

Generation and Characterization of Transgenic Potato (*Solanum tuberosum*) Roots with
Altered Levels of Hexokinase

BY

OWEN S.D. WALLY

A Thesis

Submitted to the Faculty of Graduate Studies

In Partial Fulfillment of the Requirements

for the Degree of

MASTER OF SCIENCE

Department of Plant Science

University of Manitoba

Winnipeg, Manitoba

© Copyright by Owen S. D. Wally 2002



National Library
of Canada

Acquisitions and
Bibliographic Services

395 Wellington Street
Ottawa ON K1A 0N4
Canada

Bibliothèque nationale
du Canada

Acquisitions et
services bibliographiques

395, rue Wellington
Ottawa ON K1A 0N4
Canada

Your file Votre référence

Our file Notre référence

The author has granted a non-exclusive licence allowing the National Library of Canada to reproduce, loan, distribute or sell copies of this thesis in microform, paper or electronic formats.

The author retains ownership of the copyright in this thesis. Neither the thesis nor substantial extracts from it may be printed or otherwise reproduced without the author's permission.

L'auteur a accordé une licence non exclusive permettant à la Bibliothèque nationale du Canada de reproduire, prêter, distribuer ou vendre des copies de cette thèse sous la forme de microfiche/film, de reproduction sur papier ou sur format électronique.

L'auteur conserve la propriété du droit d'auteur qui protège cette thèse. Ni la thèse ni des extraits substantiels de celle-ci ne doivent être imprimés ou autrement reproduits sans son autorisation.

0-612-80075-X

THE UNIVERSITY OF MANITOBA

FACULTY OF GRADUATE STUDIES

COPYRIGHT PERMISSION PAGE

**GENERATION AND CHARACTERIZATION OF TRANSGENIC
POTATO (*SOLANUM TUBEROSUM*) ROOTS WITH
ALTERED LEVELS OF HEXOKINASE**

BY

OWEN S.D. WALLY

**A Thesis/Practicum submitted to the Faculty of Graduate Studies of The University
of Manitoba in partial fulfillment of the requirements of the degree**

of

Master of Science

OWEN S.D. WALLY © 2002

Permission has been granted to the Library of The University of Manitoba to lend or sell copies of this thesis/practicum, to the National Library of Canada to microfilm this thesis and to lend or sell copies of the film, and to University Microfilm Inc. to publish an abstract of this thesis/practicum.

The author reserves other publication rights, and neither this thesis/practicum nor extensive extracts from it may be printed or otherwise reproduced without the author's written permission.

ACKNOWLEDGMENTS

I would like to thank the following people for their contribution to this thesis:

Dr. R. Hill for his help and guidance.

Dr. H. Duckworth and Dr. G.M. Ballance for serving on my advisory committee.

Dr. J. Rivoal for use of lab and equipment during the course of this research.

Doug Durnin and lab crew for use of their equipment and assistance.

NSERC for providing the financial support for this project.

Fellow grad student for their friendship.

My girlfriend, Janice for her support and assistance.

TABLE OF CONTENTS

| | |
|--|----|
| LIST OF TABLES | v |
| LIST OF FIGURES | vi |
| ABSTRACT | 1 |
| 1.0 INTRODUCTION | 2 |
| 1.1 Objectives | 3 |
| 2.0 LITERATURE REVIEW | 4 |
| 2.1 Introduction | 4 |
| 2.2 Occurrence of oxygen deprivation | 5 |
| 2.3 Metabolism during oxygen limitations | 6 |
| 2.3.1 Energy production | 6 |
| 2.3.2 Fermentation | 7 |
| 2.4 Induction of the hypoxic and anoxic response | 9 |
| 2.5 Aerenchyma formation | 11 |
| 2.6 Metabolic adaptations | 12 |
| 2.6.1 Anaerobic proteins | 12 |
| 2.6.1.1 Sucrose synthase | 13 |
| 2.6.1.2 Hexokinase | 15 |
| 2.6.1.3 Glucose 6-phosphate isomerase | 15 |
| 2.6.1.4 Pyrophosphate dependent phosphofructokinase | 15 |
| 2.6.1.5 Fructose-1,6-bisphosphate aldolase | 17 |
| 2.6.1.6 Glyceraldehyde-3-phosphosphate dehydrogenase | 17 |
| 2.6.1.7 Enolase | 18 |
| 2.6.1.8 Lactate dehydrogenase | 18 |
| 2.6.1.9 Pyruvate decarboxylase | 19 |
| 2.6.1.10 Alcohol dehydrogenase | 19 |
| 2.6.2 Regulatory function of anaerobic proteins | 20 |
| 2.7 Metabolic control in the glycolytic pathway | 20 |
| 2.8 Metabolic role of hexokinase | 22 |
| 2.8.1 Hexokinase function | 22 |
| 2.8.2 Hexokinase regulation | 25 |
| 2.8.1.1 Coarse control | 25 |
| 2.8.1.2 Fine control | 26 |
| 2.8.3 Hexokinase in sugar sensing | 29 |
| 2.8.4 Hexokinase in sucrose biosynthesis | 30 |
| 2.9 Plant transformations | 31 |
| 2.9.1 Plant transformation techniques | 31 |

| | |
|---|----|
| 2.9.2 Technologies used to modify gene expression in plants..... | 33 |
| 2.9.2.1 Increasing gene expression | 33 |
| 2.9.2.2 Decreasing gene expression..... | 34 |
| 3.0 MATERIALS AND METHODS..... | 37 |
| 3.1 Chemicals..... | 37 |
| 3.2 Biological material..... | 37 |
| 3.2.1 Plant material | 37 |
| 3.2.2 Root Cultures | 37 |
| 3.2.3 <i>Escherichia coli</i> stocks and cultures | 38 |
| 3.2.4 <i>Agrobacterium rhizogenes</i> stocks and cultures..... | 38 |
| 3.3 Cloning vectors | 39 |
| 3.3.1 pBK-CMV Phagemid..... | 39 |
| 3.3.2 pProEX Hta..... | 39 |
| 3.3.3 pGA643..... | 40 |
| 3.4 Plasmid amplification, purification and ligation..... | 40 |
| 3.4.1 Competent <i>E. coli</i> transformations | 40 |
| 3.4.2 <i>Agrobacterium rhizogenes</i> competent cell preparation and transformation | 41 |
| 3.4.3 Rapid plasmid preparation from <i>E. coli</i> | 42 |
| 3.4.4 Highly purified plasmids from <i>E. coli</i> | 43 |
| 3.4.4.1 High copy plasmids (SV2-G3)..... | 43 |
| 3.4.4.2 Low copy plasmids (pGA643)..... | 45 |
| 3.4.5 Small scale plasmid purification of pGA643 from <i>Agrobacterium rhizogenes</i> | 45 |
| 3.4.6 Restriction analysis | 46 |
| 3.4.7 Agarose gel electrophoresis | 47 |
| 3.4.8 DNA fragment purification..... | 48 |
| 3.4.8.1 Gel purification of DNA fragments | 48 |
| 3.4.8.2 HPLC purification of DNA fragments..... | 49 |
| 3.4.9 DNA fragment ligation | 50 |
| 3.5 Hexokinase cDNA sequencing | 50 |
| 3.6 Recombinant hexokinase immunoblotting | 51 |
| 3.6.1 SDS-PAGE and membrane electro-transfer | 51 |
| 3.6.2 Estimation of protein concentration and molecular weight | 52 |
| 3.6.3 Recombinant hexokinase expression vector | 52 |
| 3.6.4 Recombinant protein induction and purification | 53 |
| 3.6.5 Antiserum production | 56 |
| 3.6.6 Affinity purification of α -HK IgGs | 57 |
| 3.6.7 Protein extraction and quantification..... | 58 |
| 3.6.8 Immunodetection | 58 |
| 3.6.9 Quantification of HK content..... | 59 |
| 3.7 Plant transformation vectors | 59 |
| 3.7.1 pGA643 | 59 |
| 3.7.2 Sense pGA643 construct..... | 60 |
| 3.7.3 Antisense-1 pGA643 construct..... | 60 |
| 3.7.4 Antisense-2 pGA643 construct..... | 60 |

| | |
|---|-----|
| 3.7.5 Antisense-3 pGA643 construct | 61 |
| 3.7.6 <i>A. rhizogenes</i> pGA constructs | 61 |
| 3.8 <i>A. rhizogenes</i> mediated potato transformations | 63 |
| 3.9 <i>In vitro</i> hexokinase assays | 63 |
| 4.0 RESULTS AND DISCUSSION | 65 |
| 4.1 Hexokinase cDNA | 65 |
| 4.1.1 cDNA sequencing and analysis | 65 |
| 4.1.2 DNA sequence comparisons | 68 |
| 4.1.3 Amino acid sequence comparisons | 69 |
| 4.2 Production and purification of recombinant hexokinase | 73 |
| 4.2.1 <i>E. coli</i> expression vector production | 73 |
| 4.2.2 Optimizing recombinant protein induction conditions | 75 |
| 4.2.3 Recombinant protein extraction for affinity purification | 77 |
| 4.2.4 Affinity purification of recombinant protein | 80 |
| 4.2.5 Removal of 6-His tag | 83 |
| 4.2.6 Testing anti-serum for HK recognition | 85 |
| 4.3 Plant transformation vectors | 88 |
| 4.3.1 Sense construct | 88 |
| 4.3.2 Antisense constructs | 91 |
| 4.3.2.1 Antisense-1 construct | 92 |
| 4.3.2.2 Antisense-2 construct | 94 |
| 4.3.2.3 Antisense-3 construct | 95 |
| 4.3.3 Control vector | 96 |
| 4.4 Potato stem transformations | 97 |
| 4.5 Screening of transgenic roots by evaluating hexokinase protein levels | 99 |
| 4.6 Hexokinase activity measurements | 103 |
| 4.6.1 Control lines | 104 |
| 4.6.2 Sense lines | 106 |
| 4.6.3 Antisense lines | 107 |
| 4.7 Future studies | 110 |
| 5.0 CONCLUSIONS | 111 |
| 6.0 REFERENCES | 113 |

LIST OF TABLES

| | |
|---|-----|
| Table 1. Similarity between antisense sequences and STHK gene | 94 |
| Table 2. Summary of transformations and clones produced..... | 101 |
| Table 3. The efficiency of altering HK levels of the individual constructs..... | 105 |
| Table 4. Hexokinase activity of the various transgenic root lines | 108 |

LIST OF FIGURES

| | |
|---|----|
| Figure 1. Redirection of metabolism under oxygen deprivation | 8 |
| Figure 2. Glycolytic and fermentative pathways | 14 |
| Figure 3. Production of <i>E. coli</i> HK expression vector | 54 |
| Figure 4. Production of plant expression vectors..... | 62 |
| Figure 5. <i>Solanum chacoense</i> cDNA sequence | 66 |
| Figure 6. Deduced amino acid sequence of the SCHK cDNA | 67 |
| Figure 7. Hydrophobic nature of the deduced SCHK amino acid sequence | 67 |
| Figure 8. Comparison of HK amino acid sequences..... | 71 |
| Figure 9. proEX HTa containing the SCHK cDNA insert..... | 74 |
| Figure 10. The deduced amino acid sequence of the recombinant HK | 75 |
| Figure 11. Optimization of recombinant protein induction conditions..... | 76 |
| Figure 12. Localization of recombinant HK protein in soluble and insoluble fractions from <i>E. coli</i> | 78 |
| Figure 13. SDS-PAGE analysis of clarified urea supernatant of recombinant HK | 79 |
| Figure 14. Elution of affinity purified recombinant protein | 81 |
| Figure 15. Analysis of recombinant HK protein solubility after urea removal | 82 |
| Figure 16. Purification of rTEV digested recombinant HK protein | 84 |
| Figure 17. Visual quantification of the recombinant HK protein | 85 |
| Figure 18. Antiserum testing against recombinant HK | 86 |
| Figure 19. Testing and comparing purified α -HK IgGs with crude and preimmune serum on crude potato protein extracts..... | 87 |

| | |
|---|-----|
| Figure 20. TBE gel of the restriction analysis of plasmids isolated from various <i>E. coli</i> colonies containing the sense construct | 89 |
| Figure 21. Verification of proper plasmid transfer to <i>Agrobacterium</i> for S-1, AS-2 and AS-3 constructs | 90 |
| Figure 22. TBE gel of AS-1 plasmids isolated from various <i>E. coli</i> colonies..... | 92 |
| Figure 23. TBE gel of AS-1 plasmids isolated from <i>A. rhizogenes</i> | 93 |
| Figure 24. TBE gel containing plasmids from AS-2 <i>E. coli</i> colonies..... | 94 |
| Figure 25. TBE gel of AS-3 plasmids isolated from <i>E. coli</i> colonies..... | 96 |
| Figure 26. TBE gel containing digested empty pGA643 plasmids isolated from <i>A. rhizogenes</i> | 97 |
| Figure 27. Sample of immunodetection HK screening..... | 100 |
| Figure 28. HK protein levels of individual root lines | 101 |
| Figure 29. Glucokinase activity corresponding to HK protein levels..... | 109 |

ABSTRACT

Hexokinase (HK) has been shown to highly control the rate of glycolysis in animal systems. It has been hypothesized that HK may exert a similar high level of control within plant systems, especially during periods of O₂ limitations. In order to quantify the level of control transgenic potato roots were created with altered levels of HK protein and enzyme activity. A HK (SCHK) cDNA clone of *Solanum chacoense* was sequenced and analyzed. The SCHK amino acid sequence is nearly identical to *S. tuberosum* HK2. The sequence also shows a high level of similarity to other plant HKs, when compared to non-plant eukaryotic HKs the sequences share similarities in conserved binding domains. Transforming potato with SCHK using sense and antisense constructs in an *Agrobacterium rhizogenes* transformation system created transgenic roots. The resulting root lines had a range of HK protein from 0.2 to 4-fold that of the control lines, as determined by immunodetection. This alteration in protein level corresponded to an increase in phosphorylation activity using both glucose and fructose as substrates. A HK activity range of 0.6 to 6.4-fold of the control lines was observed when using glucose (GK) as substrate and 0.7 to 4.5-fold range of activity when using fructose (FK). This range in protein and HK activity is broad enough for use in determining the degree of control that HK exerts on the rate of potato root glycolysis.

1.0 INTRODUCTION

The study of hexokinase (HK) is interesting since it has been shown to be involved in many aspects of plant physiology. HK functions in primary metabolism as the first committed step in glycolysis. HK has also been shown to function in sensing the cellular sugar status of plant cells, resulting in alterations in plant gene expression.

HK is thought by many to exert a high degree of control on the rate of glycolysis during O₂ deprivation. The reasoning behind this hypothesis is that i) HK is one of 20 enzymes preferentially induced during O₂ deprivation. ii) HK is inhibited by reduction in ATP/ADP ratio and reduction in cytosolic pH, both of which occur during anoxia. iii) Evidence obtained from animal systems indicates that HK plays a key role in the rate of glycolysis. These points all indicate that HK may be a key regulatory step in the rate of plant energy production during anoxia. There is however no experimental evidence from plants to quantify the level of control that HK plays on the rate of glycolysis during anoxia.

The process of Metabolic Control Analysis (MCA) can be used to quantify the level of control that HK exerts on plant glycolysis during O₂ limitation. The MCA process requires methods of altering enzyme levels, and a mechanism for measuring the rate of flux. To determine the control that HK exerts on plant glycolysis, tissue with altered HK levels are needed and the rate of glycolytic flux can be measured by tracking radioactive metabolites.

1.1 Objectives

The ultimate objective of this research is to quantify the amount of control that HK exerts on anoxic metabolism. The objectives of this project are to develop the material necessary in order to quantify this level of control. This work includes i) to sequence and characterize a HK cDNA from *Solanum chacoense*, ii) to produce antibodies against a recombinant HK for use in screening transgenic lines, iii) to produce plant transformation vectors with HK cDNA in both sense and antisense orientations, iv) to transform potato with the HK vector and produce many transgenic lines, v) to screen the transgenic lines for the presence of altered HK protein levels and vi) to screen the transgenic lines for altered HK activity.

The transgenic root lines characterized for level of HK activity will then be used to measure the rate of glycolysis during anoxia. By comparing the rate of flux in respect to amount of in vitro enzyme activity the degree of control that HK exerts will be quantified.

2.0 LITERATURE REVIEW

2.1 Introduction

This review examines the broad adaptations that plants have developed to deal with the effects of O₂ deprivation. These adaptations include both physiological and morphological changes. The physiological changes were examined in greater detail and particular attention was paid to metabolic adaptations, including the alteration of gene and protein expression under O₂ limitation as well as the changes in enzyme activity.

The role of hexokinase (HK) under O₂ limiting conditions is thought to be part of this adaptative process. If HK is an important part of the metabolic adaptations, the level of metabolic control will be high. Therefore particular focus was paid to how metabolic control is quantified and the characteristics that make HK a likely candidate to display a high degree of control were examined in detail.

The present study hypothesizes that HK is involved in the metabolic control over the rate of plant glycolytic flux under O₂ limiting conditions. This hypothesis was based from the regulatory characteristics of plant HK and the strong degree of metabolic control observed in some animal system HKs.

Transgenic potato roots displaying altered levels of HK were generated in this work. Therefore, the strategies for altering the HK protein levels were discussed. This includes the mechanisms for plant transformations, the over-production of enzymes and the strategies for gene silencing.

2.2 Occurrence of oxygen deprivation

Throughout their lives higher plants experience many different stress conditions. These include biotic (e.g. insect predation, weeds and diseases) and abiotic (e.g. oxygen deficiency, water deficiency, salinity and temperature) stresses. Abiotic stresses are by far the most detrimental stresses to crop plants, resulting in yield losses reaching 71 % of the crops potential (Boyer 1982). Oxygen deficiency in particular is a major agricultural concern under flooded soil conditions. Excess water is the second leading cause of crop losses and represents more than 16% of crop insurance claims paid in the United States in the modern era (Boyer 1982).

Most plants require the energy generated by respiration for continued growth and development. Flooding causes O_2 diffusion into the soil to decrease dramatically, O_2 diffuses 10 000 times more slowly in H_2O than in air (Armstrong 1979). The O_2 supply within a flooded soil is quickly depleted by the plant roots and existing microorganisms within the soil. Plants experiencing a decrease in the levels of available O_2 gradually shift from normoxia (normal O_2 levels that ensure maximal respiration rates) to hypoxia (limited O_2 concentration resulting in a mixture of respiration and fermentative metabolism) to finally anoxia (complete absence of O_2 resulting in fermentation only) (Drew 1997) (Figure 1). Under field conditions, the roots rapidly become hypoxic and completely anoxic within a few hours (Fox *et al.* 1995).

2.3 Metabolism during oxygen limitations

2.3.1 Energy production

Mitochondrial respiration is dependent on O₂, which serves as the terminal electron receptor. During hypoxia, oxidative phosphorylation and the mitochondrial electron transport chain are severely impaired, and completely stopped when a state of anoxia is reached. This results in an increased steady state of NADH and FADH₂, formed by glycolysis and the Krebs Cycle (TCA). The TCA cycle functions slowly during hypoxia and is suppressed completely under anoxia in most cases (reviewed by Drew 1997). Therefore plants in general are completely dependent on glycolysis in most cases for energy production, however partial TCA function coupled with the pentose phosphate pathway generates ATP in *Echinochloa phyllogon* (Fox *et al.* 1994). However, the energy generated from glycolysis is only 2 ATP/glucose whereas the complete oxidation of glucose through respiration produces 38 ATP/glucose, therefore the rate of glycolysis is increased during O₂ limitation (reviewed by Drew 1997).

Energy utilization in plants is under stringent control. Many enzymes, especially those involved in phosphorylation and dephosphorylation reactions, are dependent on the ATP/ADP and ATP/AMP ratios (reviewed by Pradet and Raymond 1983). The energy status of a living cell as defined by Atkinson and Walton (1967) can be measured by estimating the energy charge $(ATP + \frac{1}{2} ADP) / (ATP + ADP + AMP)$. Typically the energy charge of metabolically active plant cells ranges from 0.8 to 0.9 (Pradet and Raymond 1983). A decrease in energy charge is observed during hypoxia and is further decreased when the cells become anoxic (Saglio *et al.* 1980).

2.3.2 Fermentation

Under anoxia, the generation of metabolic energy is highly coupled to the C flux through the glycolytic and fermentative pathways. The rate of glycolysis depends on the availability of NAD^+ , which serves as a co-factor. The steady state concentration of the reduced form, NADH, accumulates under anoxia and needs to be recycled for continued energy production. The regeneration of NADH to NAD^+ occurs through fermentation. Ethanol fermentation is the most common pathway for NAD^+ regeneration in plants (Figure 1). Pyruvate is decarboxylated to yield acetaldehyde through the action of pyruvate decarboxylase (PDC). Acetaldehyde is a toxic product, which is reduced to ethanol by alcohol dehydrogenase (ADH). This process regenerates NAD^+ . Lactate fermentation involves the reduction of pyruvate to form lactate through the action of lactate dehydrogenase (LDH) this reaction regenerates NAD^+ directly (Figure 1).

During the transition from normoxia to anoxia the initial glycolytic flux is directed towards lactate. Lactate production occurs concurrently with a cytosolic acidification of ~ 1 pH unit (Davies *et al.* 1974; Roberts *et al.* 1984a; Roberts *et al.* 1985). The decrease in pH inhibits LDH activity and activates PDC (Figure 1). Within a few minutes to a few hours the production of lactate levels off. The action of PDC coupled with ADH produces ethanol and CO_2 , thus taking over the role of NADH regeneration and ATP production (Davies *et al.* 1974; Roberts *et al.* 1984b). This pattern of fermentation occurs in most plants systems, however several systems have revealed alternative fermentative pathways. Sustained C-flux towards lactate has been observed in

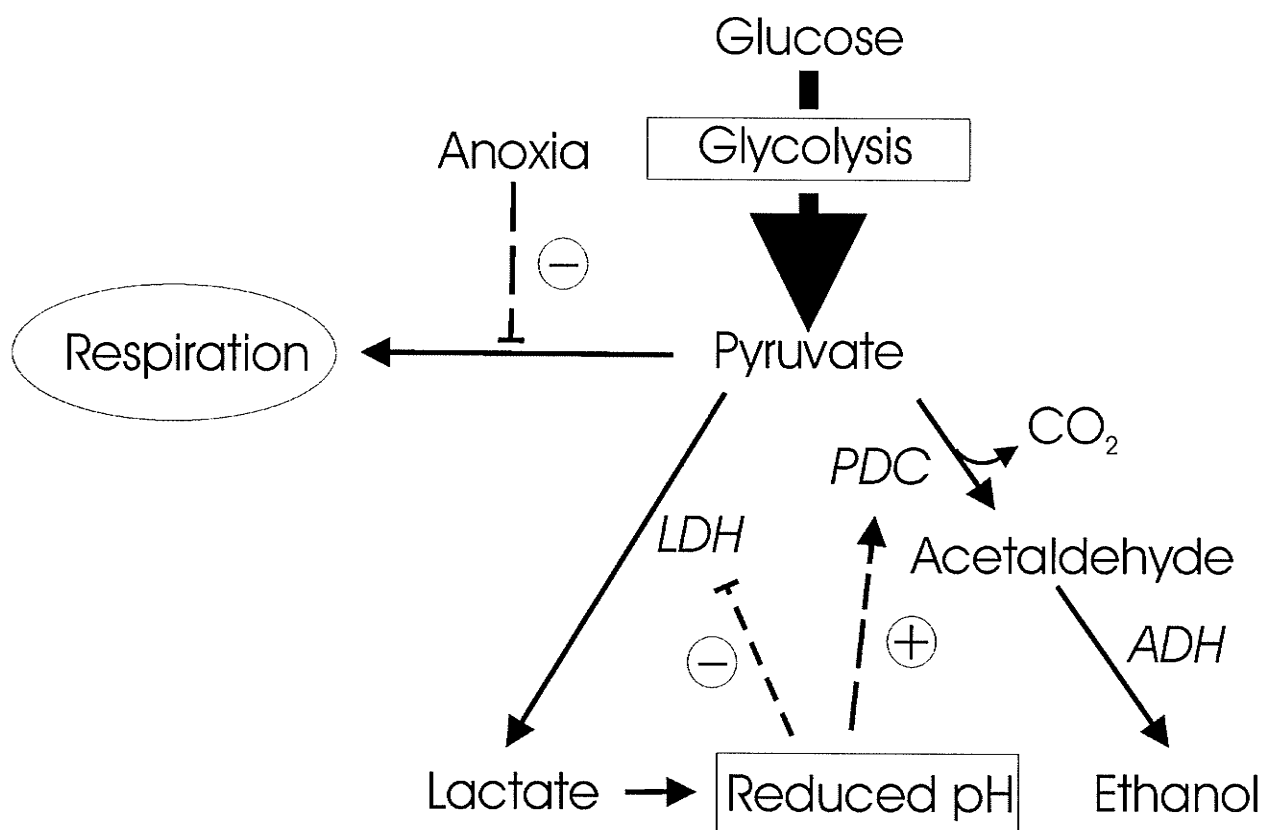


Figure 1. Redirection of metabolism under oxygen deprivation. Under anoxia the glycolytic flux is no longer directed towards respiration, but is redirected towards fermentation. Solid lines represent carbon flux, hatched lines represent regulatory mechanisms.

barley aleurone layers (Hanson and Jacobsen 1984) and in the anoxic roots of several species of the genus *Limonium* (Rivoal and Hanson 1993) several hours after transition to anoxia. In rice seedlings there is no detectable lactate formation under anoxia, however, ethanol fermentation is active (Rivoal *et al.* 1989). In hypoxically pretreated maize root tips initial fermentative C-flux is directed towards ethanol (Xia and Saglio 1992).

Other significant metabolic end products from anoxic tissue include gamma-amino butyric acid (GABA) (Fan *et al.* 1988), which is formed from the decarboxylation of glutamate through the action of glutamate decarboxylase. It is hypothesized that the

formation of GABA serves to regulate the cellular pH under anoxic conditions by absorbing excess H^+ (Menegus *et al.* 1989; Shelp *et al.* 1999). Alanine is also a significant end metabolite in root tissue (Good and Crosby 1989). Alanine is formed from pyruvate through the action of the anaerobically induced enzyme alanine aminotransferase (AAT) (Muench and Good 1994). The significance of increased alanine production under oxygen stress is not yet known.

2.4 Induction of the hypoxic and anoxic response

The exact mechanism of how plants sense their O_2 status is unknown, however there are many theories that have varying degrees of experimental support in existence. Since plant metabolism is very sensitive to the cellular energy charge, a reduction in the energy charge occurring during oxygen deprivation may serve as a signal to the oxygen status of the plant (reviewed by Drew 1997). This theory was studied using respiratory inhibitors in tobacco, where fermentation was induced under normoxic conditions (Bucher *et al.* 1994). The decrease in cellular energy status did not, however, account for the preferential induction of ADH (Bucher *et al.* 1994). In bacterial systems O_2 sensing mechanisms have been discovered and well characterized. These bacterial O_2 sensing mechanisms generally involve an O_2 binding to a protein heme group (Monson *et al.* 1992; Monson *et al.* 1995). In plants the O_2 binding to a heme group in hemoglobins has been proposed as means of sensing the O_2 status (Appleby *et al.* 1988; Sowa *et al.* 1998). Other indirect theories of plant cell O_2 sensing involve a signal linked to Ca^{++} concentration, since increased cytosolic Ca^{++} has been observed in anoxic cells and Ca^{++}

has been shown to induce ADH gene expression (Subbaiah *et al.* 1994a; Subbaiah *et al.* 1994b). Ethylene signaling has been proposed as a means of sensing the transition of normoxia to hypoxia, since ethylene production has been shown to be increased under hypoxia, and is implicated with signaling for formation of aerenchyma (He *et al.* 1996).

Within a few minutes of anoxia the roots will completely utilize their remaining ATP pool in metabolically active cells (root tips) (Sachs *et al.* 1996; Drew 1997). Evolutionary adaptations including both physiological and morphological changes allow plants to survive anoxia (reviewed by Drew 1997). Physiological changes occur quickly under anoxia, and involve altering the plant's gene and protein expressions in order to utilize the low levels of energy produced and maximize efficiency. Morphological changes occur more slowly and are generally viewed as adaptations to long-term stress. These morphological changes involve changing the plants physical structure to facilitate oxygen transport to the anoxic tissue and reestablish oxidative phosphorylation. All plant tissues are able to survive anoxia for several hours, while some anoxic tolerant plant species are able to survive for weeks without any oxygen (Barclay and Crawford 1982; Couée *et al.* 1992; Bucher and Kuhlemeier 1993).

Plants in general have an increased tolerance to anoxia if they experience a transitional period of hypoxia prior to anoxia. This process is referred to as hypoxic pre-treatment (HPT). This period of adjustment is often used in laboratory studies and allows the plants to make the necessary physiological modifications to their metabolism, gene expression and protein synthesis, while there is some energy produced through oxidative phosphorylation (Johnson *et al.* 1989). The HPT can last for a few minutes or several hours. For example an overnight (~16 hours) HPT accounts for a 3-fold increase in the

rate of glycolytic flux in maize roots (Bouny and Saglio 1996). HPT is similar to the gradual transition between normoxia, to hypoxia and finally anoxia that a plant would experience under natural conditions. The regulation of cytosolic pH is substantially better with HPT maize root tips as compared untreated root tips under anoxia (Xia and Robers 1994).

2.5 Aerenchyma formation

The ability of plants to change their physical structure as well as their physiological characteristics to deal with environmental stresses is helpful in long-term stress adaptations. Under hypoxia and anoxia some plants can form aerenchyma. Aerenchyma formation occurs by programmed cell death in which hollow air spaces are formed within the plant root cortex (Webb and Jackson 1986). These aerenchyma allow for O₂ diffusion from normoxic (above water) plant organs to the O₂ deficient (flooded) organs. This gas diffusion to O₂ deficient tissue allows for continuation of energy production through oxidative phosphorylation (reviewed by Drew 1997). Aerenchyma formation is considered to be advantageous to long term survival under anoxia, since they are present in the roots of many aquatic plants which are tolerant to long term anoxia (Drew *et al.* 1985).

The cellular degradation of the cortex leading to aerenchyma formation begins within 6-12 hours (Webb and Jackson 1986). The programmed cell death in the cortex appears to be associated with ethylene signaling (He *et al.* 1996). Genes encoding proteins associated with aerenchyma formation, including xyloglucan *endotransglycosylase* (XET), have been identified in maize and are preferentially induced under O₂ limitation

(Sachs *et al.* 1996). XET is believed to loosen cell walls required for cellular growth, this may have a function in enhancing the formation of aerenchyma (Sachs *et al.* 1996).

2.6 Metabolic adaptations

2.6.1 Anaerobic proteins

Major changes occur in gene expression under anoxia. Under O₂ deficiency, the majority of proteins synthesized under normoxia are no longer produced (Sachs *et al.* 1980). This occurs at the transcriptional level and at the translational level through the dissociation of polyribosome complexes (Hake *et al.* 1985; Sachs *et al.* 1996). During anoxia, 20 proteins represent 70% of the total protein synthesized in maize roots (Sachs *et al.* 1980). These proteins produced under limited O₂ levels are called anaerobic proteins (ANP). Induction of ANPs is the result of transcriptional up-regulation and post-transcriptional regulation. The vast majority of ANPs are involved in glycolysis and fermentation (Sachs *et al.* 1996)(Figure 2). ANPs have been characterized in maize roots, rice seedlings and a few other model systems. These proteins include: sucrose synthase (SuSy) (Springer *et al.* 1986), HK (Bouny and Saglio 1996; Fox *et al.* 1998), glucose 6-phosphate isomerase (PGI) (Kelley and Freeling 1984a), pyrophosphate-dependent phosphofructokinase (PPi-PFK) (Mertens *et al.* 1990), fructose-1,6-diphosphate aldolase (Kelley and Freeling 1984a; Kelley and Freeling 1984b), glyceraldehyde-3-phosphosphate dehydrogenase (GAPDH) (Kelley and Freeling 1984b; Russell and Sachs 1989; Ricard *et al.* 1989), enolase (Lal *et al.* 1991), ADH (Freeling 1973), LDH (Hoffman *et al.* 1986), AAT (Good and Crosby 1989; Muench and Good 1994) and PDC (Kelley 1989; Peschke and Sachs 1993).

Several of the more strongly induced ANPs (ADH and SuSy) share a conserved anoxic response element (ARE) within their promoter region. This promoter element may serve to coordinate the induction of several ANPs during the initial stages of O₂ deprivation (reviewed by Drew 1997).

2.6.1.1 Sucrose synthase

Sucrose cleavage is essentially the first step in sugar catabolism in higher plants. Reactions generally proceed through the action of invertase or via the reversible reaction catalyzed by SuSy (E.C. 2.4.1.13) (Figure 2). Although both enzymes catalyze the cleavage of sucrose, invertase is strongly inhibited by O₂ limitation (Ricard *et al.* 1998; Zeng *et al.* 1999), while SuSy has been shown to be preferentially induced under O₂ limitation in many plant systems (Springer *et al.* 1986; Ricard *et al.* 1991; Zeng *et al.* 1998). The SuSy cleavage of sucrose results in the production of fructose and UDP-glucose. Most plants generally contain 2 or 3 distinct SuSy isoforms. These isoforms typically exist as “feast or famine” enzymes, such that one isoform typically functions at low sucrose levels while the others function when sucrose is abundant (Zeng *et al.* 1998). Evidence from the study of maize SuSy mutants suggests that SuSy plays a crucial metabolic control role in sugar metabolism under anoxia (Ricard *et al.* 1998).

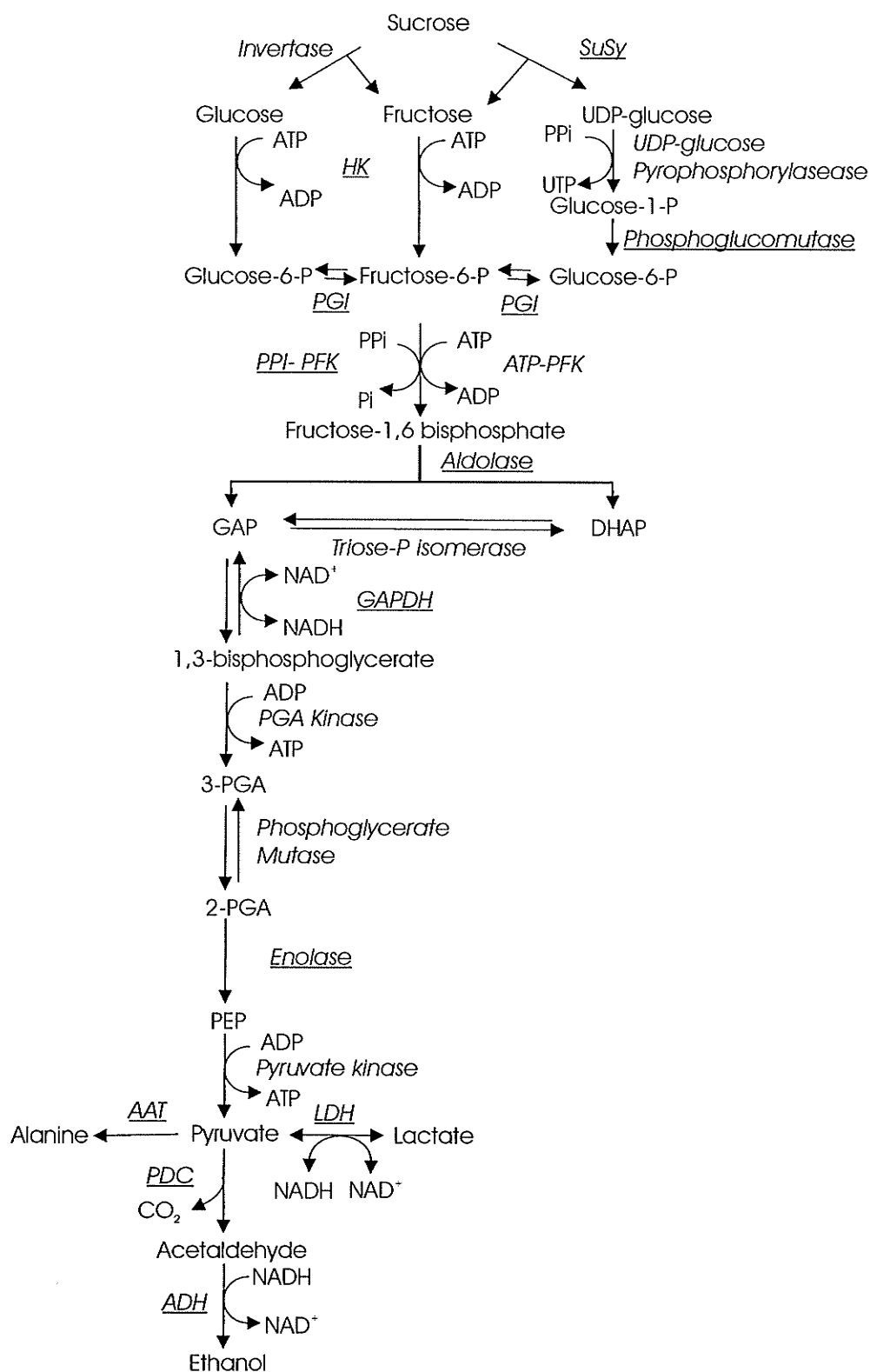


Figure 2. Glycolytic and fermentative pathways. Substrates and product are in regular text, enzymes are in italics, those showing increased expression under anoxia are underlined.

2.6.1.2 Hexokinase

HK (E.C. 2.7.1.1) catalyzes the phosphorylation of hexose sugars, typically glucose and fructose to form, glucose-6-phosphate (G6P) and fructose-6-phosphate (F6P) respectively (Figure 2). The HK-mediated step is the first dedicated step in glycolysis. HK has been shown to be preferentially induced in some plants under anoxia (Bouny and Saglio 1996; Fox *et al.* 1998). In some anoxic tolerant plant species, HK activity increases up to 4-fold the normoxic levels under anoxia (Fox *et al.* 1998).

2.6.1.3 Glucose 6-phosphate isomerase

PGI (E.C. 5.3.1.9) catalyzes the isomerization reaction converting G6P to F6P, figure 2. This equilibrium reaction occurs in both glycolysis and in sucrose biosynthesis in plants. PGI is a dimer of approximately 150 kDa native molecular weight and there are three distinct PGI isoforms that have been identified (Kelley and Freeling 1984b). PGI gene expression, protein quantity and enzyme activity have been shown to increase 2-fold after 72 hours of anoxia in maize (Kelley and Freeling 1984b), and may occur in other plant systems as well.

2.6.1.4 Pyrophosphate-dependent phosphofructokinase

PPi-PFK (E.C. 2.7.1.90) catalyzes the phosphorylation of fructose 6-phosphate to form fructose 1,6-bisphosphate using PPi as a phosphate donor (Figure 2). This reaction is completely reversible, functioning in both sucrose synthesis and glycolysis, unlike ATP dependent-PFK which function only in the glycolytic direction. PPi-PFK functions

as either a tetramer or octomer composed of 2 distinct α and β subunits. These subunits have molecular masses of 60-68 kDa (reviewed by Plaxton 1990). PPi-PFK has been shown to be preferentially induced during phosphate starvation (Duff *et al.* 1989; Theodorou *et al.* 1992) and anoxia (Mertens *et al.* 1990). PPi-PFK enzyme activity increases up to 10 fold normoxic levels within 8 days of anoxia, while ATP-PFK activity does not change during anoxia (Mertens *et al.* 1990). Plant PPi-PFK is very sensitive to the activator fructose 2,6-bisphosphate, which accumulates to physiologically significant levels in plants during anoxia (Mertens *et al.* 1990). Two ATP/hexose are generally required for glycolysis to proceed, however, the plants using PPi-PFK during glycolysis require only 1 ATP/hexose. Reducing the cellular demand on ATP used in glycolysis by 50%. PPi is produced by many biosynthetic reactions and typically hydrolyzed by plant cells and not used in metabolism (Mertens 1991).

The use of PPi as an alternative energy source under anoxia has further support through the identification of a vacuolar H^+ -pyrophosphatases (V-PPase), which are preferentially induced during O_2 limitation. Plant V-PPases were first discovered in rice (Carystinos *et al.* 1995) and have since been discovered in mung bean (Nakanishi and Maeshima 1998), *Arabidopsis* (Schumacher *et al.* 1999) and corn (Rocha and de Meis 1998) and function in the same manner as vacuolar H^+ -ATPases. The V-PPase is strongly induced by anoxia showing a 75-fold increase in protein level and enzyme activity in rice (Carystinos *et al.* 1995). Other enzymes that utilize PPi as a phosphate source under anoxia may exist, since PPi levels are relatively insensitive to plant O_2 status (Carystinos *et al.* 1995).

2.6.1.5 Fructose-1,6-diphosphate aldolase

Aldolase (E.C. 4.1.2.13) catalyzes the reversible cleavage of fructose 1,6-bisphosphate to dihydroxyacetone phosphate (DHAP) and glyceraldehyde 3-phosphate (G3P), figure 2. Aldolase exists as homotetramers with subunit molecular masses of 36-40 kDa, in cytosolic and plastidic isoforms. The cytosolic isoform have been shown to be preferentially induced under oxygen deprivation in *Acorus calamus* (Bucher and Kuhlemeier 1993) and in maize (Kelley and Freeling 1984a). An increase in gene expression of 50-60 fold was observed in the anoxic tolerant *A. calamus* after 72 hours while a 2-fold increase was seen in maize (Kelley and Freeling 1984a). The anoxic tolerant *A. calamus* shows a very high induction of aldolase during anoxic stress, which may indicate a key role in the long-term anoxic tolerance (Bucher and Kuhlemeier 1993).

2.6.1.6 Glyceraldehyde-3-phosphosphate dehydrogenase

Two isoforms of GAPDH exist in higher plants, one operational in the cytosol and the other in the plastid. Cytosolic GAPDH (E.C. 1.2.1.12) catalyzes the conversion of G3P and NAD^+ to 3-phosphoglycerate (3-PGA) and NADH (Figure 2) and has been shown to be preferential induced in rice seedlings (Ricard *et al.* 1989) and maize roots (Russell and Sachs 1989). GAPDH exists as a homo or heterotetramer, with subunits being approximately 35-40 kDa in size. Activity was shown to increase up to 3 fold in anoxic rice seedlings after 72 hours (Ricard *et al.* 1989) and up to 50% activity increase was seen in maize after 24 hours (Kelley and Freeling 1984b) (Russell and Sachs 1989).

2.6.1.7 Enolase

Enolase (E.C. 4.2.1.11) catalyzes the interconversion of 2-phosphoglycerate to phosphoenolpyruvate (PEP) (Figure 2). Generally two isoforms of enolase exist in plants, typically one cytoplasmic and one localized to the plastid (Miernyk and Dennis 1984). Enolase has been shown to be preferentially induced under hypoxia and anoxia in maize (Lal *et al.* 1991; Lal *et al.* 1998), rice (Umeda *et al.* 1994), *Echinochloa phyllopogon*, and *E. crus-galli* (Fox *et al.* 1995). In maize enolase gene expression under anoxia increased up to 5-fold, while its activity increased 2 to 3-fold (Lal *et al.* 1998). In the anoxic tolerant *E. phyllopogon*, activity increased 5-fold after 3 hours of anoxia (Fox *et al.* 1995).

2.6.1.8 Lactate dehydrogenase

LDH (E.C. 1.1.1.27) as previously stated catalyzes the reduction of pyruvate to form lactate and NAD^+ (Figure 2). LDH exists as a hetero-tetramer composed of two subunits (Rivoal *et al.* 1991). LDH is strongly induced initially during anoxia with enzyme activity continuing to increase for up to 6 days. However, gene expression and protein synthesis under anoxia begin to decrease after only 24 hours of anoxia. Increases in LDH activity of 16-fold in wheat, 3-fold in maize and 80-fold in anoxic rye roots have been observed (Hoffman *et al.* 1986).

2.6.1.9 Pyruvate decarboxylase

PDC (E.C. 4.1.1.1) catalyzes the first step bridging glycolysis and ethanol fermentation, converting pyruvate to acetaldehyde and CO₂ (Figure 2). There have been 3 PDC genes discovered in maize, encoding for 3 distinct PDC isoforms (Peschke and Sachs 1993). PDC transcript level has been shown to increase up to 20-fold under anoxia. Protein level increases 5.6-fold, and enzyme activity increases 9-fold during anoxia (Kelley 1989; Rivoal *et al.* 1997).

2.6.1.10 Alcohol dehydrogenase

ADH (E.C. 1.1.1.1) is the most studied ANP in plants. As previously stated, ADH catalyzes the reduction of acetaldehyde to form ethanol, while regenerating NAD⁺, (Figure 2). It exists in the cytoplasm as either a homodimer or heterodimer. The molecular masses of the subunits vary between plant species. Generally plants have either 2 or 3 ADH genes encoding for distinct ADH isoforms (Dennis *et al.* 1984; Dennis *et al.* 1985). ADH transcript levels can be induced at levels greater than 50-fold the normoxic levels in maize roots during hypoxia (Gerlach *et al.* 1982). Similar transcript induction has been observed in barley (Hanson *et al.* 1984) and maize shoots (Andrews *et al.* 1993). The increase in ADH activity is generally 3 to 5-fold and is tissue and species dependent (Andrews *et al.* 1994). ADH induction is consistent with long-term anoxic tolerance, since ethanol does not contribute to cytosolic acidification (Bucher and Kuhlemeier 1993).

Ethanol toxicity was thought to be a source of cellular injury during anoxia, since high concentrations of ethanol can interfere with membrane stability and metabolism. Support for this theory has disappeared since ethanol can diffuse through into the surrounding environment with relative ease and the concentrations required for cellular injury are far beyond the physiological levels produced by plants (Drew 1997).

2.6.2 Regulatory function of anaerobic proteins

The adaptative function of most ANPs in respect to metabolic regulation is largely unknown. Several of the enzymes, especially SuSy and HK have been speculated to highly controlling on the rate of C-flux through glycolysis (Bouny and Saglio 1996; Fox *et al.* 1998; Ricard *et al.* 1998). However, little experimental evidence has been conducted on the significance of ANPs. Experiments using transgenic tomato roots overproducing LDH in large quantities showed no increase in lactate production (Rivoal and Hanson 1994). These findings indicated that although LDH expression increases under anoxia the level of the protein does not control the rate of lactate fermentation (Rivoal and Hanson 1994). The LDH example is a good indication that increased gene and protein expression in the glycolytic pathway does not necessarily correspond to an increased C-flux.

2.7 Metabolic control in the glycolytic pathway

Traditionally, control over metabolic pathways was believed to be governed by one or a few so called key “pace-making”, or “rate limiting enzymes” (Newsholme and Crabtree 1979) (reviewed by ap Rees and Hill 1994). These key enzymes were identified

on the basis of one or more key characteristics: i) low extractable activity, ii) a substrate and product far from equilibrium, iii) classical sigmoidal kinetics for the enzyme, iv) and regulation by allosteric effectors (Thomas and others 1997a).

In plant glycolysis the control points are generally believed to be the two enzymes phosphofructokinase (PFK) and pyruvate kinase. However, as early as 1973 Kacser and Burns argued that all enzymes within the pathway in fact, share the regulation of flux through a metabolic pathway. This theory was supported by a formalized framework, the Metabolic Control Theory (Kacser and Burns 1973; Kacser and Burns 1995). With the advent of genetic engineering it has recently become easier to quantify the control of individual enzymes within a metabolic pathway. Enzyme levels can be easily altered by over and under-expressing their genes, while the rate of metabolic flux can be measured and tracked using radio or heavy isotopes (NMR) (reviewed by Fell 1992). The altered enzyme level can then be compared with the rate of metabolic flux to determine the extent of *in vivo* control for that particular enzyme. This procedure is referred to as Metabolic Control Analysis (MCA) (Kacser and Burns 1979) (reviewed by Fell 1992 and ap Rees and Hill 1994)), which is derived from the Metabolic Control Theory.

Even though the control over flux of a pathway is shared among the enzymes, some enzymes are more controlling than others. The level of control, which an individual enzyme exhibits, can be measured as the Flux Control Coefficient (FCC). The FCC is defined as the relative relative change in pathway flux resulting from a relative change in enzyme activity (Fell 1992; ap Rees and Hill 1994; Kacser and Burns 1995). The sum of all enzyme FCCs within a pathway is equal to 1. Enzymes having a FCC greater than 0.8

would still be considered “rate limiting”(ap Rees and Hill 1994). For example, if an enzyme has a FCC of 0.5, then doubling the enzyme concentration would increase the flux through the pathway by 50%.

MCA was used to determine the control of PFK in plant glycolysis (Thomas *et al.* 1997b). It was found that modifying PFK levels to greater than 40-fold control levels had almost no effect on glycolytic flux during normoxia (Thomas *et al.* 1997a). These findings contradict the notion that PFK is a rate-controlling enzyme in glycolysis. Evidence from these experiments indicated that the majority of control over glycolysis is upstream of the PFK step.

2.8 Metabolic role of hexokinase

2.8.1 Hexokinase function

HK has been postulated to be highly controlling on the rate of anoxic glycolytic flux (Bouny and Saglio 1996; Ricard *et al.* 1998). HK has already been shown to exhibit a high level of control on animal glycolysis and gluconeogenesis. A FCC greater than 0.7 have been observed in *Xenopus* oocytes (Ureta *et al.* 2000), human erythrocytes (Rapoport *et al.* 1974) and rat hepatocytes (Agius *et al.* 1996; De Atauri *et al.* 2001). It is possible that a similar level of control exists in plant systems, however there is no experimental evidence that quantifies the extent of HKs control.

HKs catalyze the phosphorylation of hexose sugars, which is the first committed step in the glycolytic metabolism of sugars. HKs are constitutive enzymes found in all eukaryotic and most prokaryotic cells. True HKs (EC 2.7.1.1.) utilize glucose preferentially but are able to phosphorylate, to some degree, fructose and mannose

(Cardenas *et al.* 1998). True non-specific HKs are generally only found in animal and yeast systems, while substrate-specific HKs are generally found in bacteria and plants. Substrate specific HKs or glucokinases (GK) (EC 2.7.1.2.) have a high affinity for glucose (and related aldoses such as mannose), and have significantly less affinity ($>10\times$ less) for fructose (and related ketoses) (Renz and Stitt 1993; Cardenas *et al.* 1998). GKs however, are very similar to true HKs and the nomenclature has been interchanged often (Schnarrenberger 1990).

In plants and bacteria, fructose is phosphorylated primarily by a separate family of enzymes. These fructose phosphorylating enzymes are termed fructokinases (FK) (EC 2.7.1.4.). FKs have a very high affinity ($K_m \sim 150\mu\text{M}$) and activity for fructose (Doehlert 1990; Renz and Stitt 1993; da Silva *et al.* 2001). These enzymes exist in their native configuration as homodimers composed typically of 30-40 kDa subunits (Martinez-Barajas *et al.* 1997). Since FKs are highly specific for fructose they are not considered to be part of the HK family.

Non-specific HKs have been studied extensively in mammalian and yeast systems. Multiple isoforms were initially studied in yeast which contains three distinct HKs (Womack *et al.* 1973; Gancedo *et al.* 1977). Subsequent studies have identified four distinct HKs, which were initially observed in rat hepatocytes through their electrophoretic migration characteristics. These HK isoforms appear to be present within all animal systems and are classified as HK I, II, III, and IV (Katzen *et al.* 1968) (or A, B, C, and D (Gonzalez *et al.* 1964)). Most plant species contain either two or three distinct HK isoforms.

The partially purified enzymes characterized in potato tubers (Renz *et al.* 1993) revealed a high affinity and activity towards glucose, which is the preferred substrate for all 3 HK isoforms. The K_m value for glucose ranges between 35 μ M for HK3 to 130 μ M for HK2, where as the K_m value for fructose was between 9 and 22 mM (as much as a 500-fold difference). The V_{max} values are similar between both sugars (Renz and Stitt 1993). The affinity and activity values for both of the sugars are very similar to HKs observed in corn (Doehlert 1989), tomato (Martinez-Barajas and Randall 1998), and spinach leaves (Schnarrenberger 1990).

Animal, plant and yeast HKs are able to utilize a wide range of nucleotides as substrates, however there is a strong preference to the utilization of ATP. The affinity for most HKs is approximately 10 times greater for ATP than for any other NTP (Pollard-Knight and Cornish-Bowden 1987; Doehlert 1989; Renz and Stitt 1993). Bacterial HKs however are capable of using a variety of NTPs as phosphate donors, with many enzymes having a similar affinity for ITP as with ATP (Hengartner and Zuber 1973). There have also been HKs characterized from bacteria which utilize ADP (Kengen *et al.* 1995) and polyphosphate (Phillips *et al.* 1993).

The native molecular masses of the different HK isoforms are typically in either the 50 or 100 kDa range in both animal and yeast systems (reviewed by Wilson 1995 and Cardenas *et al.* 1998)). The native molecular masses differ just as significantly in plants, ranging from 38 kDa in castor beans (Miernyk and Dennis 1983) to as large as 100 kDa in wheat germ (Higgins and Easterby 1974). The masses of the isoforms also vary within species with 39 and 59 kDa isoforms found in maize (Doehlert 1989) and 50 and 100 kDa HKs discovered in wheat germ (Higgins and Easterby 1974).

In most plant systems the HKs appear to be monomers (Fox *et al.* 1998). This appears to also be the case in animal systems (Cardenas *et al.* 1998). However, several fungal, bacterial and protozoa have oligomeric HKs, which are generally homodimers (Cardenas *et al.* 1998). In rare cases structures as large as hexamers have been observed, for example: the protozoa *Trypanosoma bruceia* has a HK with a native molecular mass of 300 kDa composed of six 50-kDa subunits (Misset *et al.* 1986).

The detailed molecular structure and substrate binding characteristics of HK were first determined with the yeast HK (Anderson *et al.* 1978a; Anderson *et al.* 1978b) and has since been determined in mammalian HK (Sebastian *et al.* 1999). The high degree of amino acid similarity in substrate binding regions between most HKs implies that there are similar structural characteristics among most HKs (reviewed by Wilson 1995). The yeast HK consists of 2 distinct regions, a “large lobe” and a “small lobe” (Bennett, Jr. and Steitz 1980). Between the lobes a cleft exists in which the sugar substrates bind. The binding of the substrate initiates a conformational change in the protein, changing from an “open cleft” when no sugar is bound to a “closed cleft” in the presence of sugar (Anderson *et al.* 1978b).

2.8.2 Hexokinase regulation

2.8.2.1 Coarse control

The HK isoform composition in distinctive tissues and at the developmental state of the tissue varies considerably within an organism. Tissue specific isoforms have been studied primarily in mammalian systems (Griffin *et al.* 1992), while relatively little analysis has been conducted on plant systems. A detailed study on potato indicated a

dramatic change in the isoform composition of tubers in respect to their developmental stage (Renz *et al.* 1993). This showed a glycolytic dependence on FK (FK1 and FK2) in young tubers, corresponding to an initial activity of sucrose cleavage by SuSy (Renz *et al.* 1993). As the tubers aged and eventually began to germinate the activities of HK1 and HK2 become more prominent correlating to increased invertase cleavage of available sucrose. The change in HK isoforms also varied between the potato tissue, leaves having primarily FK3 activity, which was completely absent from the tubers (Renz *et al.* 1993). This alteration in HK composition between tissues may be due to the preferential induction of HK based on sugar availability. For example in tomato fruit FK gene expression was shown to be induced by fructose concentrations at physiological levels (20 mM) (Kanayama *et al.* 1998).

2.8.2.2 Fine Control

HKs in general are very sensitive to feedback inhibition by their products. In animal systems HK I, II and III are extremely sensitive to G6P, while HK IV (GK) is insensitive to physiological levels of G6P (reviewed by Cardenas *et al.* 1998). The substrate specific HKs in plants, however, behave more like animal true HK in terms of feedback inhibition. G6P has been shown to inhibit potato and tomato HK by non-competitive binding ($K_i = 4.1$ mM) (Renz and Stitt 1993; Martinez-Barajas and Randall 1998). This is highly significant since G6P concentrations of 3-7 mM are present in potato tubers (Hajurezaei and Stitt 1991). ADP the other product of the HK reaction is also involved in feedback inhibition. ADP inhibits HK by competitive binding to the ATP site of the enzyme. The sensitivity of different HK isoforms varies greatly. In potato

tubers K_i value for ADP ranges from 40 μ M in HK1 to 108 μ M in HK3 (Renz and Stitt 1993), and similar values have been observed in corn (Doehlert 1989) and tomato (Martinez-Barajas and Randall 1998). Studies performed by Doehlert et al. (1989) indicated that corn kernel GKs were inhibited by glycolytic intermediates other than G6P; 3 mM PEP and 1 mM G3P inhibited GK activity by 10 and 25% respectively.

Hexose sugars, other than fructose, competitively bind to HK and inhibit glucose phosphorylating activity. The different HK isoforms of potato and spinach were shown to have their activity inhibited by 50 and 70% with the addition of 10 mM mannose (Renz and Stitt 1993; Schnarrenberger 1990).

Classic HK inhibitors discovered working with animal and yeast HKs generally inhibit plant HKs as well. These inhibitors are generally amino sugars and hexose analogues, such as glucosamine, N-acetylglucosamine, 2-C-hydroxymethyl glucose (Salas *et al.* 1965) and mannoheptulose (Martinez-Barajas and Randall 1998).

Plant FKs are not as strongly inhibited by feedback inhibition as the HKs. Typically FKs are not inhibited by even high concentrations of G6P. However, many of the isoforms are weakly inhibited by F6P (Renz and Stitt 1993) (Martinez-Barajas *et al.* 1997). The inhibition by ADP is also significantly lower in FKs, the K_i value for ADP in tomato is 400 μ M (Martinez-Barajas *et al.* 1997) while inhibition of *Arabidopsis* FK is not detected until the concentration reaches 10 mM (Gonzali *et al.* 2001). Inhibition by glycolytic intermediates other than F6P has not been observed. An interesting characteristic of plant FKs is that they are typically inhibited by their own substrate fructose. In corn the K_i value for fructose was 1.42 and 4.1 mM respectively (Doehlert 1990), whereas values of 3-21 mM were observed in potato (Renz and Stitt 1993). These

values for the most part are below the physiologically occurring concentrations of the sugars, indicating very stringent control on fructose metabolism.

In biological systems metal cofactors are essential for optimal enzyme function, this is no different in regards to plant HKs, which require metal ions to chelate ATP. Like most kinases, HK utilizes Mg^{+2} (Mg-ATP) preferentially (Turner *et al.* 1977). However, other divalent cations can serve to chelate ATP to a lesser degree these include: Mn^{+2} , Co^{+2} and Ni^{+2} (Salas *et al.* 1965). Excess free Mg^{+2} can also strongly inhibit the function of all HKs. Generally Mg^{+2} concentrations greater than 10 times the ATP concentrations will severely inhibit the HK activity (Turner *et al.* 1977). As with some plant enzymes (e.g. pyruvate kinase), the presence of K^{+} serves as a crucial enzyme activator for HK. HK activity increases proportionately until the K^{+} concentration reaches 20-40 mM, at which point the optimal ion levels is reached. K^{+} becomes inhibitory to HK activity in concentrations greater than 100mM (Gonzali *et al.* 2001).

Unlike most plant enzymes, which are preferentially induced under anoxia, HK shows sensitivity to the reduced pH occurring under anoxia (Bouny and Saglio 1996). The pH during oxygen deficiency decreases rapidly in most plants, from 7.2-7.5 to 6.8 within as little as 20 minutes (Roberts *et al.* 1984a; Roberts *et al.* 1984b). In potato HK1, HK2, FK1 and FK2 all show a drop in sugar phosphorylating activity of approximately 50% from normoxic to anoxic pH levels (Renz and Stitt 1993). Similar findings were found in maize kernel HKs (Doehlert 1989), maize roots (Bouny and Saglio 1996) as well as in tomato (Martinez-Barajas and Randall 1998).

HK is strongly inhibited by two conditions that occur during anoxia: a decrease in the cytosolic pH, and a decrease in ATP/ADP ratio. This along with the fact that HKs

have been shown to be highly controlling in animal glycolytic systems, suggests that HK is a highly controlling enzyme in plant anoxic metabolism. This has been postulated in several publications (Doehlert 1989; Bouny and Saglio 1996; Fox *et al.* 1998; Ricard *et al.* 1998), however no detailed quantification of the control has been published.

2.8.3 Hexokinase in sugar sensing

Sugars serve not only as metabolic substrates and structure components, but have also been shown to be important regulatory components. Sugars serve in the regulation of gene expression, metabolic rate, cell cycle and development (Jang *et al.* 1997). HK has been associated with glucose sensing in mammalian, yeast and plant systems (reviewed by Koch *et al.* 2000; Rolland *et al.* 2001; Rolland *et al.* 2002). The predominant work with plants was conducted with transgenic *Arabidopsis* expressing a wide range of HK activities through use of sense and anti-sense transformations (Jang *et al.* 1997). *Arabidopsis* over-expressing HK showed a decrease in seedling growth and hypocotyl greening as compared to wild type and HK under-expressing plants. This decreased growth and inability to form proper leaves was also observed in tomato, with similar findings (Dai *et al.* 1999). The reduced growth of the transgenic plants was assumed to be the result of repression of many photosynthetic genes (Jang *et al.* 1997). The genes that were repressed by the HK glucose signal were: chlorophyll a/b binding protein, ribulose-1, 5-bisphosphate carboxylase and plastocyanin (Jang *et al.* 1997; Dai *et al.* 1999). Nitrate reductase on the other hand, was induced by the HK signal (Jang *et al.* 1997). The sugar signaling itself was independent of glycolysis since a similar repression was found using 2-deoxyglucose. 2-deoxyglucose binds HK and is phosphorylated efficiently, however, 2-

deoxyglucose 6-phosphate cannot be metabolized. A secondary set of evidence came from the use of *Arabidopsis* transformed with yeast HK. In this case the gene repression was not observed even with an over-production of glucose phosphorylating ability (Jang *et al.* 1997), proving that metabolite production is not the critical aspect of HK sugar signaling.

The exact mechanism of the HK sugar sensing is unknown although it is believed that signaling may be due to a conformational change of the plant HK when bound to glucose (Koch *et al.* 2000).

2.8.4 Hexokinase in sucrose biosynthesis

Reduced carbon from photosynthesis is transported to the cytoplasm as glucose and triose-phosphates (triose-P) (Schleucher *et al.* 1998). The transport of glucose accounts for as much as 75% of the reduced C transported to the cytosol (Schleucher *et al.* 1998). Both triose-P and glucose are used for sucrose biosynthesis. HK mediates the phosphorylation of glucose to G6P, required for the biosynthesis of sucrose (Veramendi *et al.* 1999). Use of *Arabidopsis* glucose transporter mutants revealed a 5-fold starch build up in the mature leaves following their light period (Trethewey and ap Rees T. 1994). It was hypothesized that the inability to transport glucose from the chloroplast resulted in feedback inhibition of the starch degradation pathways, and an excessively starchy phenotype (Trethewey and ap Rees T. 1994). In transgenic potato with reduced HK expression, increases in leaf starch levels were observed (Veramendi *et al.* 1999). Increased concentrations of glucose were present in the antisense HK potato leaves, resulting in feedback inhibition of glucose transporters and increased leaf starch

(Veramendi *et al.* 1999). These findings indicate that HK plays a key role in the production of sucrose from photosynthetically fixed carbon (Veramendi *et al.* 1999).

2.9 Plant transformations

2.9.1 Plant transformation techniques

The use of genetic engineering to introduce foreign genes into plant species has become a powerful tool for agricultural benefits and for detailed understanding of gene function. Agriculture has been revolutionized by the recent production of herbicide and pest resistant crops.

Genetic engineering is also a powerful tool to study the physiological function of genes. This is accomplished by altering the expression level of a single gene, by either increasing or decreasing the gene expression level. The effect of altering the protein level can be deduced by closely examining physiological characteristics in transgenic lines engineered.

Many techniques for inserting foreign DNA into plant systems have been developed including: *Agrobacterium*-mediated transformations, viral transformation, microinjection, electroporation, and particle bombardment (reviewed by Lessard *et al.* 2002 and Potrykus 1991).

Of all these transformation techniques, the most widely used method of plant transformation is the use of *Agrobacterium* (reviewed in Hooykaas 1989 and de la Riva *et al.* 1998). *Agrobacterium* is a soil bacterium that utilizes plants to produce its food source opines. *Agrobacteria* are attracted to a plant wound signal, arising generally from insect predation or direct physical wounding. During *Agrobacterium* infection, part of an

endogenous Ti-plasmid is inserted into the plant's genome. This transferred DNA (T-DNA) encodes genes for opine production and oncogenic genes responsible for tumour (*A. tumefaciens*) or root (*A. rhizogenes*) production (de la Riva *et al.* 1998). Opines are produced by condensation between amino acids and carbohydrates or organic acids. They are synthesized within the transformed plant tissue (callus or roots) and used by the *Agrobacterium* as a carbon and nitrogen source (de la Riva *et al.* 1998). The genes from the T-DNA encoding for opine synthesis can be replaced with foreign DNA, through use of a binary vector, and used to insert these novel genes into plants. One of the early limitations of *Agrobacteria* transformations was the inability to insert DNA into cereal crops, in recent years however more virulent strains of *Agrobacteria* have been developed that can transform most agriculturally important crops (Hernalsteens *et al.* 1984; Schafer *et al.* 1987; Hiei *et al.* 1994; Hansen 2000).

The most commonly used *Agrobacterium* system is that of *A. tumefaciens* (reviewed by Hooykaas 1989 and de la Riva *et al.* 1998). *A. tumefaciens* inserts the T-DNA into the plant cells, which then form callus tissue. Calli are non-differentiated plant cells, which can be used to regenerate whole plants using various hormone treatment for shoot and root formation (de la Riva *et al.* 1998). Each callus generated by *A. tumefaciens*, is the result of multiple transformations, therefore plant regeneration must be conducted on media containing a selectable element (generally a herbicide or antibiotic) (Lessard *et al.* 2002).

An alternative transformation system is that of *A. rhizogenes*, which transfers foreign DNA into plants as efficiently as *A. tumefaciens* does (Chilton *et al.* 1982 reviewed by Giri and Narasu 2000 and Shanks and Morgan 1999). *A. rhizogenes* has the

advantage of producing hairy roots instead of calli. Each root produced arises from a single transformation event, resulting in clonal material. The ability to grow on media absent of exogenous hormones is a reliable method to screen for successful transformations. These hairy roots are physiologically similar to normal roots, however they tend to have a “highly branching” phenotype and demonstrate plagiotrophism (lateral growth) (Shanks and Morgan 1999). This allows for rapid production of material. Unlike callus the roots can be characterized directly for the presence of the transgene. If whole plants are required the roots can be used to regenerate whole plants, using various treatments with exogenous hormones (Giri and Narasu 2000).

2.9.2 Technologies used to modify gene expression in plants

2.9.2.1 Increasing gene expression

The production of plant lines over-expressing a particular gene is relatively simple. The DNA encoding for the desired protein is placed in a plant expression vector in the sense orientation under the control of a promoter. The choice of promoter can vary depending on the particular application. Constitutive promoters are most commonly used for continuous gene expression; inducible promoters offer an inducible response expression of the gene and tissue specific promoters for gene product isolated to a particular tissue (reviewed by Lessard *et al.* 2002). The most common promoter used in plant transformations is the cauliflower mosaic virus 35S (CAMV 35S) promoter (Benfey *et al.* 1990). The CAMV 35S promoter is very well characterized and has relatively high gene expression. A wide range of gene over-expression can be produced using a sense construct under the control of a CAMV 35S promoter, depending on the location of DNA

integration in the plant genome. For example in potato transformed using the sense construct of HK1 under the control of CAMV 35S resulted in a 5-fold increase in HK activity in leaves and a 2-fold increase in tubers (Veramendi *et al.* 1999).

2.9.2.2 Decreasing gene expression

Gene silencing was discovered inadvertently in transformed organisms containing a non-homologous copy of foreign gene. These genes were silenced pre-transcriptionally by DNA-DNA or DNA-RNA interactions, which induced a *de novo* methylation of the transgene (Matzke and Matzke 1995). Gene silencing was initially viewed as an annoyance, since it made the production of stable transgenic lines more difficult. It did, however, reveal a powerful tool for scientists by allowing them to develop new techniques for decreasing the translation of endogenous genes. In plant biotechnology there are three genetic mechanisms available to reduce the levels of endogenous proteins: co-suppression, anti-sense RNA and RNA interference (RNAi).

Gene silencing by co-suppression involves inactivation of an endogenous gene, through use of a transgene in the sense orientation (Napoli *et al.* 1990; van der Krol *et al.* 1990a). This mechanism of gene silencing was also discovered accidentally while attempting to overproduce pigment producing genes in petunia, only to find that the transgenes along with the endogenous genes were inactivated (Napoli *et al.* 1990). Co-suppression was thought to occur only in plants but it has since been observed in fungi (Cogoni and Macino 1999; van West *et al.* 1999), *Drosophila* (Pal-Bhadra *et al.* 1999), *Paramecium* (Ruiz *et al.* 1998) and mice (Bahramian and Zarbl 1999). The exact

mechanism for gene silencing is unknown, however, it is thought that multiple gene copies may lead to DNA methylation and silencing (Kooter *et al.* 1999).

Recently it was discovered in *Caenorhabditis elegans* that injecting a small length double stranded RNA (dsRNA) of 21-25 nucleotides in length dramatically silences genes containing that sequence (Fire *et al.* 1998). This process known as RNAi has been shown to be effective in degrading and silencing mRNA in a variety of organisms (reviewed by Fire 1999; Boshier and Labouesse 2000). Stable gene silencing has been accomplished by producing constructs encoding mRNA that form “hairpin” loops of 21-25 nucleotides long (Chuang and Meyerowitz 2000). However, the exact mechanism of RNAi gene silencing is unknown.

The most common strategy of gene silencing used is that of anti-sense constructs. Constitutively expressed genes in anti-sense orientation are transcribed, hybridizing to the complementary sense mRNA strand. The dsRNA duplex can no longer be translated and is degraded by RNase, therefore being reduced. The plant cells degrade the dsRNA complexes. The degradation is thought to be part of the plant cells host viral defense mechanism (Wassenegger and Pelissier 1998).

Anti-sense gene silencing occurs naturally in bacteria, animal and plant systems. Initial anti-sense gene reduction experiments were conducted on mice (Izant and Weintraub 1984). Subsequent experiments showed that previously inserted sense genes could be silenced in plants, using this technique (Rothstein *et al.* 1987). The degree of gene expression reduction was dependent on the antisense: sense RNA ratio the higher this ratio the greater the suppression. RNA stability and the secondary structure of the RNA also influence the degree of suppression, this is often reliant on the type and size of

construct used (van der Krol *et al.* 1990b). Using various lengths of anti-sense sequences can increase the odds of successful gene silencing (van der Krol *et al.* 1990b). The similarity required for gene reduction varies, however the higher the sequence similarity the greater the reduction (van der Krol *et al.* 1988a). In transgenic potato tubers use of antisense HK1 gene resulted in nearly complete silencing of HK1 and approximately 50% reduction of HK2, which shares approximately 85% similarity with HK1 (Veramendi *et al.* 1999).

Using an anti-sense DNA construct under the control of a CAMV 35S promoter can potentially produce potato root lines displaying a range of reduced gene and protein expression. This technique of gene suppression has been successful in reducing HK activity in potato using a single antisense construct (Veramendi *et al.* 1999).

Using the MCA approach on HK, a greater understanding of the regulation of plant primary metabolism can be achieved. In this thesis, this will be accomplished by using genetic engineering to produce potato roots, which have altered levels of HK. Then by comparing the rate of glycolytic flux under anoxia to the extractable HK activity, we can determine the FCC of HK, an important parameter of its *in vivo* function.

3.0 MATERIALS AND METHODS

3.1 Chemicals

All chemicals used were purchased from either Sigma Chemical Co. or Fisher Scientific Inc. unless otherwise stated and were of analytical grade or higher.

3.2 Biological material

3.2.1 Plant material

Mature *Solanum tuberosum* tubers (cv. Russet Burbank) were planted in standard potting soil (2 parts loam: 1 part sand: 1 part peat: 1 part vermiculite) placed over a ~4cm layer of packed peat. Potatoes were allowed to grow in growth chambers at 23 °C with 12 hour light periods for 2 weeks without watering. Weekly watering was performed following plant emergence using a watering solution containing 0.2 g of 20:20:20 fertilizer/l. Plants were grown for up to 8 weeks and used as the primary material for transformations.

3.2.2 Root cultures

Potato root cultures were grown and maintained on MS based media (Murashige and Skoog 1962) supplemented with 0.5 mg/l thiamine-HCl, 150 mg/l L-asparagine and 30 g/l sucrose adjusted to pH 5.7 with KOH prior to autoclaving. Solid MS media in petri plates (2.5 g/l phytagel) were used to maintain the root cultures; these plates were produced by transferring several root tips (20-30) to fresh plates every 3 weeks. Liquid

MS root cultures of 50 and 100 ml were produced by inoculation of the media with 20-30 root tips from plates and maintained in 250 and 500 ml flasks respectively agitated continually using a gyratory shaker at 150 rpm. Root material was harvested from liquid cultures after 2 to 3 weeks, the fresh material being flash frozen using liquid N₂ and stored at -80 °C until needed. Roots from solid media were used for initial screening of transgenic lines, while roots from liquid cultures were used for activity measurements.

3.2.3 *Escherichia coli* stocks and cultures

Competent *E. coli* cell lines of DH5 α (supE44 Δ lacU169 ϕ 80 lacZ Δ M15 *hsd*R17 *rec*A1 'endA1 *gyr*A96 thi-1 *rel*A1), HB101 (*hsd*20 (*r*_B⁻, *m*_B⁻), *rec*A13, *rps*L20 (streptomycin^R), *leu*, *pro*A2), and BL21 (DE3)(*E. coli* B, F⁻, *dcm*, *ompT*, *hsd*S (*r*_B⁻*m*_B⁻), *gal* λ (DE3)) were generously prepared and donated by Dr. Sonia Dorion (Université Laval).

E. coli was grown at 37 °C on Luria-Bertani (LB) media (10 g/l bacto tryptone (Difco), 5 g/l yeast extract (Difco) and 5 g/l NaCl pH adjusted to 7.5 with NaOH prior to autoclaving). Solid media was produced on petri plates by addition of 15 g/l bacto agar. Liquid media cultures required high-speed agitation (250 rpm) on a gyratory shaker.

3.2.4 *Agrobacterium rhizogenes* stocks and cultures

Agrobacteria rhizogenes strain A4 was generously donated by Dr. D. Tepfer (INRA, Versailles, France). *A. rhizogenes* was grown at 28 °C on mannitol yeast ammonium (MYA) media (containing 5 g/l yeast extract, 0.5 g/l casaminoacids, 8 g/l mannitol, 2 g/l (NH₄)₂SO₄ and 5 g/l NaCl pH adjusted to 6.6 prior to autoclaving with

NaOH) plates (15 g/l bacto agar) and liquid agitated at 200 rpm with a gyratory shaker. A4 stocks were maintained over long periods in 25% (v/v) glycerol stocks, which were flash frozen in liquid N₂ and store at -80 °C.

3.3 Cloning vectors

3.3.1 pBK-CMV Phagemid

The phagemid vector pBK-CMV (Stratagene) is derived from ZAP express lambda vector (Stratagene). It contains a kanamycin resistance gene and *ColE1* origin of replication for selection and rapid amplification in *E. coli*. The multiple cloning site contains 17 unique restriction sites. The vector contains the *lac* promoter for prokaryotic expression as well as the CMV 35S promoter for eukaryotic expression. The *f1* origin of replication also allows for production and packaging of single-stranded DNA (ssDNA) from either the sense or anti-sense strand in the presence of the *f1* phage.

3.3.2 pProEX HTa

The pProEX HTa (Invitrogen) vector was designed for expression of foreign proteins within *E. coli*. The foreign protein is under the control of a *trc* inducible promoter enabling control over gene and protein production. The vector adds a 6-His sequence to the foreign protein for rapid purification of the protein on a Ni-affinity resin. A 7 amino acid spacer peptide containing a rTEV protease site is added for removal of the 6-His tag. The plasmid contains an ampicillin resistance gene and a pBR322 origin of replication. The *f1* origin of replication also allows for production and packaging of ssDNA from either the sense or anti-sense strand in the presence of the *f1* phage.

3.3.3 pGA643

The binary vector pGA643 was designed to transfer foreign DNA into a plant system within *Agrobacterium* with the aid of a helper plasmid (Ri plasmid in *A. rhizogenes*). Both *Agrobacterium* and *E. coli* origins of replication are present in pGA643. Tetracycline (2 mg/l in *E. coli* and 5 mg/l in *A. rhizogenes*) and kanamycin (10 mg/l *E. coli* and 25 mg/l in *A. rhizogenes*) resistance genes provide selectable markers for bacteria. The multiple cloning site contains 9 restriction sites. A cauliflower mosaic virus (CAMV) 35S promoter allows for constitutive gene expression within plants.

3.4 Plasmid amplification, purification and ligation

3.4.1 Competent *E. coli* transformations

Standard *E. coli* transformation involved incubating 100 ng of plasmid with 90 μ l of competent *E. coli* and 10 μ l of 10X TCM buffer (containing final concentration 10 mM Tris (hydroxymethyl) aminomethane (Tris)-HCl pH 7.5, 10 mM CaCl_2 and 10 mM MgCl_2) in a 1.5 ml Eppendorf tube on ice for 30 min. Following the incubation the transformation mixture containing the competent cells was heat shocked at 42 °C for precisely 2 min in a water bath. Immediately after heat shock 1 ml of aerated 37 °C LB media was added to the transformation mixture, followed by a 1 hour incubation at 37 °C. After incubation the cells were precipitated by centrifugation for 30 s, then resuspended in 100 μ l of LB. The resuspended cells were then plated onto LB plates containing the appropriate antibiotic concentrations for the plasmid used. Transformed *E. coli* colonies

were stored as 25% (v/v) glycerol stocks, which were flash frozen in liquid N₂ and stored at -80 °C.

3.4.2 *Agrobacterium rhizogenes* competent cell preparation and transformation

A. rhizogenes were transformed using a modification of the transformation protocol of An *et al.* (1988). A preculture was started using 5 ml of MYA inoculated from a glycerol A4 stock stored at -80 °C and grown for 30 hours with vigorous shaking. A culture of 50 ml of fresh MYA was inoculated with the preculture and allowed to grow until an OD₆₀₀ of 0.5-1 was achieved (10-12 hours). Cells were placed on ice to halt growth after appropriate OD₆₀₀ was reached, and then precipitated by clinical centrifugation (~1000g) for 7 min at room temperature. The supernatant was removed and the pellet was resuspended in 1 ml of sterile ice cold 20 mM CaCl₂. An aliquot of 100 µl of the resuspended cells were placed into chilled sterile Falcon tubes (Simport model # T406-2A) containing approximately 1 µg of the appropriate pGA643 plasmid. The cells with the DNA were flash frozen in liquid N₂ and left frozen for a minimum of 5 min. The tubes were then place in a 37 °C water bath for precisely 5 min to heat shock the cells. To the heat shocked cells, 1 ml of fresh MYA was added, followed by a 4 hour incubation at 28 °C with gentle agitation (~100 rpm) to allow for the expression of the antibiotic resistance genes. Following incubation the cells were precipitated by a 1-min centrifugation at 12 500g and the pellets resuspended in 100 µl of fresh MYA. The 100 µl of cell suspension was then plated onto solid MYA media containing 25 mg/l kanamycin sulfate (Invitrogen) and 5 mg/l tetracycline. The plates

were incubated and the positive transformants emerged within 5-7 days. Transformed *A. rhizogenes* were stored as glycerol stocks, methods described previously.

3.4.3 Rapid plasmid preparation from *E. coli*

Plasmids for diagnostic restriction analysis were prepared using a rapid alkaline lysis “mini-prep” protocol. All steps in this protocol were performed at room temperature unless otherwise stated, and all centrifugations were done using a microcentrifuge at 12 500g. Liquid *E. coli* cultures of 2 ml were grown for 16-20 hours and centrifuged for 1 min in order to harvest the cells. The cells were resuspended in 100 µl of cold sterile buffer I (25 mM Tris-HCl pH 8.0, 1 mM EDTA and 1% (w/v) glucose) by vortexing for 30 s. To the resuspended cells, 200 µl of buffer II (0.2 M NaOH and 1 % (w/v) sodium dodecyl sulfate (SDS)) was added and mixed by inverting the tube 5-7 times. To the sample, 150 µl of cold buffer III (3M KCH₃COO and 1.8 M CH₃COOH) was then added followed by vortexing for 30 s, the samples were then incubated on ice for 15 min. To the mixture, 450 µl of cold PCI (50:48:2 % (v/v) phenol: chloroform: isoamyl alcohol and 0.1 % (w/v) hydroxyquinoline) was added and was vortexed for 30 s followed by centrifugation for 15 min. The samples were separated into 2 phases, and the aqueous phase containing the plasmid DNA was carefully removed and placed into a new sterile Eppendorf tube. To the aqueous phase, 450 µl of isopropanol was then added and was mixed by vortexing for 30 s, followed by a 15 min centrifugation. The supernatants were carefully removed and 450 µl of ice cold 80 % (v/v) ethanol was added to the DNA containing pellet and centrifuged for 15 min. The ethanol was removed from the plasmid DNA pellets and were left to dry (30-60 min) at which time they were resuspended in 20

μl of 10 mM Tris-HCl pH 8.5 and stored at -20 °C until needed. These DNA preparations were used for confirmation of successful transformations, for the presence and correct orientation of inserts and for *A. rhizogenes* transformations.

3.4.4 Highly purified plasmids from *E. coli*

3.4.4.1 High copy plasmids (SV2-G3)

Highly purified plasmids were prepared using the Qiagen Midi-prep system with a modified protocol for high and low copy plasmids. For high copy plasmid (SV2-G3) preparations 5 ml of LB (Kanamycin 50 mg/l and ampicillin monosodium 100mg/l) was inoculated with *E. coli* cells containing the desired plasmid and grown for 16 hours with vigorous shaking. Five hundred μl of the grown culture was used to inoculate 50 ml of fresh LB media, and the culture was allowed to grow for an additional 16 hours. Cells were harvested by centrifugation at 6000g at 4 °C for 15 min. The cells were resuspended in 4 ml of buffer P1 (containing 50 mM Tris-HCl pH 8.0, 10 mM EDTA and 100 mg/l RNase A) by vortexing. Four ml of buffer P2 (containing 200 mM NaOH and 1% (w/v) SDS) was then added to lyse the cells, which were mixed gently by inverting the tube 5 or 6 times. Four ml of the cold buffer P3 (3.0 M KCH₃COO pH 5.5) was quickly added to neutralize the lysed cells, and mixed by inverting tube and incubating on ice for 15 min. Following the incubation the mixture was centrifuged twice at 20 000g at 4 °C for 30 min removing the supernatant containing the plasmid DNA. The supernatant was then loaded onto a QIAGEN-tip 100 column, which had been previously equilibrated with 4 ml of buffer QBT (containing 750 mM NaCl, 50 mM morpholinopropane sulfonic acid (MOPS) pH 7.0, 15% (v/v) isopropanol and 0.15% (v/v) Triton X-100), using gravity

flow. The column was washed twice with 10 ml of buffer QC (containing 1.0 M NaCl, 50 mM MOPS pH 7.0 and 15% (v/v) isopropanol). The DNA was eluted from the column by loading 5 ml of buffer QF (containing 1.25 M NaCl, 50 mM Tris-HCl pH 8.5 and 15% (v/v) isopropanol) onto the column. The eluted DNA was precipitated by adding 3.5 ml of isopropanol to the sample and centrifuging at 15 000 g at 4 °C for 30 min. The isopropanol was discarded and the DNA pellet washed with 2 ml of 70% (v/v) ethanol, which was further centrifuged at 15 000g for 10 min. The ethanol was discarded and the DNA pellet allowed to air dry. It was then resuspended in 200 µl of 10 mM Tris-HCl pH 8.5. The DNA was further purified, since this Midi-prep protocol consistently had high levels of protein, by PCI extraction and sodium acetate (NaCH₃COO) precipitation. To do this, 200 µl of cold PCI was added to the resuspended plasmid, which was mixed by vortexing for 30 s and centrifuged for 15 min at 12 500g. The aqueous phase was transferred to a new Eppendorf tube and subjected to a second PCI extraction. To the DNA, 20 µl of 3 M NaCH₃COO pH 5.2 was added, which was mixed by vortexing. To the mixture, 450 µl of absolute ethanol was added, which was mixed and incubated at – 20 °C for 12-16 hours. The sample was then centrifuged at 12 500 g for 15 min to precipitate the DNA. The ethanol was discarded and the pellet washed with 1 ml of 80% (v/v) ethanol, followed by centrifugation of 1 min. The supernatant was discarded, and the pellet air-dried and then resuspended in 200 µl of 10 mM Tris-HCl pH 8.5. The OD₂₆₀: OD₂₈₀ was measured to evaluate purity of DNA, ratios >1.7 was acceptable.

3.4.4.2 Low copy plasmids (pGA643)

The protocol used for purification of low copy number plasmids was similar to that of high copy stated above with several exceptions. The culture volume used was 1 litre of LB media (kanamycin 10 mg/l and tetracycline 2 mg/l). The harvested cells were resuspended in 20 ml of buffer P1, lysed with 20 ml of buffer P2 and neutralized with 20 ml of buffer P3. After the second centrifugation step to remove cellular debris, 42 ml of isopropanol was added to the supernatant and incubated at -20°C for 30 min. Following the incubation the sample was centrifuged at 15 000g at 4°C for 30 min to precipitate the DNA. The pellet was then resuspended in 500 μl of TE buffer (containing 10 mM Tris-HCl pH 8.0 and 1 mM EDTA), and brought to a final volume of 5 ml by adding buffer QBT. The sample was then processed as per high copy plasmids.

3.4.5 Small scale plasmid purification of pGA643 from *A. rhizogenes*

Agrobacterium plasmid purification was modified from the protocol described in An *et al.* (1988). For this protocol all centrifugation took place using a microcentrifuge at 12 500g at room temperature. A culture of MYA (1 ml containing 25 mg/l kanamycin and 5 mg/l tetracycline) was inoculated with a single *A. rhizogenes* colony and grown for 16 hours. The cells were transferred to a 1.5 ml Eppendorf tube, precipitated by centrifugation for 30 s, and resuspended by vortexing for 30 s in 100 μl of cold sterile buffer I (containing 25 mM Tris-HCl pH 8.0, 50 mM glucose and 10 mM EDTA). The cellular suspension was incubated at room temperature for 10 min. Following incubation 200 μl of fresh buffer II (containing 200 mM NaOH and 1% (w/v) SDS) was added to

lyse the cells, followed by inverting the tube 6 times and allowed to incubate at room temperature for an additional 10 min. To the lysed cells, 30 μ l of phenol equilibrated with 60 μ l of buffer II was added, followed by vortexing for 15 s. One hundred and fifty μ l of 3 M NaCH_3COO pH 4.8 was added to the tube to neutralize the sample, which was mixed by inverting 10 times then allowed to incubate at -20°C for 15 min. The sample was then centrifuged for 5 min, and the resulting supernatant transferred to a new tube. To the tube 1 ml of ice cold 95% (v/v) ethanol was added and mixed by vortexing for 10 s and incubated at -80°C for 15 min. The DNA was precipitated by centrifugation for 5 min and resuspended in 500 μ l of sterile 0.3 M NaCH_3COO pH 7.0. To the tube, 1 ml of cold 95% (v/v) ethanol was added, and mixed by inverting 10 times and incubated at -80°C for 15 min. The DNA was precipitated by centrifugation for 15 min and the supernatant was carefully discarded. The pellet was washed with 1 ml of cold 70% (v/v) ethanol, vortexed for 30 s and centrifuged for 3 min. The ethanol was discarded and the pellet air dried, then resuspended in 30 μ l of TE and stored at -20°C until needed. These DNA preparations were used to confirm the successful transformation of *A. rhizogenes* with pGA643, the presence of the correct insert (size and orientation).

3.4.6 Restriction analysis

All restriction endonucleases were purchased from Invitrogen. Restriction digests were performed using an estimated 5 units of enzyme per μg of DNA, the reactions proceeding for 1 hour at 37°C unless otherwise specified. The addition of 5 units of ribonuclease A was required for rapidly purified plasmids. The supplied reaction buffers were used for single digests, but when multiple enzymes were used together the reaction

buffer with the best performance for all the enzymes was used (complete list available at http://www.invitrogen.com/Content/TechOnline/molecular_biology/manuals_pps/react.pdf).

3.4.7 Agarose gel electrophoresis

DNA samples were mixed with 6X loading buffer (0.25% (w/v) bromophenol blue and 40% (w/v) sucrose in H₂O), and were loaded onto the appropriate gel. Tris-Borate EDTA (TBE) gels containing 1% or 0.7% (w/v) agarose (Invitrogen) and 0.5 µg/ml ethidium bromide in TBE buffer (working solution 89 mM Tris base, 89 mM boric acid and 2 mM EDTA) were used for diagnostic analysis. The molecular markers λ DNA/*Hind*III fragments and/or 1 Kb Plus DNA ladder (Invitrogen) were used in every agarose gel. These gels were run using a Kodak Biomax QS710 or MP1015 electrophoresis tanks with TBE buffer at 80 or 120 volts respectively until adequate band separation was achieved (45 min- 90 min respectively). Ethidium bromide intercalates DNA, and in this state fluoresces when illuminated by ultraviolet (UV) light. For analytical purposes, DNA was visualized by illuminating the gel with short wave (260 nm) UV light using a Geldoc transilluminator. For preparative electrophoresis Tris-acetate EDTA (TAE) gels containing 1% (w/v) agarose and 0.5 µg/ml ethidium bromide in TAE buffer (working solution 40 mM Tris-acetate and 1 mM EDTA) were used.

3.4.8 DNA fragment purification

3.4.8.1 Gel purification of DNA fragments

Insert DNA required for construct ligation were purified from agarose gels using the QIAEX II (Qiagen) gel extraction system (http://www.qiagen.com/literature/handbooks/qexII/1011033_qiaexII.pdf). All steps were carried out at room temperature unless otherwise stated. All centrifugation was done using a microcentrifuge at 12 500g. The DNA bands were carefully cut out of the gel with a minimal amount of excess agarose (approximately 300 mg for the width of 4 wells), and placed in a sterile 1.5 ml Eppendorf tube. The agarose was dissolved by adding 3 volumes (900 µl) of the supplied buffer QX1 and the DNA fragment was bound through the addition of 30 µl of the supplied QIAEX II beads. The mixture was incubated in a 50 °C water bath for 10 min, vortexing for 5 s every 2 min. The sample was then centrifuged for 30 s and the supernatant was discarded. The pellet was washed and resuspended in 500 µl of QX1 by vortexing and centrifuging for 30 s 3 times, each time discarding the supernatant. The pellet was then washed and resuspended in 500 µl of the supplied buffer PE by vortexing and centrifuging for 30 s an additional 3 times, discarding the supernatants. Following the washes the DNA was eluted from the pellet by resuspending it in 30 µl of 10 mM Tris-HCl pH 8.5 by vortexing, then centrifuging for 30 s with the supernatant containing the DNA being collected. The elution was repeated, pooling the supernatants and storing them at -20 °C until needed. DNA was quantified visually by comparing the ethidium bromide florescence intensity of the purified fragment with the 1 650 bp fragment from the 1 KB+ molecular ladder, with standard loads of 10-80 ng.

3.4.8.2 HPLC purification of DNA fragments

The vector fragments for the constructs were isolated from digested plasmids by HPLC using a Waters Gen-Pak FAX column (4.6 mm X 100 mm) with a Waters Alliance 2690 separations module. The chromatography was performed using a 2 eluent buffer system. Buffer A consisted of 25 mM Tris-HCl pH 8.0 and 1 mM EDTA, while buffer B consisted of 25 mM Tris-HCl pH 8.0, 1 mM EDTA and 1 M NaCl. 10 µg of digested DNA was run at 37 °C at 0.75 ml/min with a linear gradient from 30 % buffer B to 100% buffer B over 40 min. After the gradient the column was washed with 5 ml of 0.04 M H₃PO₄. Peaks were detected using a Waters 996 photodiode array detector at 260 nm. Fractions were collected using a Waters fraction collector II in time mode set to collect each fraction in 30 s samples.

After chromatography the fragment sizes were confirmed by agarose gel electrophoresis. Following the gel, the fractions containing the appropriate fragment were pooled and precipitated by adding 3 volumes of 95% (v/v) ethanol/ 0.12 M NaCH₃COO and incubating at -20 °C overnight. The DNA was then precipitated by centrifugation for 15 min at 12 500g, the supernatant was decanted and the pellet washed by vortexing with 1 ml of 70% (v/v) ethanol before being centrifuged for 5 min. The ethanol was discarded, the pellet air-dried and resuspended in 50 µl of 10 mM Tris-HCl pH 8.5 and stored at -20 °C until needed. DNA was quantified as per the gel extraction protocol.

3.4.9 DNA fragment ligation

Ligation reactions were performed using T4 DNA Ligase (Invitrogen). All ligations were performed with 3 ratios of insert to vector: 3:1, 6:1 and 9:1 (10-30 fmoles of vector: 30-280 fmoles insert) in a total volume of 20 μ l. Double cohesive end ligations were incubated at room temperature for 1 hour using the following reaction mixture; 4 μ l of 5X reaction buffer (containing final concentrations 50 mM Tris-HCl, 10 mM MgCl₂, 1 mM ATP, 1 mM dithiothreitol (DTT) and 5% (w/v) polyethylene glycol-8000), 1 U of T4 ligase, and appropriate insert to vector ratio, with the total volume brought to 20 μ l with sterile H₂O. All ligations with blunt ends were incubated at 14 °C for 24 hours using 5 U of T4 ligase. Following the incubation the ligation mixture was used to transform competent *E. coli* cells.

3.5 Hexokinase cDNA sequencing

The plasmid SV2-G3 was obtained from Dr. Daniel Matton (University of Montréal). SV2-G3 contained a full length cDNA clone of *Solanum chacoense* HK, within the phagemid vector pBK-CMV. SV2-G3 was transformed into HB101 cells, amplified from a 50 ml culture and purified using Qiagen Midi-prep system. Five μ g of purified SV2-G3 was sequenced by Dr. Ingeberg Roewer (National Research Council of Canada), using the Big Dye Terminator 2.0 kit based on the Sanger method (Sanger *et al.* 1977). Fluorescently labelled reaction products were analyzed on a 377 DNA sequencer (ABI) using T3 and T7 primers.

3.6 Recombinant hexokinase immunoblotting

3.6.1 SDS-PAGE and membrane electro-transfer

Clarified protein extracts were denatured by boiling in SDS sample buffer for 15 min (SDS buffer contains final concentration of 60 mM Tris-HCl pH 6.8, 10% (v/v) glycerol, 1% (w/v) SDS, 0.1M DTT, 0.002 % (w/v) bromophenol blue). SDS-polyacrylimide gel electrophoresis was performed according to Laemmli (1970) (Laemmli 1970) at room temperature using a 4 % (w/v) acrylamide (Invitrogen): 0.107% bis-acrylamide stacking and 12 %: 0.32 % (w/v) separating gel. Gels were run to completion (approximately 80 min) in SDS-PAGE buffer (25 mM Tris, 190 mM glycine and 0.1% (w/v) SDS) at 120 volts. All gels were run with Bio-Rad SDS-PAGE low range molecular weight standards. Following electrophoresis the gels were either stained directly using Coomassie Blue or they were electro-transferred onto polyvinylidene (PVDF) membranes for immunodetection.

Gels were stained with Coomassie Blue stain (containing 0.1% (w/v) Coomassie Brilliant Blue R250, 50% (v/v) methanol and 10% (v/v) glacial acetic acid) for approximately 30 min. Destaining was done by washing the gel 3 or 4 times with destain (containing 25% (v/v) methanol and 10 % (v/v) glacial acetic acid) for 20 min. Following destaining the gels were dried between 2 sheets of cellophane for 2 hours under vacuum at 80 °C using a gel drier (BioRad, model #583).

Electro-transfer was performed by transferring the separated proteins to a 45 µm pore PVDF membrane in ice-cold TGM transfer buffer (25 mM Tris, 190 mM glycine and 20% (v/v) methanol) using a Bio-Rad (Mini Trans-Blot cell) transfer apparatus at

100 volts for 60 min. The blots were stained for 1-2 min in Ponceau S (1% (w/v) in 1% (v/v) acetic acid) then washed with H₂O to verify protein transfer.

3.6.2 Estimation of protein concentration and molecular weight

Quantification of protein concentrations was conducted by visually comparing the Coomassie Blue staining intensity of the protein band to the 45 kDa standard (ovalalbumin) in the BioRad low molecular weight standards, of which 0.5 µg was loaded per SDS-PAGE.

Estimation of MW was based on the relative mobility (R_f). The MW standards were used to generate a standard equation plotting the R_f of the protein = distance migrated by the protein/ distance migrated by the protein front against the \ln of the MW of the protein. Equations were produced from these lines, and the MW of the samples was determined.

3.6.3 Recombinant hexokinase expression vector

The prokaryotic expression system pProEX HT (Invitrogen) was used since it has a removable 6-histidine peptide sequence. This 6-His tag allows for pH dependent binding to the supplied Ni purification resin, which allowed us to rapidly purify the recombinant protein.

The general strategy used for the construction of the recombinant HK expression vector is outlined in Figure 3. SV2-G3 was digested to completion with *Xho*I, followed by partial *Eco*RI digestion (1 min 37 °C, reaction halted through addition of 2.5 volumes of PCI). These digestions produced DNA fragments of 1618,

923 and 695 bp in length. The 1.6 Kb fragment was isolated by gel extraction. The isolated fragment was ligated into pProEX HTa prepared by digestion with *Eco*RI, *Xho*I and purified by HPLC. The ligation reaction proceeded using cohesive end ligation protocol. The ligated plasmid was used to transform competent DH5 α *E. coli* cells (Figure 3). The successfully transformed cells formed colonies on LB plates (50 mg/l kanamycin and 100 mg/l ampicillin) after 16 hours. Diagnostic restriction analysis was performed on the rapidly purified plasmids using *Eco*RI and *Xho*I to confirm insert was successfully integrated.

3.6.4 Recombinant protein induction and purification

Recombinant protein was obtained using a modified version of the protocol supplied with the pProEX HT system. This involved inoculating 500 ml of LB broth containing (100 mg/l ampicillin and 50 mg/l kanamycin) with an isolated colony containing the pProEX-HK plasmid. The culture was grown until an OD₆₀₀ of 0.6 was obtained. Isopropyl-beta-D-thiogalactopyranoside (IPTG) (0.6mM final concentration) was added to the culture to induce the prokaryotic *trc* promoter, and the culture was allowed to grow for an additional 5 hours. All subsequent procedures were performed at 4 °C unless otherwise stated. The cells were harvested by centrifugation at 10 000g for 10 min and resuspended in 40 ml of lysis buffer (containing 50 mM Tris-HCl, pH 8.5, 5 mM DTT, 1 mM phenylmethylsulfonyl fluoride (PMSF), 1 mM benzamidine, 1 mM ϵ - amino n-caproic acid (ϵ -CA), and 0.1% (v/v) triton X-100). The cells were lysed by passing them twice through a French press at 18 000 psi. The recombinant protein

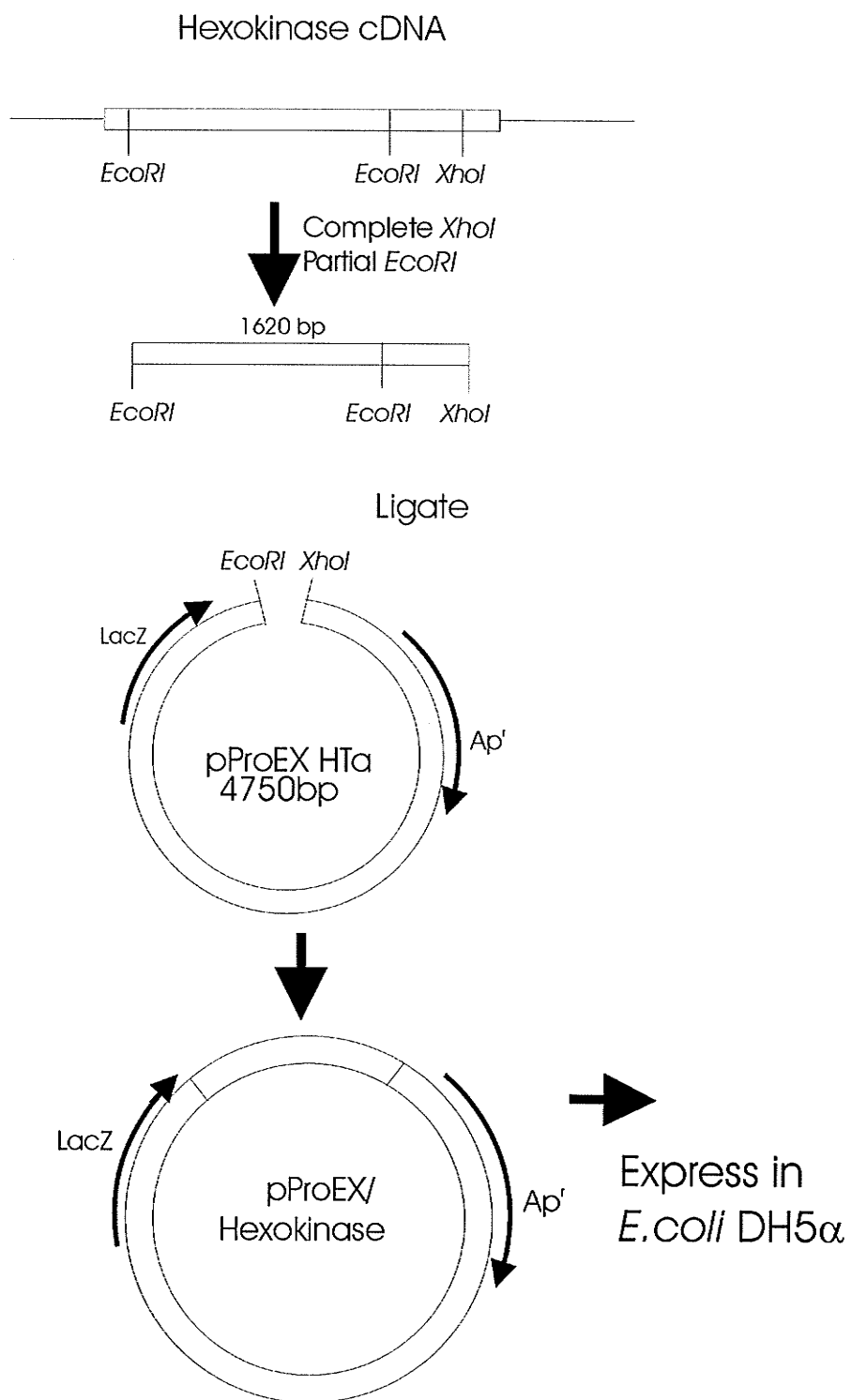


Figure 3. Production of *E. coli* HK expression vector. SV2-G3 was digested completely with *XhoI* and partially with *EcoRI* to produce a 1620 bp insert. The insert was ligated into *EcoRI/XhoI* digested proEX HTa and transformed in DH5 α cells.

along with the cellular debris was precipitated by centrifugation at 10 000g for 25 min, and the supernatant was removed. Purification buffers B, C, D, and E all contained 6M urea, 0.1 M NaH_2PO_4 , and 10 mM Tris-HCl at the given pH. The pellet was resuspended in buffer B (pH 8) by vigorous shaking (200 rpm) for 1 hour. Cellular debris were removed by centrifugation at 10 000g for 15 min. The clarified sample was incubated for 1 hour with 1 ml of Ni affinity resin (settled volume), and then loaded onto the supplied column (10 mm X 50 mm). The column was washed with 4 volumes of buffer B, followed by 2 volumes of buffer C (pH 6.3). The recombinant protein was then eluted from the column with 2 ml of buffer D (pH 5.9) and 2 ml buffer E pH (4.5) in 1 ml fractions. The eluted protein was visualized by SDS-PAGE. Fractions containing the recombinant HK were pooled (4 ml total volume), and their pH was raised by addition of 1 ml 1 M Tris-HCl pH 8.5. The protein sample was dialyzed against 50 mM Tris-HCl pH 8.5 and 5 mM DTT for 16 hours. The dialyzed sample was then centrifuged at 13 000 g for 25 min to remove any remaining insoluble components. The sample was stored at 4 °C (16 hours) until it was further processed.

In order to remove the 6-His purification tag from the recombinant protein, the 3 ml of protein solution were incubated with 200 U of rTEV protease for 3 hours at 30 °C with TEV reaction buffer (containing final concentration 50 mM Tris-HCl pH 8.0 and 0.5 mM EDTA) and 30 μl of 0.1 M DTT. Following proteolytic cleavage the rTEV buffer was replaced to buffer F (containing 50 mM NaH_2PO_4 pH 8.0, 300 mM NaCl and 10 mM imidazole) by loading the 3 ml of protein sample onto 2 buffer F equilibrated PD-10 gel filtration columns (Amersham Pharmacia Biotech). The protein was collected by loading an additional 1 ml of buffer F onto each of the columns. The

desalted protein solutions were pooled, incubated with the Ni affinity resin (1 ml settled volume) for 1 hour, and then loaded onto the supplied column. The flow through contained the recombinant protein lacking the 6-His purification tag. Washing the column with 8 ml of buffer G (containing 50 mM NaH_2PO_4 pH 8.0, 300 mM NaCl and 20 mM imidazole) followed by 3 ml of buffer H (containing 50 mM NaH_2PO_4 pH 8.0, 300 mM NaCl and 250 mM imidazole) eluted the rTEV and any non-cleaved recombinant protein, which was analyzed by SDS-PAGE. A total of 12 ml of recombinant protein mixture was concentrated 6-fold by centrifugation of a YM-30 Centricon tube (Millipore) at 4°C for 4 hours at 5000g. Protein concentration was confirmed visually by comparing Coomassie Blue staining intensity of an SDS-PAGE gel. Approximately 200 μg of recombinant protein was produced.

3.6.5 Antiserum production

Purified recombinant HK was run on a 20 ml preparative SDS-PAGE. Polypeptides were stained with Coomassie Blue and the band corresponding to the recombinant HK (~50 kDa) was excised. The HK protein was electro eluted using a Bio-Rad electroplater according to the directions of the manufacturer. The protein solution (200 μg in 500 μl) was separated into 3 injection volumes, of 300 μl and two 100 μl booster injections. Antibodies were raised using a 2-kg New Zealand White rabbit. After collection of the preimmune serum, recombinant HK (300 μl , emulsified in complete Freund's adjuvant) was injected subcutaneously into the back of the rabbit. Booster injections were performed at days 14 and 21 with 100 μl of recombinant HK emulsified in incomplete Freund's adjuvant. Blood was collected on day 28, 35 and 42

the final bleed by cardiac puncture. The serum was collected after centrifugation at $1500 \times g$, frozen in liquid N_2 , and kept at $-20^\circ C$.

3.6.6 Affinity purification of α -HK IgGs

Crude anti-serum was affinity purified against recombinant HK using a modification of the method described by Plaxton (1989). All steps were performed at room temperature unless otherwise stated. Fifteen μg of recombinant HK per lane was run on a 12% SDS-PAGE and electro-transferred to a PVDF membrane. After staining with Ponceau S the membrane was air dried. The band corresponding to 53 kDa (HK) was carefully excised from the blot, placed in a 2 ml Eppendorf tube, wetted with methanol for 1 min and then with H_2O for 15 min. The membrane strips were incubated in 1.5 ml of blocking solution for 1 hour and then washed 3 times by vortexing for 45 s with 1.5 ml of TBST. The membrane strips were then incubated for 1 hour with 1.5 ml of crude rabbit α -HK anti-serum, and washed to remove the remaining antiserum by vortexing 4 times 30s with 1.5 ml of TBST. Lightly vortexing the membranes with 1.5 ml of cold elution buffer (containing 20 mM glycine-HCl pH 3.0, 500 mM NaCl, 0.04% (w/v) NaN_3 and 0.25 % (v/v) Tween 20) for 2 min eluted the bound IgGs. The elution was removed and added to a fresh tube which contained 15 μl of 1M Tris and 150 μl of 5% (w/v) BSA in TBST, mixed, flash frozen with liquid N_2 and stored at $-80^\circ C$. The procedure was repeated 18 times with the same membranes, incubating with crude antiserum for 15 min each subsequent time.

3.6.7 Protein extraction and quantification

Root samples of 300-500 mg were extracted in a 1:1.5 weight to volume ratio of roots to ice cold extraction buffer. The extraction buffer was modified from Renz and Stitt (1993) (containing 100 mM Tris-HCl pH 8.0, 10 mM MgCl₂, 10 mM KCl, 1 mM EDTA, 1 mM ethylene glycol-bis (β -aminoethyl ether)- N, N, N', N'-tetraacetic acid (EGTA), 1 mM PMSF, 1 mM benzamidine, 1 mM ϵ -CA, 5 mM DTT, 5% (w/v) Polyvinylpolypyrrolidone (PVPP), 10% (v/v) glycerol and 0.1% (v/v) Triton X-100). Roots proteins were extracted using a pre-cooled mortar and pestle containing approximately 50 mg of sea sand. Extracts were clarified by 4 °C centrifugation at 12 500g for 10 min. The extract supernatants were analyzed for protein content using the Bradford protein assay (Bradford 1976) on a microplate reader (Molecular Devices VERSAmax) using Bio-Rad protein reagent with a bovine serum albumin (BSA) standard. Crude protein samples of 20 μ g were loaded onto SDS-PAGE and used in primary screening.

3.6.8 Immunodetection

All steps in immunodetection were carried out at room temperature and under constant agitation (150 rpm) on a gyratory shaker. Non-specific protein binding was blocked by incubating the membranes in a 3 % (w/v) skim milk solution in TBST (containing 50mM Tris-HCl pH 7.6, 150mM NaCl, 0.05% (v/v) Tween 20 and 0.02% (w/v) NaN₃) for a minimum of 60 min. The blocking solution was removed and the membranes washed 3 times for 10 min with TBST. Affinity purified α -HK IgGs (1:3 dilution in 3% (w/v) BSA TBST solution) were added to the membranes and incubated for 60 min. After washing them 3 times in TBST, the membranes were incubated with

the secondary antibody (a 1:10 000 dilution of goat α -rabbit alkaline phosphatase antibodies (Promega) in 3% (w/v) BSA TBST solution) for 60 min. Thereafter, the membranes were washed an additional 3 times with TBST. Staining was accomplished by incubating the membrane in 0.33 mg/ml nitroblue tetrazolium salt (NBT) and 0.165 mg/ml 5-bromo-4-chloro-3-indolyl-phosphate (BCIP) in alkaline phosphatase buffer (a solution containing 100 mM Tris-HCl pH 9.5, 5 mM MgCl_2 and 100 mM NaCl) for approximately 10 min (or until bands were clearly visible).

3.6.9 Quantification of hexokinase content

The intensities of HK bands from immunoblots were quantified by comparing the peak areas of the bands from digitally scanned (Deskscan II, Hewlett Packard) immunoblots using the Image J software system (<http://rsb.info.nih.gov/ij/>). The HK levels within the individual protein extracts were compared to the peak intensity of a control transformation line and a relative HK protein level was then determined.

3.7 Plant transformation vectors

3.7.1 pGA643

The binary vector pGA643 (An *et al.* 1988) was used for all plant transformation constructs. The plasmid was purified using Qiagen Midi-prep for low copy plasmids. *E. coli* pGA643 was grown on LB 10 mg/l kanamycin and 2 mg/l tetracycline. Clones were only maintained on LB plates for a maximum of 2-3 days, in order to prevent mutations. For potato transformation experiments, one control construct, one sense construct, and 3 anti-sense constructs were engineered. For all constructs the plasmids

were used to transform competent HB101 *E. coli*. A general scheme for the production of the plant transformation vectors is demonstrated (Figure 4).

3.7.2 Sense pGA643 construct

The sense construct was prepared by digesting the HK cDNA from SV2-G3 with *Cla*I (31 bp upstream) and *Hinc*II (1834 bp downstream). The 1875 bp fragment was then ligated into a *Cla*I, *Hpa*I digested pGA643 using blunt end ligation protocols. Positive colonies were confirmed by digesting prepared plasmids with *Bam*HI and *Dra*I (Figure 4).

3.7.3 Antisense-1 pGA643 construct

Antisense-1 was prepared by digesting the HK cDNA with *Xba*I (12 bp upstream) and *Eco*RV (600 bp downstream). The 612 bp fragment was ligated into pGA643 digested with *Xba*I and *Hpa*I using the blunt end ligation protocol. Positive clones were confirmed by digesting the prepared plasmids with *Bam*HI and *Cla*I (Figure 4).

3.7.4 Antisense-2 pGA643 construct

Antisense-2 was prepared by digesting pGA643 with *Hpa*I. 10 µg of pGA643 was digested with *Hpa*I and then dephosphorylated by incubating with 150 U of bacterial alkaline phosphatase (BAP)(Invitrogen), in BAP reaction buffer (final concentration 10 mM Tris-HCl pH 8.0) for 1 hour at 65 °C. The BAP was removed by PCI extraction and NaCH₃COO precipitation. The insert was prepared by digesting the

HK cDNA in SV2-G3 with *EcoRV* (611 bp downstream) and *HincII* (1834 bp upstream), and was ligated into the prepared vector using the blunt end protocol. Positive clones were confirmed by digesting the prepared plasmids with *BamHI* (Figure 4).

3.7.5 Antisense-3 pGA643 construct

Antisense-3 was prepared by digesting the HK cDNA with *XbaI* (12 bp upstream) and *HincII* (1834 bp downstream). The 1846 bp fragment was ligated into pGA643 digested with *XbaI* and *HpaI* using the blunt end protocol. Successful transformants were confirmed by digesting with *BamHI* (Figure 4).

3.7.6 *A. rhizogenes* pGA constructs

Rapidly purified construct DNA and a pGA643 plasmid were used to transform *A. rhizogenes* using the protocol described previously. Transformed colonies grew on MYA plates containing 25 mg/l kanamycin and 5 mg/l tetracycline. The transformants were confirmed by restriction analysis using the enzymes described above for each construct.

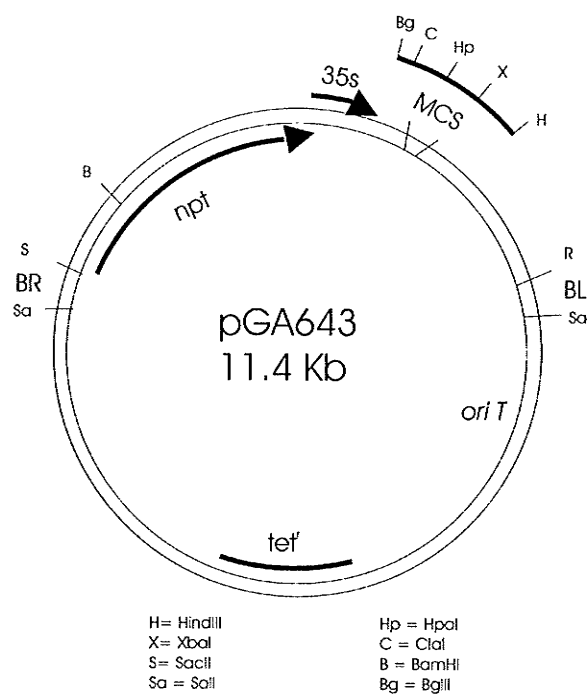
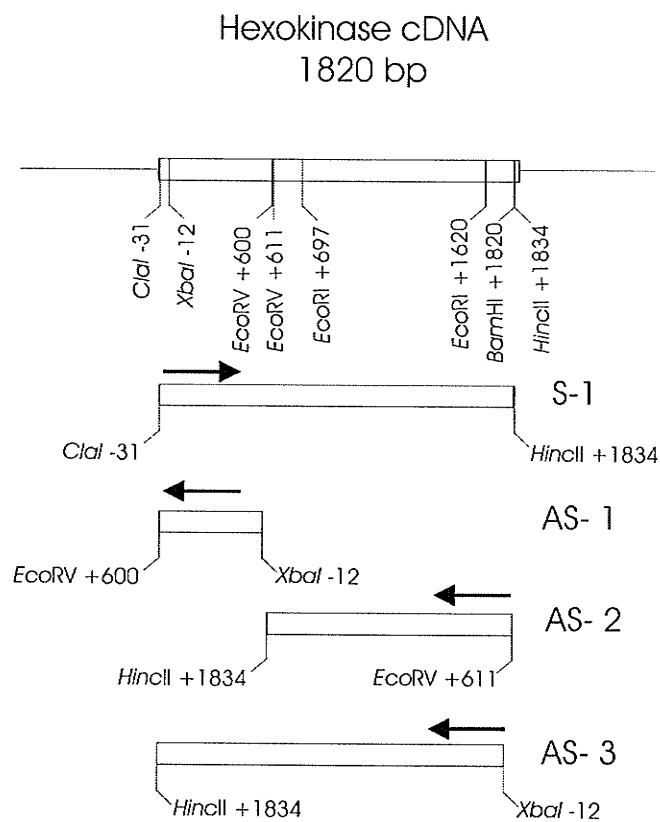


Figure 4. Production of plant expression vectors.

3.8. *A. rhizogenes* mediated potato transformations

Potato petioles from plants 4-6 weeks old were used for transformations. Leaves were removed from plants with stems being surface sterilized for 10 min in a solution containing 10% (v/v) commercial bleach and 0.005% (v/v) Tween 20. The sterilized stems were washed 4 times in sterile H₂O for 10 min per wash. Sterile washed stems were cut into 2-3 cm segments and placed in reverse orientation into small jars containing ~40 ml of solid MS based media (4 g/l phytagel). The freshly wounded stem tissue was then infected by a single colony of *A. rhizogenes* from a 3-4 day old MYA (25 mg/l kanamycin 5mg/l tetracycline) plate streaked with the desired pGA643 vector using a flamed platinum wire. The infected tissue was then incubated in a growth cabinet at 23 °C until transgenic roots of 1-2 cm emerge from the infected stem segments. Emerging transgenic roots were sub-cultured 3 times by transferring only the freshly grown tissue onto petri plates containing solid MS media (2g/l phytagel) with reducing concentrations of antibiotics 500, 500, 200-mg/l carbenicillin. Following sub-culturing the individual transgenic root lines were maintained on solid antibiotic free MS media.

3.9 *In vitro* hexokinase assays

Rapidly growing root tissue samples of 250-400 mg, were harvested from liquid MS media blotted dry, flash frozen and stored at -80 °C until needed. Protein was

extracted as previously described, except that a 3:1 buffer to root ratio was used. The volumes of the clarified extracts were carefully measured then loaded onto a PD-10 desalting column at 4 °C previously equilibrated with 50 ml of desalting buffer (containing 20 mM Tris-HCl pH 8.0, 5 mM MgCl₂, 1 mM DTT and 20% (v/v) glycerol). Desalting buffer was added to the column such that the extract volume totaled 2.5 ml, and allowed to flow by gravity. The protein is eluted from the PD-10 column by loading an additional 3 ml of desalting buffer onto the column. Activity assays were conducted on the desalted protein extracts using a protocol modified from Turner *et al.* (1977) which uses a glucose-6-phosphate dehydrogenase (G6PDH) coupled reaction at 25 °C monitoring the production on NADH at 334nm using a Molecular Devices VERSAmax microplate reader. Desalted extracts of 10, 20 and 30 µl were assayed in an assay buffer (containing final concentration 50 mM Tris-HCl pH 8.0, 50 mM KCl, 5 mM MgCl₂, 0.3 mM NAD⁺, 5 mM DTT, 1 mM ATP, 1U/ml G6PDH and 5 mM glucose), to a total volume of 200 µl. The background activity was determined by performing the same assay in duplicate without glucose, and was subtracted from the total activity. Substituting glucose for 5 mM fructose and adding 1 U/ml phosphoglucosomerase determined total fructose phosphorylation activity. Specific activity for each line was determined by calculating the activity per mg of total protein, in terms nmoles min⁻¹ mg protein⁻¹ (mU).

4.0 RESULTS AND DISCUSSION

This section will describe and discuss the relevant results in regards to production and screening of transgenic potato lines with altered HK levels. The results presented will examine the sequence of the *Solanum chacoense* HK cDNA clone, the production of recombinant HK for antibody production, the production of plant transformation vectors, production of transgenic potato lines, screening the lines for HK protein levels and screening the transgenic lines for altered HK activity.

4.1 Hexokinase cDNA

4.1.1 cDNA sequencing and sequence analysis

Solanum chacoense HK cDNA was sequenced as described in Materials and Methods. The sequence was determined to be 1808 bp in length (Figure 5). The coding sequence begins with an ATG codon at position 64 and terminates with the TGA stop codon at position 1552 (Figure 5). The poly-A tail begins at position 1790. The cDNA was translated using Expasy Translate (<http://us.expasy.org/tools/dna.html>) in 5'-3' reading frame 1, and predicted a 496 amino acid polypeptide with an expected molecular mass of 53.751 kDa (Figure 6). The isoelectric point was calculated using ProtParam (<http://us.expasy.org/cgi-bin/protparam>) and determined to be 6.07. The hydrophobic nature of the deduced amino acid sequence was analyzed using ProtScale (<http://ca.expasy.org/cgi-bin/protscale.pl>), with the Kyte and Doolittle algorithm. The presence of a high abundance of valine and alanine residues near the expected protein's

N-terminus predicts a highly hydrophobic region (Figure 7). This is indicative of a possible membrane anchor region in the protein.

```

1   GGA TCC AAA GAA TCA ATC CCA ATT CCC CTT CTC TAT CAT TTT TTC CTT AAT CGG ATA GTA
61  AGG ATG AAG AAG GCG ACG GTG GCT GCG GTG GTG GTA GGT ACA GCG GCG GCG GTA GCT GTG
121 GCG GCG CTC ATC ATG CGC CAC CGC ATG GGT AAA TCG AGC AAA TGG GCA CGT GCC AGG GCA
181 ATT CTG AAG GAA TTC GAG GAG AAA TGT GCC ACC CCA GAT GGC AAG CTG AAG CAA GTG GCT
241 GAT GCC ATG ACG GTG GAG ATG CAC GCC GGA CTC GCC TCT GAA GGC GGC AGC AAG CTC AAG
301 ATG CTT ATT AGC TAT GTC GAT AAT CTC CCT ACT GGC GAT GAA GGA GGA GTC TTT TAT GCA
361 TTG GAT CTT GGT GGA ACA AAT TTT CGA GTA TTG CGG GTG CAA TTG GGG GGA AAA GAT GGT
421 GGC ATT ATC CAT CAA GAA TTT GCG GAG GCA TCA ATT CCT CCA AAT TTG ATG GTT GGA ACT
481 TCA GAA GCA CTT TTT GAC TAT ATT GCG GCA GAA CTT GCA AAA TTC GTA GCT GAA GAA GGA
541 GAA GAG TTT CAT CCA CCT CCT GGT AGG CAG AGA GAA TTA GGC TTC ACC TTC TCG TTC CCA
601 ATA ATG CAG ACT TCA ATC AAT TCT GGA ACT CTT ATC AGG TGG ACG AAA GGT TTC TCC ATT
661 GAT GAC ACG GTT GGC AAA GAT GTT GTT GCA GAA CTG ACA AAA GCA ATG CAA AAA CGA GAA
721 ATT GAT ATG AGG GTC TCA GCG CTT GTG AAT GAT ACT GTT GGA ACA TTG GCT GGT GGT AGA
781 TTC ACC AAT AAG GAT GTA TCC ATT GCT GTG ATA TTA GGT ACT GGG ACC AAT GCA GCA TAT
841 GTG GAA CGG GGT GAG GCA ATT CCC AAA TGG CAC GGT CCT CTG CCT AAA TCT GGA GAA ATG
901 GTG ATC AAT ATG GAA TGG GGT AAC TTT AGG TCC TCC CAC CTT CCC TTG ACA GAG TAC GAT
961 CAT GCT ATG GAT ACC GAT AGT TTA AAT CCT GGT GAA CAG ATA TTT GAG AAG ATA TGT TCT
1021 GGC ATG TAC TTG GGA GAA ATT TTA CGC AGA GTT CTA CTT AGA ATG GCT GAA GAA GCT GGC
1081 ATT TTT GGC GAG GAA GTT CCT CCA AAA CTC AAG AAT TCA TTC ATA TTG AGG ACA CCT GAA
1141 ATG TCT GCT ATG CAT CAT GAC ACA TCC TCT GAT TTG AGA GTG GTT GGC GAC AAG TTG AAG
1201 GAT ATC TTA GAG ATA TCC AAT ACC TCC TTG AAG ACA AGG AGA TTA GTT GTT GAG CTG TGT
1261 AAT ATT GTT GCA ACA CGT GGC GCC AGA CTT GCG GCA GCT GGG ATC TTG GGC ATT ATC AAA
1321 AAG ATG GGA AAG GAT ACA CCC AGG GAA AGT GGT CCA GAA AAG ATT GTC GTA GCC ATG GAT
1381 GGC GGA TTG TAT GAA CAT TAT ACA GAA TAC AGT AAG TGC TTG GAG AAC ACT TTG GTT GAA
1441 TTA CTT GGA AAG GAA ATG GCC ACA AGT ATT GTT TTC AAG CAC GCG AAT GAT GGT TCT GGC
1501 ATT GGC GCT GCA CTC CTT GCG GCC TCT AAC TCC GTG TAT GTT GAA GAC AAG TGA GAG TGA
1561 TCA AAA TGA TAT TTA GCT AGA GGA AAC TCC ATT TAC CTT TTA TAT TAT GTT TTT TCT CTG
1621 GCC TTT TCT TTT TGG ATT CTC TCT CTC CTT TTT GGT TCT TCT TAC AAT TAT TTC CAG AAT
1681 TTT CCA GCA CTT GTA CTT GGT TTT CTA GGA TAT TAT TCC TGG GAA TGC CAA CAT ATT TCT
1741 TCT GGA AAA GGG TGC AAA GAA ATT ATA TGA AAC TCA GCA TTG CTT ATT CAA AAA AAA AAA
1801 AAA AAA AC

```

Figure 5. *Solanum chacoense* cDNA sequence. The nucleotide sequence of SCHK determined using a modification of the Sanger method (Sanger and others 1977). Coding region begins with ATG codon at position 64, terminates at the stop codon TGA at position 1552, marked in bold. The poly-A tail begins at position 1790 and is underlined.

```

1  MKKATVAADV VGTAADVAVA ALIMRHRMGK SSKWARARAI LKEFEKCAT PDGKLKQVAD
61 AMTVMHAGL ASEGGSKLKM LISYVDNLPD GDEGGVFYAL DLGGTNFRVL RVQLGGKDG
121 IIHQEFAEAS IPPNLMVGTS EALFDYIAAE LAKFVAEEGE EFHPPPGRQR ELGFTFSFPI
181 MQTSINSGLT IRWTKGFSID DTVGKDVVAE LTKAMQKREI DMRVSALVND TVGTLAGGRF
241 TNKDVSIAVI LGTGTNAAYV ERAQAIPKWH GPLPKSGEMV INMEWGNFRS SHLPLTEYDH
301 AMDTDSLNPQ EQIFEKICSG MYLGEILRRV LLRMAEEAGI FGEEVPPKLK NSFILRTPEM
361 SAMHHDTSDD LRVVGDKLKD ILEISNTSLK TRRLVVELCN IVATRGARLA AAGILGIKK
421 MGKDTPRESG PEKIVVAMDG GLYEHYTEYS KCLENTLVEL LGKEMATSIV FKHANDGSGI
481 GAALLAASNS VYVEDK

```

Figure 6. Deduced amino acid sequence of the SCHK cDNA. The cDNA was translated 5'-3' in frame 1, using the ATG codon at nucleotide 64 and the TGA stop codon at nucleotide position 1552.

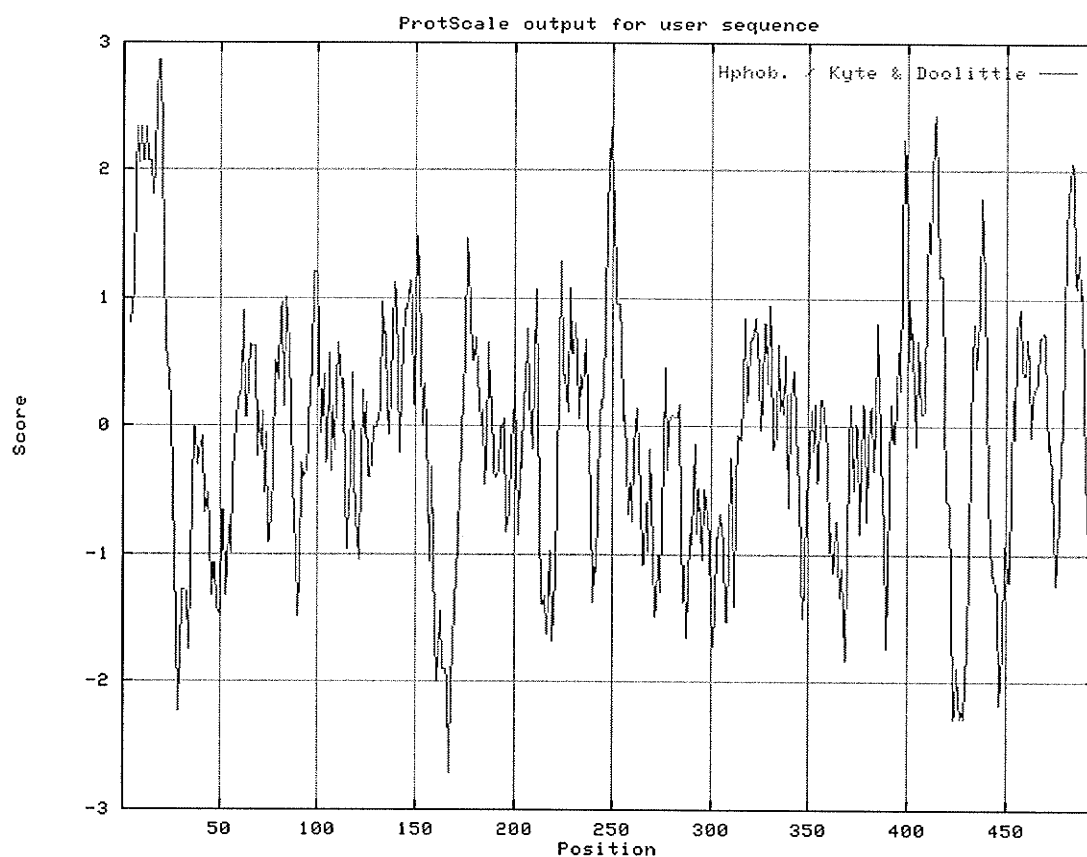


Figure 7. Hydrophobic nature of the deduced SCHK amino acid sequence. Increasing number indicate a higher degree of hydrophobicity, based on individual amino acid scores: A = 1.800, R = -4.500, N = -3.500, D = -3.500, C = 2.500, Q = -3.500, E = -3.500, G = -0.400, H = -3.200, I = 4.500, L = 3.800, K = -3.900, M = 1.900, F = 2.800, P = -1.600, S = -0.800, T = -0.700, W = -0.900, Y = -1.300, V = 4.200.

The hydrophobic nature of the deduced protein is similar to the nature of HK1 and HK2 of *S. tuberosum*, and other plant HKs including: *Arabidopsis* HK1 and HK2 (Jang *et al.* 1997), tomato HK1 (Martinez-Barajas and Randall 1998) and HK2 (Menu *et al.* 2001) and tobacco HK1 (Wiese *et al.* 1999) among others. These HKs have been noted as having N-terminus membrane anchoring regions.

The benefit of membrane anchoring of the N-terminus would likely assist in binding the HK to the outer membrane of the chloroplast and mitochondria. This would allow the HK access to the ATP generated by these organelles (Wiese *et al.* 1999). This membrane anchor appears to be conserved throughout the plant HKs, while it is not present in mammalian or yeast enzymes.

4.1.2 DNA sequence comparisons

The DNA sequence obtained was compared to published sequences using Blastn similarity search (<http://www.ncbi.nlm.nih.gov/BLAST>). The results obtained indicated high similarities to other plant HKs. As expected, the highest degree of similarity was between the *S. chacoense* HK (SCHK) cDNA and *S. tuberosum* HK2 (STHK2). The sequences had near identical nucleotide sequences at the 5' end, having 1576/1585 identities with no gaps for >99% similarity (-2 penalty for mismatches and -5 penalty for gaps). The sequences differed slightly at the 3' end having 132/138 identities with 3 gaps, for 95% similarity.

High similarities were observed between SCHK and *S. tuberosum* HK1 (STHK1) as well. The sequences displayed 1101/1296 identities with 11 gaps for 85% similarity. The sequence for potato HK3 has not yet been published and could not be compared.

Comparison of SCHK to other plant HKs also revealed relatively high similarities, 96% with tomato HK2, 82 % with *Prunus persica* HK2 and 82% with *Arabidopsis thaliana* HK2.

Comparison to non-plant hexokinase gene sequences revealed significantly lower nucleotide similarities. There was only 21% similarity between the 50 kDa human HKIV and similar findings with other mammalian HKs. Yeast HKA and HKB had only 19 and 18% sequence similarities with SCHK.

4.1.3 Amino acid sequence comparison

The deduced amino acid sequence of SCHK had a 99% similarity with the amino acid sequence of STHK2. The internal sequences and the C and N-termini were nearly identical between the two peptides with the only minor deviations apparent (Figure 8). Similarities between STHK1 and SCHK were less in the amino acid sequences, as there was only 75% homology between the two peptides. There were some differences throughout the sequences with the major differences occurring between amino acids 75 through 95 (Figure 8).

Comparisons of SCHK to other plant HK amino acid sequences revealed high levels of similarities, which is consistent with previous reports (Jang and others 1997; Menu and others 2001). There is 90% similarity between SCHK and tomato HK2, 86% to tobacco HK1, 80% and 70% to *Arabidopsis* HK1 and HK2, 79% to spinach HK1 and 77% to rice HK1. This high degree of sequence similarity is expected due to the conserved nature of the plant enzymes.

Figure 8. Comparison of HK amino acid sequences. A comparison of the predicted amino acid sequences of *S. chacoense* SCHK, *Saccharomyces cerevisiae* Yeast HKA and HKB (Stachelek *et al.* 1986), *S. tuberosum* STHK1 (AC# 064390) and STHK2 (AC# Q95Q76), *A. thaliana* ATHK2 (Jang *et al.* 1997) and human HK4 (Tanizawa *et al.* 1991). Arrow H, from position 4-24 is a transmembrane region. Arrow P1, from 99-120 and arrow P2, from 254-273 are phosphate binding domains 1 and 2 (Bork *et al.* 1992). Arrow A, from positions 458-476 is the adenosine binding domain (Bork *et al.* 1992). Arrow S, from position 173-192 is the sugar binding domain (Bork *et al.* 1993). The numbering above the sequences is the relative position of the amino acid residues. Identical residues are indicated by "*", highly conserved residues by ":", mildly conserved residues by "." and gaps by "-".

10 20 30 40 50 60 70 80 90

YeastHKA -----MVHLGPKKQARKGSMADVPEKELMDEIHQLEDMFTVDSETLRKVVKHFIDELNKGLTKKGGN---IPMIPGWVMEF
 YeastHKB -----VHLGPKKQARKGSMADVPEKELMQQIENFEKIPTVPTETLQAVTKHFISELEKGLSKKGGN---IPMIPGWVMDF
 STHK2 MKKATVGA VVVGTA AAVAAVAALIMRHRMGKSSKWARARAILKEFEKCATPDGKLKQVADAMTVEMHAGLASEGGSK--LKMLISYVDNL
 SCHK MKKATVAAVVVGTA AAVAAVAALIMRHRMGKSSKWARARAILKEFEKCATPDGKLKQVADAMTVEMHAGLASEGGSK--LKMLISYVDNL
 STHK1 MKKVTVGA VVVGTA AAVCAVAALIVNHRMRKSSKWARARAILKEFEKCATPDGKLKQVADAMTVEMHAGLASEGGSK--SRCLSPMSIIS
 ATHK2 MGKAVAVATTVCVAVCAAAALIVRRMRKSSAGKWARVIEILKAFEDCATPIAKLRQVADAMTVEMHAGLASEGGSK--LKMLISYVDNL
 HumanHK4 -----MLDDRARMEAAKKEKVEQILAEFQLQEEDLKKVMRRMQKEMDRGLRLLETHEEASVKMLPTVYRST

→ H ←

100 110 120 130 140 150 160 170 180

YeastHKA PTGKESGNYLAIDLGGTNLRVVLVKLSGNH---TFDDTQSKYKLPDMRTTKHQEELWSFIADSLKDFMV---EQELLNTKDTLPLGFT
 YeastHKB PTGKESGDFLAIDLGGTNLRVVLVKLGDDR---TFDDTQSKYRLPDAMRTTQNPDELWEFIADSLKAFID---EQFPQGISPIPLGFT
 STHK2 PTGDEGGVFFYALDLGGTNFRVLRVQLGGKDDG--IIHQEFAEASIPPNLMVG-TSEALFDYIAAELAKFVAEEGEEFHPPPGRQRELGFT
 SCHK PTGDEGGVFFYALDLGGTNFRVLRVQLGGKDDG--IIHQEFAEASIPPNLMVG-TSEALFDYIAAELAKFVAEEGEEFHPPPGRQRELGFT
 STHK1 QLVMLKGVFFYALDLGGTNFRVLRVQLGGKDDG--IIHQEFAEASIPPNLMVG-TSDALFDYIAAELAKFVAEEGEEFHPPPGRQRELGFT
 ATHK2 PSGDETGFYFALDLGGTNFRVLRVQLGGKDDG--VVKREFKEESIPPHLMTG-KSHELFDYIVDLAKFVATEGEDFHLPPGRQRELGFT
 HumanHK4 PEGSEVGDFLSLDLGGTNFRVLRVQLGGKDDG--VVKREFKEESIPPHLMTG-KSHELFDYIVDLAKFVATEGEDFHLPPGRQRELGFT

→ P1 ←

190 200 210 220 230 240 250 260 270

YeastHKA FSPASQNKINNEGILQRWTKGFDIPNVEGHVPLQLNEISKR-ELPIEIVALINDTVGTLIASYYTDPETKMGIIFGTGVNGAFYDVVS
 YeastHKB FSPASQNKINNEGILQRWTKGFDIPNIEHNDVVPMLQKQITKR-NIPIEVVALINDTTGTLVASYYTDPETKMGIIFGTGVNGAYYDVCS
 STHK2 FSPFPIQTSINSGLTIRWTKGFSIDDTVGKDVVAELTKAMQKR-EIDMRVSALVNDTVGTLAGGRFTNKDVSIIVILGTGTNAAYVERAQ
 SCHK FSPFPIQTSINSGLTIRWTKGFSIDDTVGKDVVAELTKAMQKR-EIDMRVSALVNDTVGTLAGGRFTNKDVSIIVILGTGTNAAYVERAQ
 STHK1 LLIPSNADFNNSGTLIMRWTKGFSIDDAVGQDVVGELTKAMKEK-VLDMRVSAVNDTVGTLAGGRFTNKDVSIIVILGTGTNAAYVERAQ
 ATHK2 FSPFVKQLSLSSGTLINWTKGFSIDDTVGKDVVGELVKAMERV-GLDMLVAALVNDTVGTLAGGRFTNKDVSIIVILGTGTNAAYVERAQ
 HumanHK4 FSPFVRHEDIDKGIILLNWTGKFKASGAEGNNVGLLRDAIKRRGFEMDVVAMVNDTVATMISCYIEDHQCEVGMIVGTGCNACVMEEMQ

S ←

→ P2

280 290 300 310 320 330 340 350 360

YeastHKA DIEKLEGLKLADDIPSNSPMAINCEYGSFD-NEHLVLPRTKYDVAVDEQSPRPGQQAPEKMTSGYYLGEILLRLVLELNEKGLMLKQDQLS
 YeastHKB DIEKLGKLSDDIPSPAPMAINCEYGSFD-NEHVVLPRTKYDITIDEESPRPGQQTPEKMTSGYYLGEILLRLALMDMYKQGFIFKNQDLS
 STHK2 AIPKWHG---PLPKSGEMVINMEWGNFR-SSHLPLT--EYDHAMDNTSLNPGEQIFEKICSGMYLGEILRRVLLRMAEEAGIFGEEVPP
 SCHK AIPKWHG---PLPKSGEMVINMEWGNFR-SSHLPLT--EYDHAMDNTSLNPGEQIFEKICSGMYLGEILRRVLLRMAEEAGIFGEEVPP
 STHK1 AIPKWHG---PVPKSGEMVINMEWGNFR-SSHLPLT--EYDHAMDNTSLNPGEQIFEKICSGMYLGEILRRVLLRMAEEAGIFGEEVPP
 ATHK2 AIPKWHG---LLPKSGEMVINMEWGNFR-SSHLPLT--EYDHAMDNTSLNPGEQILEKISGMYLGEILRRVLLRMAEEAGIFGEEVPP
 HumanHK4 NVELVEG-----DEGRMCVNTWGAFGDSGELDEFLELYDRVDESSANPGQQLYEKILGGKYMGEILVRLVLLRLVDENLLFHEASE

←

370 380 390 400 410 420 430 440 450

YeastHKA K-LKQPYIMDTSYPARIEDDPFENLEDTDIFQKDFGVK-TTLPERKLIRRLCELIGTRAARLAVCGIAAICQKRGYKTG-----HI
 YeastHKB K-FDKPFVMDTSYPARIEEDDPFENLEDTDLFQNEFGIN-TTVQERKLIRRLSELIGARAARLSVCGIAAICQKRGYKTG-----HI
 STHK2 K-LKNSFILRTPMSAMHHDTSDDLVRVVGDKLKDILEISNTSLKTRRLVVELCNIVATRGARLAAAGILGIIKKMGKDTPRESGPEKIVV
 SCHK K-LKNSFILRTPMSAMHHDTSDDLVRVVGDKLKDILEISNTSLKTRRLVVELCNIVATRGARLAAAGILGIIKKMGKDTPRESGPEKIVV
 STHK1 QSLKDSFVLRTPDMSAMHHDTSDDLVRVVGDKLKDILEISNTSLKTRRLVVELCNIVATRGARLAAAGILGIIKKMGKDTPRESGPEKIVV
 ATHK2 K-LKIPFIIRTPMSAMHHDTSDDLVRVVGDKLKDILEISNTSLKTRRLVVELCNIVATRGARLAAAGILGIIKKMGKDTPRESGPEKIVV
 HumanHK4 Q-LRTRGAFETRFVSQVESDTRDKQIYN--ILSTLGLR-PSTTDCDIVRRACESVSTRAAHMCSAGLAGVINRMRESRSED--VMRITV

460 470 480 490 500 510 520

YeastHKA AADGSVYKYPGFKKAAAKGLRDIYGTGASKD-PITIVPAEDSGAGAAVIAALSEKRIAEGKSLGIIGA
 YeastHKB AADGSVYKYPGFKKAAANKLDIYGTQTSLLDYPIKIVPAEDSGAGAAVIAALAKQRIAEGKSLGIIGA
 STHK2 AMDGGLYEHYTEYSKLENTLVLLG--KEMATS--IVFKHANDSGGIGALLAASNSVYVEDK-----
 SCHK AMDGGLYEHYTEYSKLENTLVLLG--KEMATS--IVFKHANDSGGIGALLAASNSVYVEDK-----
 STHK1 AMDGGLYEHYTEYSKLENTLVLLG--EELATS--IVFVHSNDSGGIGALLRASHSMYLEDQA-----
 ATHK2 AMDGGLYEHYTEYSKLENTLVLLG--DEVSES--VEVILSNDSGGIGALLAASHSQYLEDDSETS--
 HumanHK4 GVDGSVYKLPSPFKERPHASVRLRTP-----SC-EITFIESESGSGRGAALVSAVACKACMLGQ-----

→ A ←

Compared to non-plant eukaryotic HK SCHK has a significantly lower degree of sequence similarities. There are 33 and 34% similarities with yeast HKA and HKB.

While the 50 kDa mammalian HK4 has 33% similarity to SCHK. This is indicative of a very distant common ancestor of the plant, yeast and animal HKs (Cardenas *et al.* 1998).

Figure 8 displays the sequence comparisons between seven 50 kDa eukaryotic HK amino acid sequences. The plant HKs STHK1, STHK2, SCHK and ATHK2 all contain a putative 20 amino acid hydrophobic region between residues 4-24. The hydrophobic nature of this region is shown in Figure 7, at the N-terminus. There are two phosphate binding regions (starting at positions 99 and 254) along with an adenosine binding domain (starting at position 458) shared by all 7 amino acid sequences (Figure 8). The phosphate binding domains interacts with the β and γ phosphates from ATP, while the adenosine binding domain interacts with the adenosine portion of ATP (Bork *et al.* 1992). These domains were identified by amino acid similarities between different protein families of sugar kinases and ATPases (Bork *et al.* 1992; Wilson 1995). The sugar binding domain is indicated starting at position 173, which was identified by sequence similarities between sugar kinases (Bork *et al.* 1993).

The phosphate 1 binding domain (Figure 8, P1 residues 99-120) was highly conserved between all seven HKs compared, which, several identities and several highly conserved residues. The phosphate 2 domain (Figure 8, P2 residues 254-273) was also highly conserved among all seven of the sequences. The adenosine and sugar binding domain, however as not as highly conserved (Figure 8, S residues 173-192 and A residues 458-476). There are some identities in the region, however this is not throughout

the sequence. It is unlikely that these differences are due to different substrate specificities, since all HKs aligned have a preference for glucose and ATP.

The degree of amino acid sequence similarity is similar between plant HKs and the yeast HKs, as well as 50 kDa mammalian HKs. This is consistent with the conclusion that there was an ancestral 50 kDa HK in eukaryotes (Cardenas *et al.* 1998). The divergence between the plant, vertebrate and yeast HKs occurred at the same time, based on relatively equal similarities between the 3 classes of 50 kDa HKs (Cardenas *et al.* 1998).

4.2 Production and purification of recombinant hexokinase

4.2.1 *E. coli* expression vector production

The *E. coli* expression vector was assembled as described in the Materials and Methods section. The expression vector was used to transform DH5 α *E. coli*, resulting in 42 positive colonies growing on the antibiotic selection media (LB 50 mg/l kanamycin and 100 mg/l ampicillin). The positive colonies were tested for the presence and proper orientation of the HK insert, through *EcoRI*/*XhoI* digestion of purified plasmid. All of the 36 colonies tested displayed DNA bands of 900 and 700 bp as expected (the plasmids isolated from 9 colonies are shown in (Figure 9), indicating the presence of the insert and in the correct orientation for proper protein production. Colony #3, (Figure 9 lane 3), was used as the *E. coli* line for protein production, since a high level of plasmid was produced.

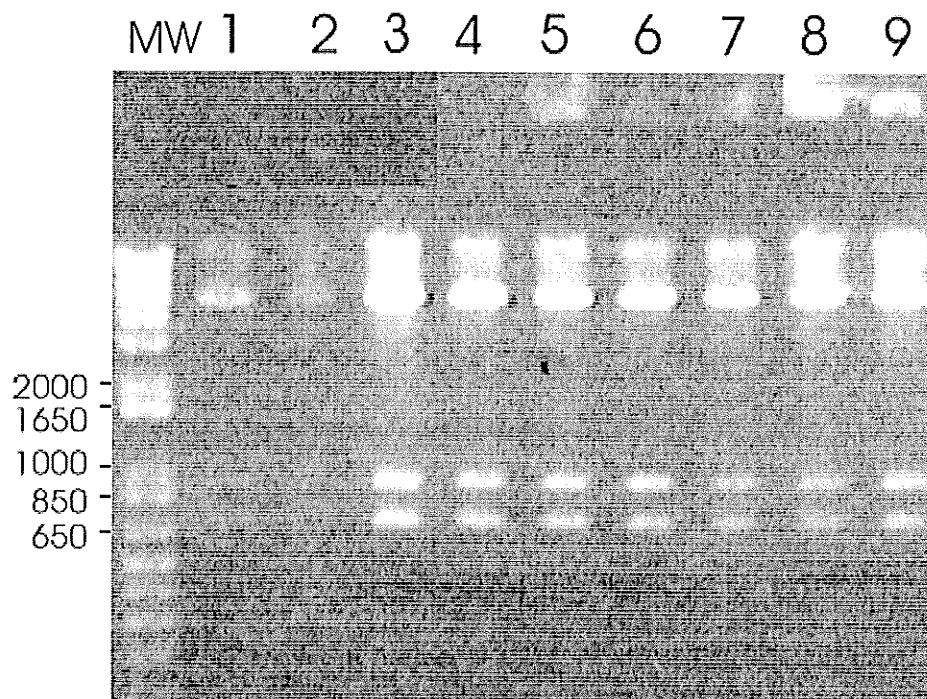


Figure 9. proEX HTa containing the SCHK cDNA insert. TBE gel of plasmids isolated from different resistant colonies digested with *EcoRI*/*XhoI* in lanes 1-9. MW is 1 kb+ molecular weight markers.

The truncated cDNA insert along with the additional codons added for 6-His sequence purification and protease cleavage region encode for a polypeptide of 52.8 kDa are shown in Figure 10. After removal of the 6-His tag by rTEV the polypeptide will have a molecular mass of 49.8 kDa.

```

1  MSYYHHHHH DYDIPTTENL YFQ*GAMDPE-FEEKCATPDGK LKQVADAMTV EMHAGLASEG
61  GSKLKMLISY VDNLPTGDEG GVFYALDLGG TNFRVLRVQL GGKDGGIIHQ EFAEASIPP
121 LMVGTSEALF DYIAAELAKF VAEEGEEFHP PPGRQRELGF TFSFPIMQTS INSGTLIRWT
181 KGFSIDDTVG KDVVAELTKA MQKREIDMRV SALVNDTVGT LAGGRFTNKD VSIIVILGTG
241 TNAAYVERAQ AIPKWHGPLP KSGEMVINME WGNFRSSHLP LTEYDHAMDT DSLNPGEQIF
301 EKICSGMYLG EILRRVLLRM AEEAGIFGEE VPPKLKNSFI LRTPEMSAMH HDTSSDLRVV
361 GDKLKDILEI SNTSLKTRRL VVELCNIVAT RGARLAAAGI LGIIKKMGKD TPRESGPEKI
421 VVAMDGGGLYE HYTEYSKCLE NTLVELLGKE MATSIVFKHA NDGSGIGAAL LAASNSVYVE
481 DK

```

Figure 10. The deduced amino acid sequence of the recombinant HK. 29 amino acid residues were added to the truncated SCHK cDNA for use in affinity purification. The transition from SCHK to additional sequence is marked by -. The rTEV protease cleavage site is marked by *. The 6-His purification tag is highlighted.

4.2.2 Optimizing recombinant protein induction conditions

Small scale induction experiments were performed to determine the optimal conditions for recombinant HK expression in *E. coli*. Cell cultures were grown in duplicate until OD₆₀₀ of 0.5-0.6 were obtained, at which point IPTG was added to one of the cultures to induce the *trc* promoter. Protein profiles obtained under various the induction conditions are shown in Figure 11. Substantial increase in a protein slightly larger than the 49.5 kDa molecular marker is visible in all of the induced cultures (lanes 2,4,6 and 8). Based on relative mobility this band corresponds to approximately 53 kDa, which was the mass predicted from the nucleotide sequence. Maximal protein induction was visible in lanes 2 and 6, both conditions corresponding to 5 hours of induction at 37 °C. The sample in lane 6 was stored overnight at 4 °C. The protein yield was determined solely by visualization, since no difference was observed by storing the sample overnight at 4 °C. A 5 hour induction at 37 °C was used as standard induction procedure.

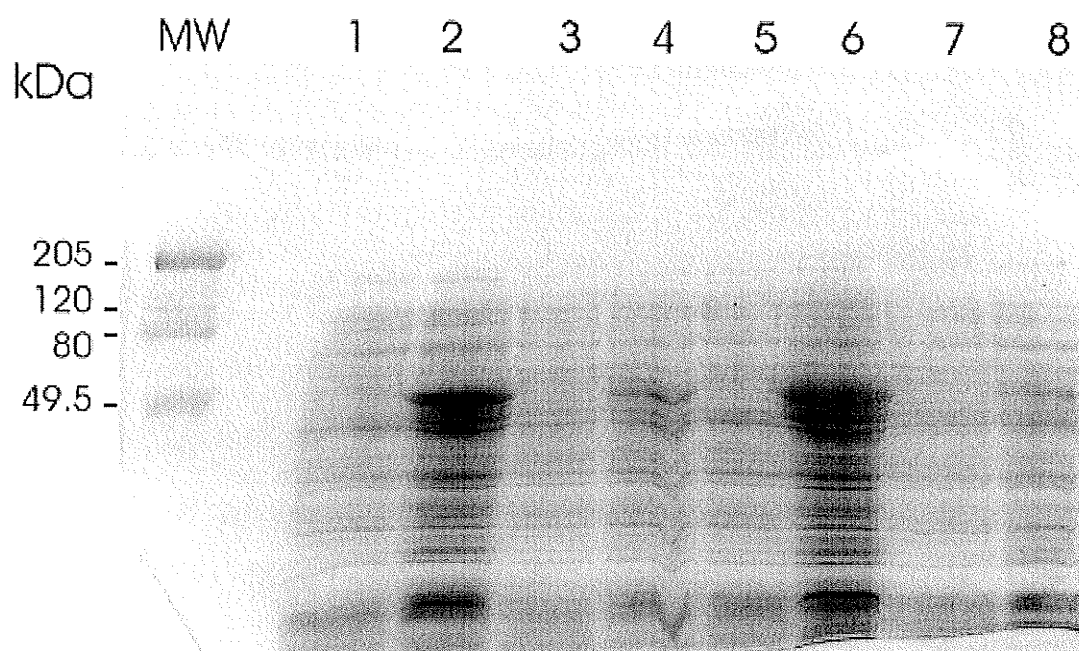


Figure 11. Optimization of recombinant protein induction conditions. SDS-PAGE of crude protein extracts from DH5 α containing the proEX:HK plasmid, the recombinant protein induced with the addition of IPTG under different conditions. All lanes were loaded with 15 μ l of crude extracts denatured in 5 μ l of 4X SDS sample buffer. Lanes 1 and 2 were grown for 5 hours at 37 $^{\circ}$ C, lane 2 was induced. Lanes 3 and 4 were grown for 5 hours at 30 $^{\circ}$ C, lane 4 was induced. Lanes 5 and 6 were grown for 5 hours at 37 $^{\circ}$ C then left overnight at 4 $^{\circ}$ C, lane 6 was induced. Lanes 7 and 8 were grown for 3 hours at 37 $^{\circ}$ C, lane 8 being induced. MW is Bio-Rad high prestained molecular weight markers.

4.2.3 Recombinant protein extraction for affinity purification

Large-scale induction of protein was carried out as described in the Materials and Methods. The lysed cells were centrifuged to pellet the cellular debris, at which point the presence of protein was determined in both the supernatant and pellet by SDS-PAGE. If the protein was in the supernatant it would be possible to proceed with protein purification under native conditions. The pellet was resuspended in 6M urea and compared to the denatured supernatant by SDS-PAGE (Figure 12). From this gel it was clearly visible that the majority of the recombinant protein was in the pellet. This indicated that all subsequent purification steps should be performed under denaturing conditions.

When the dissolved pellet was clarified by centrifugation a significant amount of pellet was again produced. The pellet produced was analyzed for protein content by SDS-PAGE (Figure 13). The majority of the protein remained in the urea solution (lane labeled SNT Figure 13). There was no detectable protein band in the 50 kDa range visible in the precipitate (lane labeled pellet Figure 13). Therefore, the clarified redissolved pellet was used for protein purification.

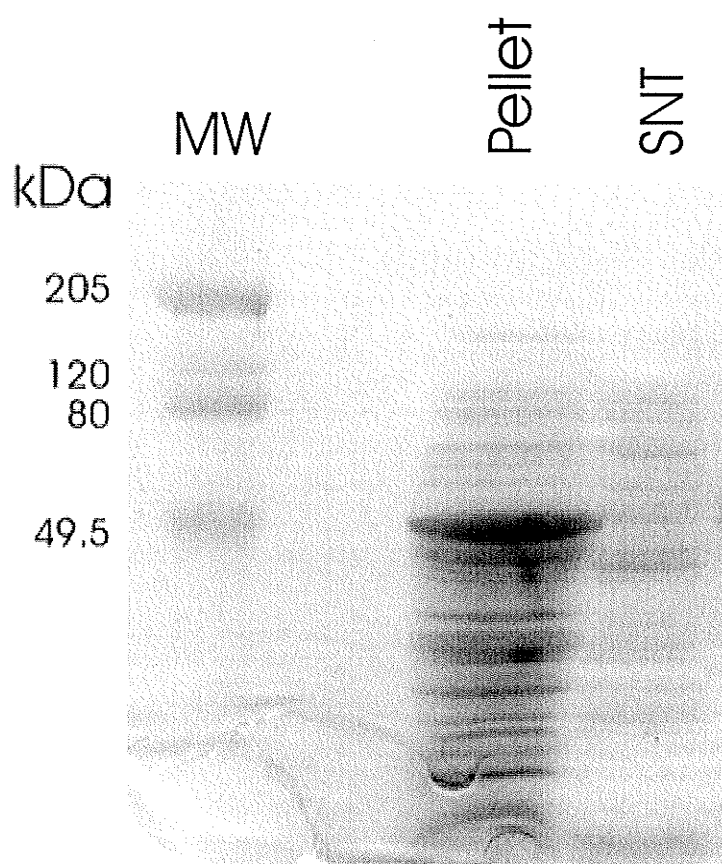


Figure 12. Localization of recombinant HK protein in soluble and insoluble fractions from *E. coli*. SDS-PAGE of resuspended pellet protein and soluble protein lane marked SNT. Pellet contains 20 μ l of precipitated material resuspended in urea and denatured in SDS sample buffer. SNT contains 20 μ l of soluble material denatured in SDS sample buffer. MW is Bio-Rad high molecular weight prestained markers.

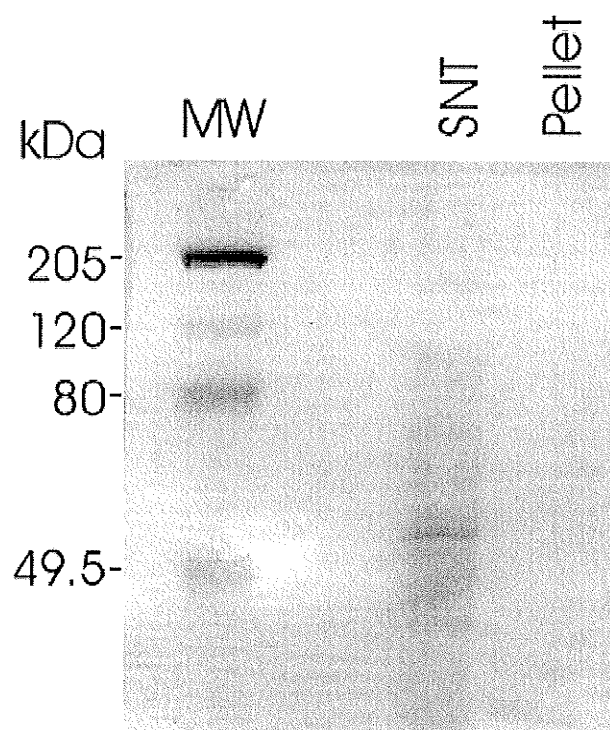


Figure 13. SDS-PAGE analysis of clarified urea supernatant of the recombinant HK. SDS-PAGE of 20 μ l of urea denatured supernatant (SNT) and 20 μ l of resuspended and denatured pellet material. MW is Bio-Rad high molecular weight prestained markers.

4.2.4 Affinity purification of the recombinant HK

The protein solubilized in urea was incubated with the Ni-affinity resin batchwise. The suspension was then poured into the supplied column as described in the Materials and Methods section. A substantial amount of recombinant HK was present in the flow through fraction (lane 1, Figure 14), indicating that the affinity resin was overloaded. Presumably, all of the proteins larger than the recombinant HK did not bind to the resin and were present in the flow through. The two washes contained protein with a molecular mass similar to that of the recombinant HK. The proteins in the wash fractions represented proteins, which were presumably loosely bound to the Ni resin (lanes 2 and 3 Figure 14). Significant amounts of protein with a similar molecular mass to the recombinant HK eluted at pH 5.9 (lanes 4 and 5 Figure 14), however the majority of the protein eluted at pH 4.5 (lanes 6 and 7 Figure 14). The eluants were then pooled together and pH was adjusted (lanes 4-7 Figure 14).

The pooled samples contained urea, which was removed in order for the rTEV protease to cleave the 6-His tag. This was accomplished by overnight dialysis against a buffer (containing 50 mM Tris-HCl pH 8.5 and 5 mM DTT). Following dialysis significant amounts of precipitate were visible in the protein sample. The solution was clarified by centrifugation, and the supernatant and pellet were analyzed by SDS-PAGE (Figure 15). The lack of protein present in the redissolved pellet (lane 3 Figure 15) indicates that the protein remained in solution following dialysis.

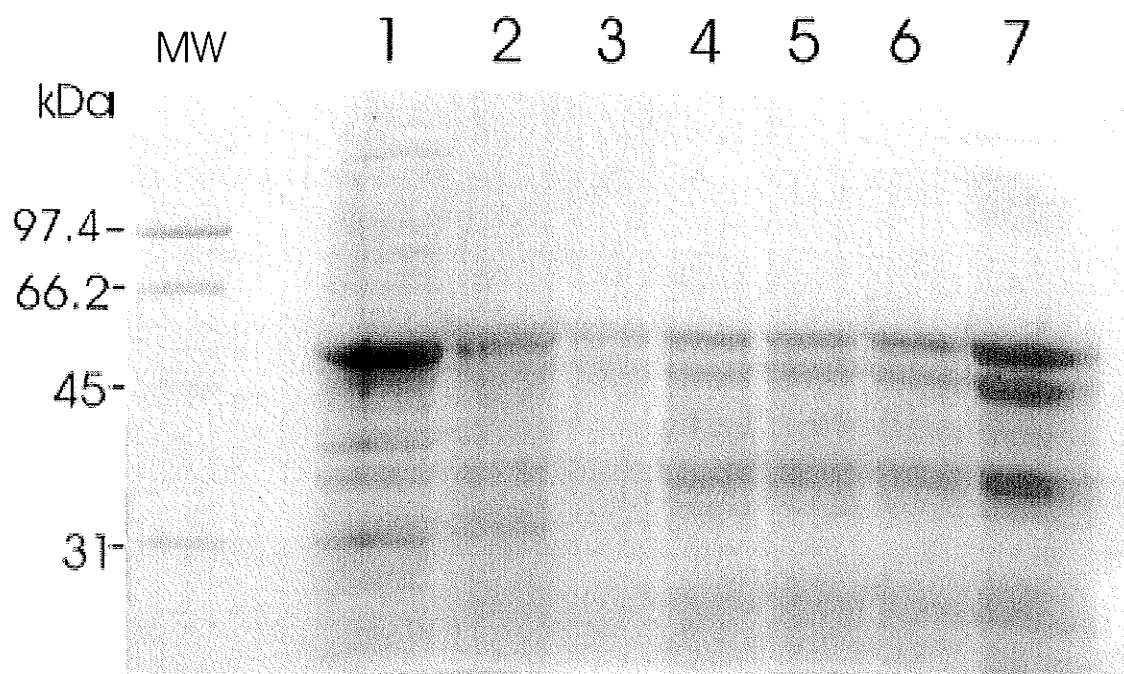


Figure 14. Elution of affinity purified recombinant protein. SDS-PAGE samples (20 μ l) eluting from Ni affinity column. Lane 1 contains the flow through, which was the material that did not bind to the column. Lanes 2 and 3 were 4 ml washes at pH 6.3 and contained unbound protein. Lanes 4 and 5 were elutions of 1 ml each at pH 5.9. Lanes 6 and 7 were elutions of 1 ml each at pH 4.5. MW is Bio-Rad low range molecular weight standards.

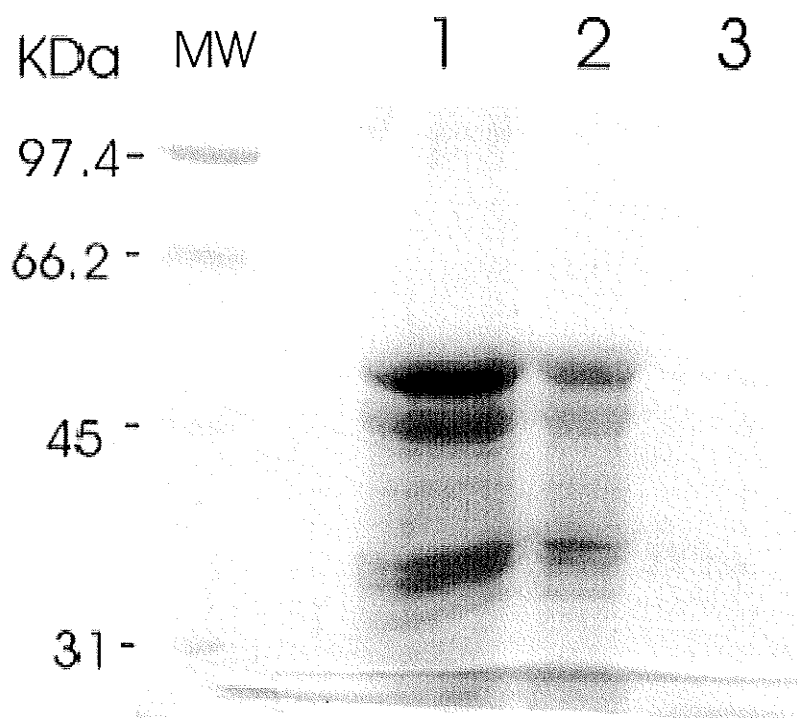


Figure 15. Analysis of recombinant HK protein solubility following dialysis. SDS-PAGE of 20 μ l samples denatured in SDS sample buffer. Lane 1 contains protein, prior to dialysis. Lane 2 contains the supernatant, which was the soluble fraction after the removal of urea by dialysis. Lane 3 contains the pellet, which was the insoluble fraction after urea was removed and the suspension centrifuged. MW is Bio-Rad low range molecular weight standards.

The presence of protein bands smaller than the recombinant HK was hypothesized to be products of proteolytic degradation, which occur *in vivo*. This conclusion was supported by the fact that the protein bands of lower molecular weights had a 6-His tag, since they were bound to the resin. The ratios of these bands were identical throughout all of the purification fractions

4.2.5 Removal of the 6-His tag

The 6-His tag was removed by incubation of approximately 2 mg of recombinant HK with 200 U of rTEV protease. Following the proteolytic reaction, the protein was incubated with the Ni affinity resin (1 ml settled volume), and then poured into a 10 X 50 mm purification column. The protein present in the flow through (lane 2 Figure 16) was the processed recombinant HK. The size was decreased by approximately 3 kDa as compared to the undigested proteins (lane 1, Figure 16). Washing the column with 4 ml of wash buffer (20 mM imidazole) eluted negligible amounts of protein (lanes 3 and 4, Figure 16). Loading elution buffer (250 mM imidazole) onto the column, eluted protein that was unsuccessfully digested by the protease along with the rTEV (lanes 5,6 and 7, Figure 16).

The flow through was concentrated using Centricon YM-30 units, as described in the Materials and Methods. The protein was concentrated 6-fold to a final volume of 2 ml. The amount of protein was estimated by visualization of a SDS-PAGE (Figure 17). By comparing with staining intensity of the molecular weight markers it was estimated that there was a total amount of 400 μg of recombinant HK (to be 0.2 μg protein/ μl of solution). The 50 kDa protein was isolated from the smaller protein fragments by electro-elution. The protein was then used to produce rabbit α -HK anti-serum.

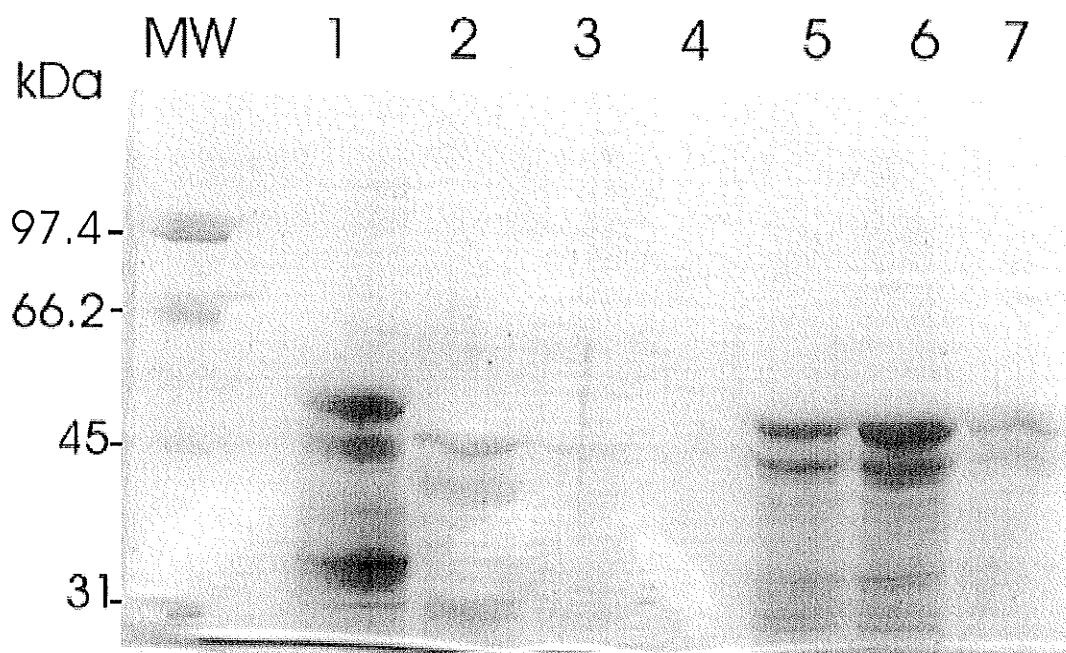


Figure 16. Purification of rTEV digested recombinant HK protein. SDS-PAGE of fractions from the purification of processed recombinant HK following rTEV digestion. Each lane contains 20 μ l of sample denatured in SDS sample buffer. Lane 1 contains undigested protein. Lane 2 contains the column flow through. Lanes 3 and 4 were washes of 4 ml each (20 mM imidazole). Lanes 5, 6 and 7 are eluted (250 mM imidazole) proteins, which were bound to the Ni affinity matrix. MW is Bio-Rad low range molecular weight standards

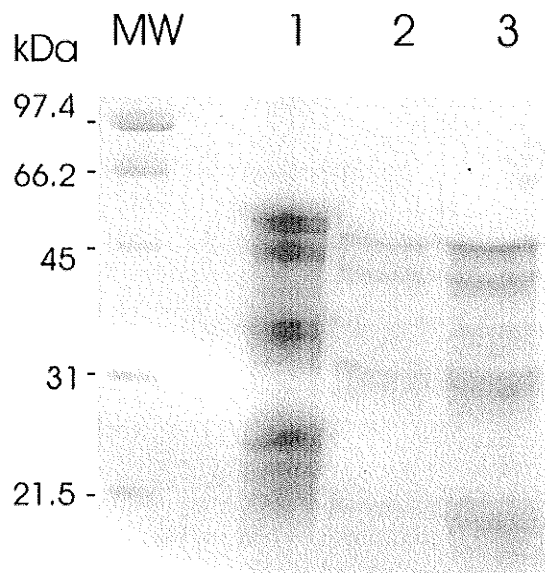


Figure 17. Visual quantification of the recombinant HK protein. SDS-PAGE loaded 20 μ l of sample denatured in SDS sample buffer. Lane 1 contains undigested protein. Lane 2 contains the digested protein with rTEV prior to concentration. Lane 3 contains the concentrated digested protein. MW is Bio-Rad low range molecular weight standards.

4.2.6 Testing the anti-serum for HK recognition

Crude anti-serum was used to estimate specificity for recognition of the recombinant protein. Recombinant protein (2 μ g) was electro-transferred to a PVDF membrane, after SDS-PAGE. The membrane was probed, using a 1/1000 dilution of crude anti-serum and compared to a membrane probed with a 1/500 dilution of pre-immune serum (Figure 18). The anti-serum recognized many protein bands, all of which were equal or smaller in size than the recombinant HK. There was no recognition of the recombinant HK with the pre-immune serum. Multiple bands recognized by the crude antiserum may have been due to the fact that there was proteolytic degradation of recombinant HK *in vivo*, or that possibly additional *E. coli* proteins were injected accidentally into the rabbit. The antibody titer was sufficient to produce adequate band

intensity with 2 μ g of recombinant protein using a 1/1000 dilution of crude antiserum (Figure 18 lane IS).

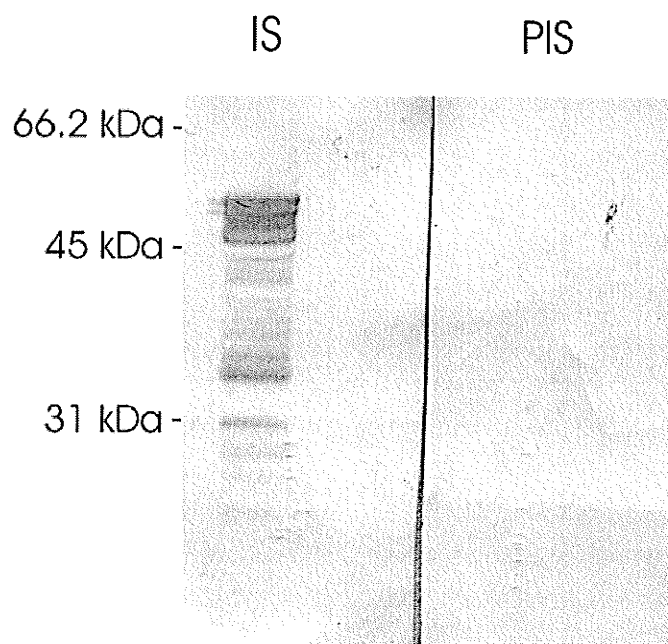


Figure 18. Antiserum testing against recombinant HK. Immunoblot of 2 μ g of recombinant protein in lanes IS and PIS. IS was screened with 1/1000 dilution of crude anti-serum. PIS was screened using a 1/500 dilution of preimmune serum. Staining was allowed to develop for 5 min. Molecular mass was determined using Bio-Rad low range molecular weight standards.

The specificity of the crude antiserum was low when crude potato extracts were probed. The crude-antiserum when used in immunodetection of crude potato extracts resulted in some unspecific protein recognition (Figure 19). This was similar to what was observed with antibodies raised against recombinant Arabidopsis HK1 (Jang *et al.* 1997). For this reason the antibodies (IgGs) were affinity purified. When purified there was significantly less background interference and several of the interfering bands of the crude antiserum were removed (Figure 19). The affinity purified α -HK IgGs were more

specific to proteins with molecular mass corresponding to potato HKs (Figure 19). The pre-immune serum had some faint protein recognition, however, the signal intensity was negligible as compared to the purified IgGs (Figure 19).

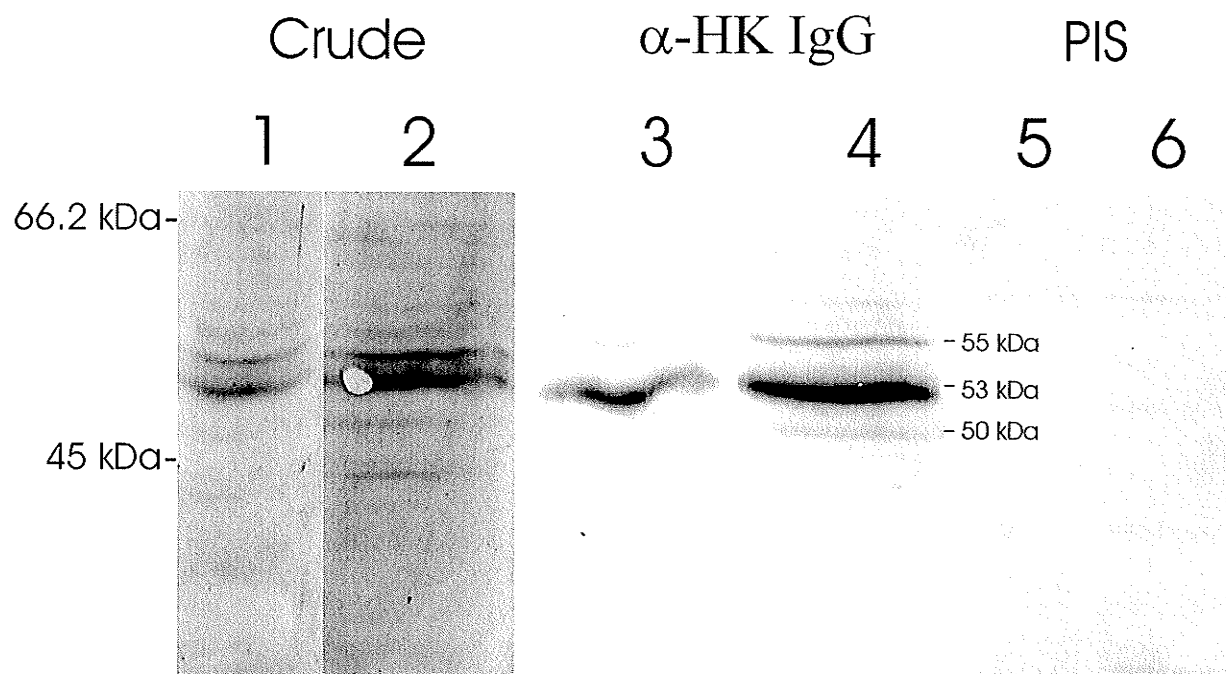


Figure 19. Testing and comparing purified α -HK IgGs with crude and preimmune serum on crude potato protein extracts. Lanes 1, 3 and 5 were loaded with 10 μ g of denatured control potato root extracts. Lanes 2, 4 and 6 were loaded with 20 μ g protein from potato extracts. Lanes 1 and 2 were probed with 1/250 dilution of crude antiserum. Lanes 3 and 4 were probed with affinity purified IgGs (1 in 3 dilution), while lanes 5 and 6 were probed with 1/250 dilution of crude preimmune serum. Development time of 5 minutes was done for all blots. Molecular mass was determined using Bio-Rad low range molecular weight standards.

The affinity purified α -HK IgGs recognized 2 main bands at 55 and 53 kDa respectively (Figure 19). There is also a minor band, which appears at 50 kDa. The band appearing at 53 kDa corresponds to a protein of the molecular weight of the gene published for STHK2. The 55 kDa band corresponds to the predicted molecular mass of

the gene published for STHK1. The minor band that appears at 50 kDa is presumably a degradation product of the existing HKs, since the intensity of this band increases with increasing HK levels. A major protein band of approximately 54 kDa was present when screening using the crude antiserum, however since it was removed after affinity purification it is not believed to be a HK isoform (Figure 19).

There has been only one report of the production of antibodies against plant HKs in the literature (Jang *et al.* 1997). This is interesting since there have been many studies in isolating and characterizing the different plant HK isoforms. Western blots are invaluable in determining the comparative levels of the protein concentration in various tissue, and induction conditions. The lack of antibodies to plant HKs may indicate difficulties involved in producing the required protein or low immunogenic responses in animals. However, the reasoning for the lack of antibodies developed is difficult to ascertain, since researchers typically do not publish results from unsuccessful experiments.

4.3 Plant transformation vectors

4.3.1 Sense construct

The HK over-expressing vector was assembled as described in the Materials and Methods. The full length cDNA was inserted between the *HpaI* and *ClaI* site of pGA643. When the ligated vector was transformed into HB101 cells, two different ligation conditions resulted in the production of three antibiotic resistant colonies (LB 10 mg/l kanamycin and 2 mg/l tetracycline). These colonies were named A1, B1 and B2. Plasmids isolated from these colonies were analyzed by digestion with, *BamHI* and

*Bam*HI/*Cla*I. Of the three colonies tested only colonies A1 and B2 generated the 2.3 kb fragment from the *Bam*HI digest (Figure 20, lanes 4 and 8) and the 1.8 and 2.3 kb bands from the *Bam*HI/*Cla*I digest (Figure 20, lanes 5 and 9). A reduction in size of the top fragment of B1 digested with *Bam*HI/*Cla*I indicates the presence of insert, however there were no clear bands at 1.8 and 2.3 kb (Figure 20, lane 7).

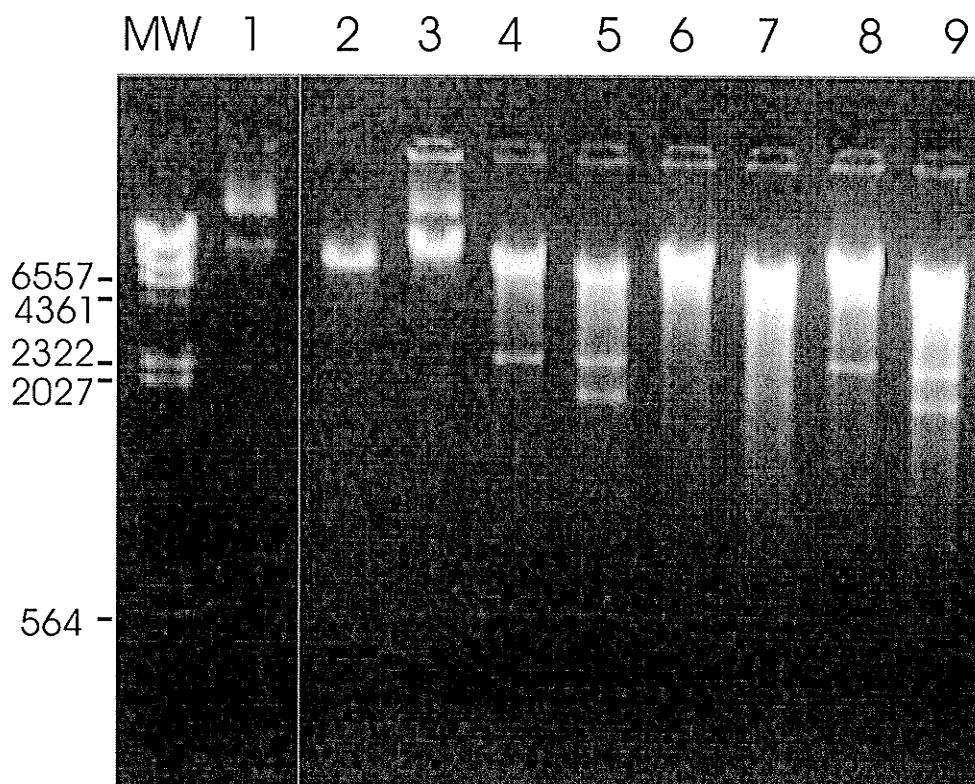


Figure 20. TBE gel of the restriction analysis of plasmids isolated from various *E. coli* colonies containing the sense construct. Lane 1 contains undigested pGA643. Lane 2 is pGA643 digested with *Bam*HI. Lanes 3,4 and 5 is A1 plasmid undigested, *Bam*HI digested and *Bam*HI/*Cla*I digested respectively. Lanes 6 and 7 is B1 plasmid *Bam*HI digested and *Bam*HI/*Cla*I digested respectively. Lanes 8 and 9 is B2 plasmid *Bam*HI digested and *Bam*HI/*Cla*I digested respectively. MW is λ /*Hind*III DNA standards.

Plasmids isolated from colonies A1 and B2 were used to transform *A. rhizogenes* A4. The A1 plasmid resulted in no antibiotic resistant *A. rhizogenes* (MYA with 20 mg/l kanamycin and 4 mg/l tetracycline) colonies being formed. The B2 isolated plasmid produced four *A. rhizogenes* antibiotic resistant colonies, named B21, B22, B23 and B24. The plasmids from the 4 colonies were analyzed for the presence of the insert by digesting with *Bam*HI. All 4 plasmids produced the appropriate 2.3 kb band (Figure 21 lanes 2-5), and were used in plant transformations.

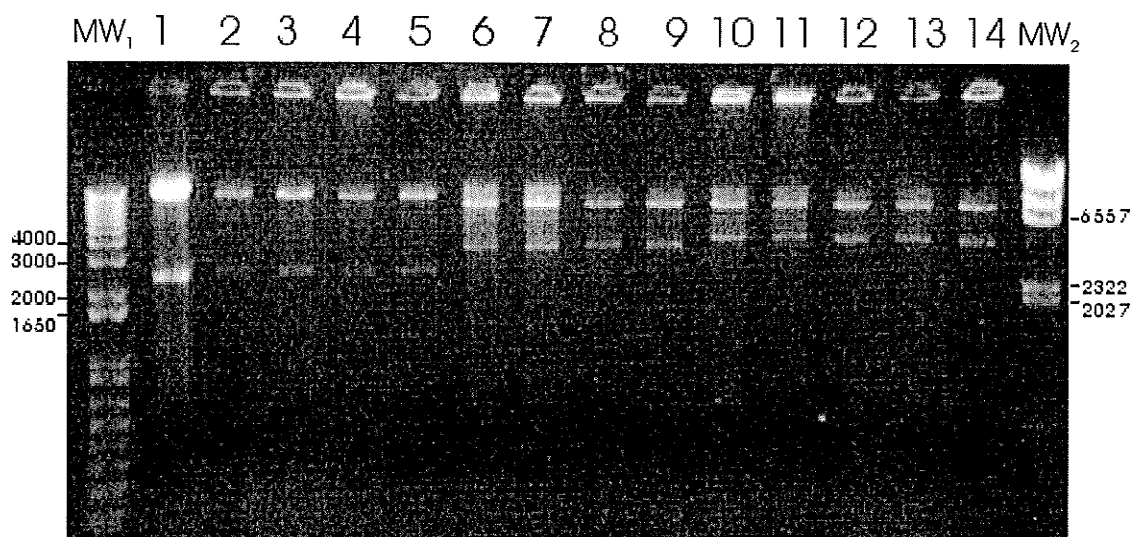


Figure 21. TBE gel of S-1, AS-2 and AS-3 constructs from *A. rhizogenes*. Lane 1 in *E. coli* isolated plasmid B2 digested with *Bam*HI. Lanes 2-5 contain isolated plasmids B21-B24 digested with *Bam*HI. Lanes 6-9 contain isolated plasmids AD21-AD24 digested with *Bam*HI. Lanes 10-14 contain isolated plasmids AG11, AG12, AG21, AG22 and AG51 respectively digested with *Bam*HI. MW₁ is 1 KB+ molecular markers while MW₂ is λ /HindIII DNA standards.

4.3.2 Antisense constructs

The different antisense constructs used vary in the length of sequence used: AS-1 is 612 bp, AS-2 is 1223 and AS-3 is 1846 bp. Comparing the individual shortened antisense sequences with the STHK1 and STHK2 sequences indicate relatively equal levels of similarity between all 3 constructs. Table 1 summarizes the similarity between each antisense sequence and STHK1 and STHK2. Similarity was very high between all three antisense sequences and STHK2, with 99 or 98 % identities. The level of HK2 repression was anticipated to be high. The homology of the antisense sequences to STHK1 was somewhat lower, ranging from 87% for AS-1 to 84 % for AS-2 and AS-3. However, the efficiency of gene reduction using antisense technology is difficult to predict and may rely on chance to produce the correct identities between sequences (Inouye 1988; van der Krol *et al.*1988b).

Table 1. Similarity between antisense sequences and STHK genes. The similarity between the various antisense sequences used was compare to STHK1 and STHK2 using Blast2 alignments. The scores are based on % identities with standard gap penalties. AS-1 is antisense-1, AS-2 antisense-2 and AS-2 antisense-3.

| HK Gene | Antisense Construct | | |
|---------|---------------------|------|------|
| | AS-1 | AS-2 | AS-3 |
| STHK1 | 87 % | 84 % | 84 % |
| STHK2 | 99 % | 98 % | 99 % |

4.3.2.1 Antisense-1

The antisense-1 construct used the 5' end sequence of the SCHK cDNA in the anti-sense orientation. The 612 bp fragment was ligated between the *HpaI* and *XbaI* sites of pGA643, and used to transform HB101 cells. The transformation produced six antibiotic resistant colonies from three different ligation reactions. These colonies were named J1, J2, J3, K1, K2 and L1. The plasmids isolated from these colonies were analyzed by *BamHI* and *BamHI/ClaI* restriction digestion. The plasmids containing the insert in antisense orientation were expected to produce a 3.1 kb fragment from the *BamHI/ClaI* digest as opposed to 2.5 kb fragment, which is produced by the empty pGA643 plasmid (Figure 22). From Figure 22 it is clear that colonies K1 (lane 3), K2 (lane 4) and L1 (lane 5) produced the appropriate sized fragments, as well as colony J3 (not shown).

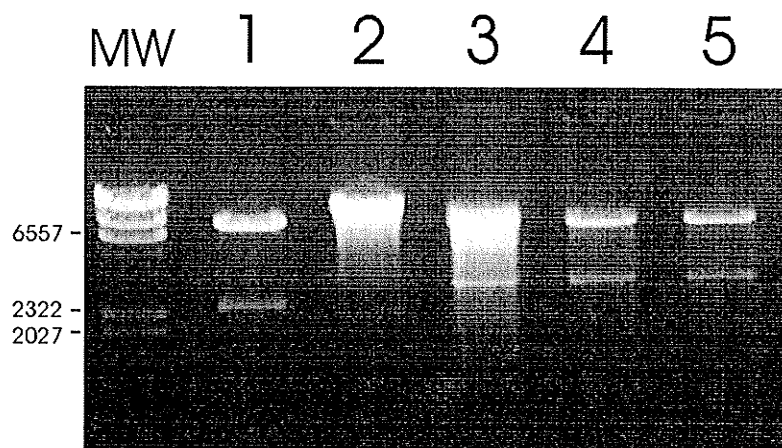


Figure 22. TBE gel of AS-1 plasmids isolated from various *E. coli* colonies. Lane 1 contains pGA643 digested with *BamHI/ClaI*. Lane 2 contains plasmid K1 digested with *BamHI*. Lane 3, 4 and 5 contain plasmids K1, K2 and L1 digested with *BamHI/ClaI*. MW is λ /HindIII DNA standards.

The plasmids isolated from J3, K1, K2 and L1 were used to transform *A. rhizogenes*. Over 50 antibiotic resistant colonies resulted from these 4 transformations. From these, two *A. rhizogenes* colonies from each plasmid were analyzed for the presence of the transformation vector. These colonies were named J31, J32, K11, K12, K21, K22, L11 and L12 respectively (Figure 23 lanes 1-8). Plasmids isolated from these colonies produced the appropriate 2.5 kb band when digested with *Bam*HI (Figure 23). These *A. rhizogenes* colonies were used to transform potatoes.

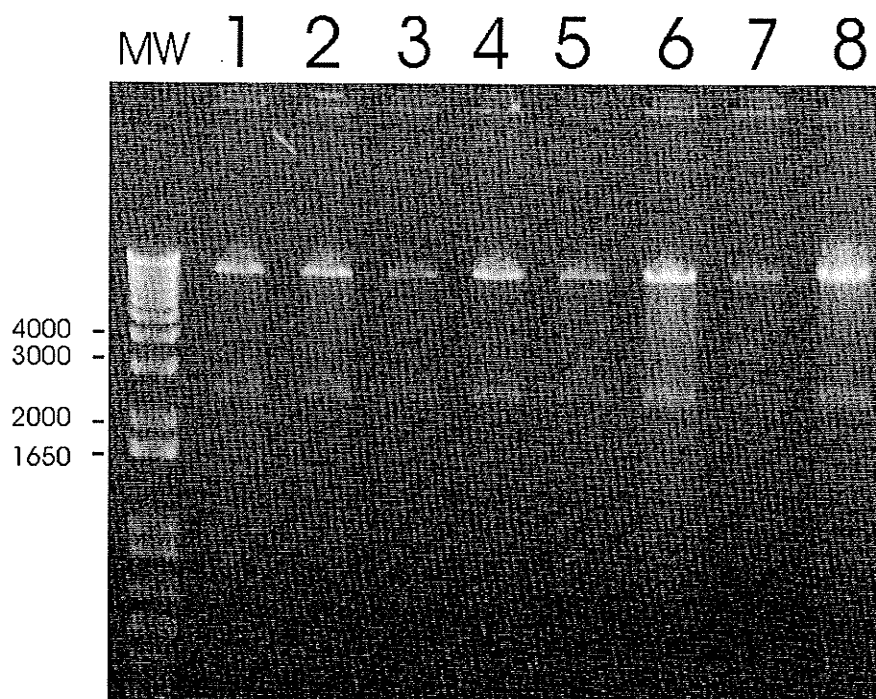


Figure 23. TBE gel of AS-1 plasmids isolated from *A. rhizogenes*. Lanes 1-8 contain plasmids J31, J32, K11, K12, K21, K22, L11 and L12 digested with *Bam*HI respectively. MW is 1 kb+ DNA standards.

4.3.2.2 Antisense-2 construct

The antisense-2 construct used the 3' end of the SCHK cDNA in antisense orientation. The 1223 bp insert was blunt ended, and could be inserted in either the sense or anti-sense orientation at random, in the *HpaI* site of pGA643. The ligated plasmids were used to transform HB101 cells. Six antibiotic resistant colonies were produced from three separate ligation reactions. These resistant colonies were labeled AC1, AD1, AD2, AD3, AD4 and AE1. Plasmids isolated from the resistant colonies were digested using *BamHI*, if the insert was in the antisense orientation a 3.7 kb fragment would be generated, if the insert was in the sense orientation a 2.5 kb fragment would be generated. Of the six plasmids tested only AD2 and AD4 produced a 3.7 kb fragment, which is the correct size (Figure 24 lanes 3 and 5).

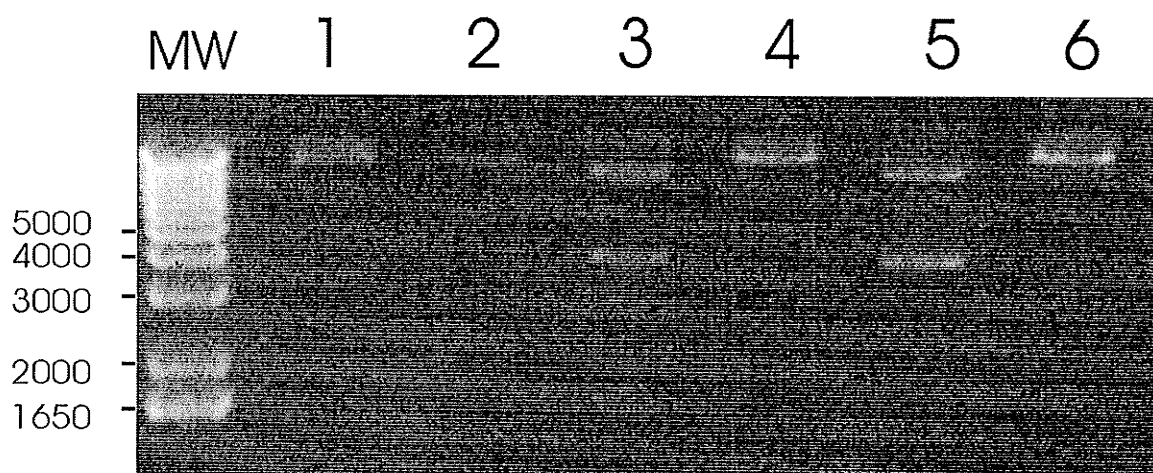


Figure 24. TBE gel containing plasmids from AS-2 *E. coli* colonies. Lanes 1-6 contain the plasmids AC1, AD1, AD2, AD3, AD4 and AE1 digested with *BamHI* respectively. MW is 1 kb+ molecular markers.

The plasmids from AD2 and AD4 were used to transform *A. rhizogenes*. A total of 12 antibiotic resistant colonies grew, all of which were from the AD2 plasmid. Four of the 12 colonies were analyzed for the presence of the correct insert. These colonies were named AD21, AD22, AD23 and AD24 (Figure 21 lanes 6-9). All of the plasmids analyzed by restriction digestion with *Bam*HI produced the appropriate 3.7 kb fragment. The confirmed *A. rhizogenes* lines were then used to transform potato.

4.3.2.3 Antisense-3 construct

The antisense-3 construct used the full length SCHK cDNA in antisense orientation. The 1846 bp fragment was inserted between the *Hpa*I and *Xba*I sites of pGA643. The ligated plasmids were used to transform HB101 cells. Ten antibiotic resistant colonies were obtained from three separate ligation reactions. These colonies were labeled AF1, AF2, AG1, AG2, AG3, AG4, AG5, AI1, AI2 and AI3. Plasmids isolated from these colonies were analyzed by restriction digestion with *Bam*HI. Plasmids containing the insert were expected to produce a 4.3 kb fragment from the *Bam*HI digestion (Figure 25). The plasmids from the colonies AG1 (lane 3), AG2 (lane 4), AG3 (lane 5), AG5 (lane 7), AI1 (lane 8) and AI2 (lane 9) all produced DNA fragments of the proper length.

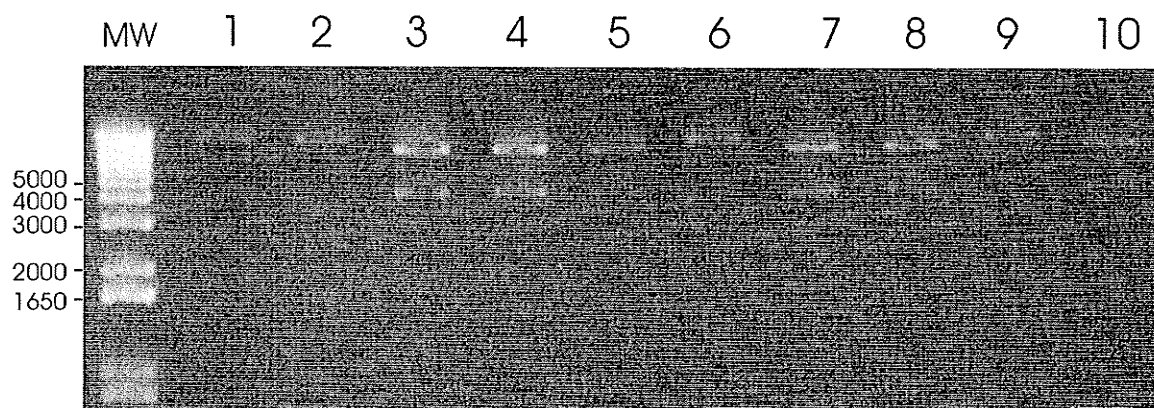


Figure 25. TBE gel of AS-3 plasmids isolated from *E. coli* colonies. Lanes 1-10 contain the plasmids AF1, AF2, AG1, AG2, AG3, AG4, AG5, AI1, AI2 and AI3 all digested with *Bam*HI. MW is 1 kb+ molecular markers.

These five plasmids were used to transform *A. rhizogenes*. More than 60 antibiotic resistant A4 colonies were formed. Of these resistant colonies two from each plasmid were selected. They were named AG11, AG12, AG21, AG22, AG31, AG32, AG51, AG52, AI11 and AI12 respectively. No antibiotic resistant colonies were formed from the AI12 plasmid. Plasmids were isolated and analyzed by digestion with *Bam*HI. All of the plasmids tested generated the expected 4.3 kb fragment (Lanes 10-14, figure 21). These plasmid containing *A. rhizogenes* lines were used to transform potato.

4.3.3 Control vector

pGA643 plasmids, undigested and with no insert were used to produce control root lines. These were required to ensure that the transformation events did not cause alterations in the tissues metabolic activity. When used to transform *A. rhizogenes* four

colonies were isolated on MYA 20 mg/l kanamycin and 4 mg/l tetracycline. These colonies were named P1, P2, P3 and P4. Presence of the plasmid was confirmed using restriction analysis with *Bam*HI/*Cla*I a 2.5 kb fragment was produced, as expected (Figure 26). These *A. rhizogenes* colonies containing the pGA643 plasmid were then used to transform potato.

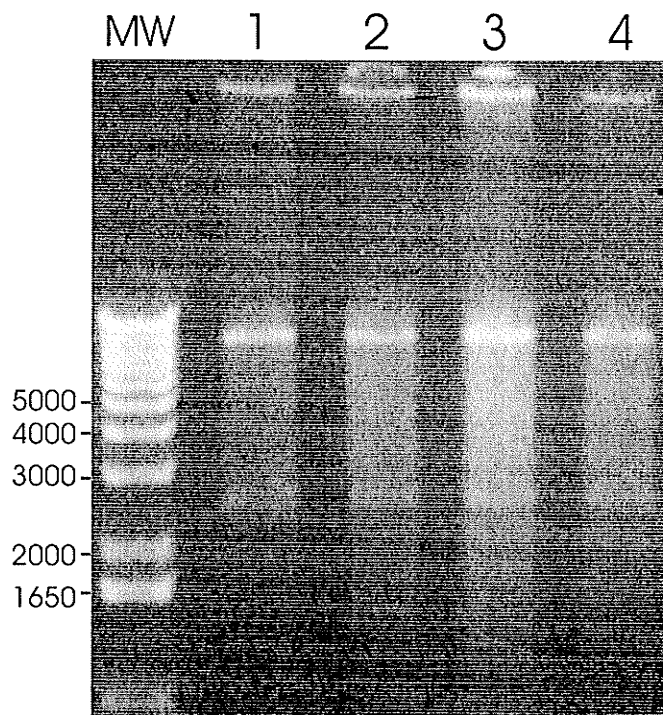


Figure 26. TBE gel containing digested empty pGA643 plasmids isolated from *A. rhizogenes*. Lane 1-4 contain plasmids from colonies P1-P4 respectively, each digested with *Bam*HI/*Cla*I. MW is 1 kb+ molecular markers.

4.4 Potato stem transformations

Following the verification of vector with the correct insert in *A. rhizogenes*, potato transformations were performed. The transformations took place in small sterile jars, which contained either 3 or 4 sterile stem segments. Seven separate transformation sets

were performed. The total number of available lines was in excess of 500, however the maintenance of these lines was unnecessary and were not subcultured to completion, due to rapid identification of lines with altered HK protein levels.

The 281 subcultured lines represented a population comprising all the *E. coli* produced vectors, and the majority of the successfully transformed *A. rhizogenes* with confirmation of the presence of the appropriate transformation vector (Table 2).

Table 2. Summary of transformations and clones produced. S-1 is the sense construct. AS-1, AS-2 and AS-3 have been previously defined. The control transformations are potatoes transformed with an empty pGA643 vector.

| Vector | Number of Transformations Events | Number of Clones |
|---------|-------------------------------------|------------------|
| S-1 | 31 | 30 |
| AS-1 | 94 | 89 |
| AS-2 | 34 | 65 |
| AS-3 | 80 | 82 |
| Control | 37 | 15 |
| Total | 276 | 281 |

The individual root lines were labeled based on the *A. rhizogenes* line used in their production. For instance *A. rhizogenes* line B23 gave rise to the root lines B23001-B23020. The numbering of the root lines was based on the order in which they were placed onto antibiotic free MS media.

4.5 Screening of transgenic roots by evaluating hexokinase protein levels

The primary screening for altered HK levels was performed by immunodetection using affinity purified IgGs raised against the recombinant HK. Comparisons were made between the staining intensity of the HK band of 53 kDa of the transgenic lines and that of the control lines, using the ImageJ software. The HK levels were expressed as a proportion of the control HK level. An example is presented in Figure 27. A protein extract of the pGA643 transformed control line P2007 was loaded in lane 1 and serves as the reference for all the other lines tested. AD21008 loaded in lane 2 had 0.45-fold HK level as control, in lanes 3 AD23019, lane 4 AD24007, lane 5 AD24011 and lane 6 L12006 there is no difference compared to the control line. AG51008 loaded in lane 7 displayed 0.5-fold the control HK level, while B22003 loaded in lane 8 displays 4-fold the control HK level. The extraction and immunoblotting of all lines displaying altered HK was repeated with similar results to ensure that alteration in HK was not artifactual.

Many lines were screened to identify the distinct clones with altered HK levels (Table 3). The production of overexpressing lines was relatively efficient. The screening of 13 clones led to eight sense lines that represented a broad range of altered HK levels (Table 3). The degree of HK overexpression ranged from 1.5 to 4-fold control levels (Figure 28). The discovery of the eight sense lines removed the need for the further screening of additional sense lines. This level of increased protein is similar to but slightly lower than the 5 to 10-fold increase in HK protein observed in transgenic *Arabidopsis* seedlings over producing HK1 (Jang *et al.* 1997).

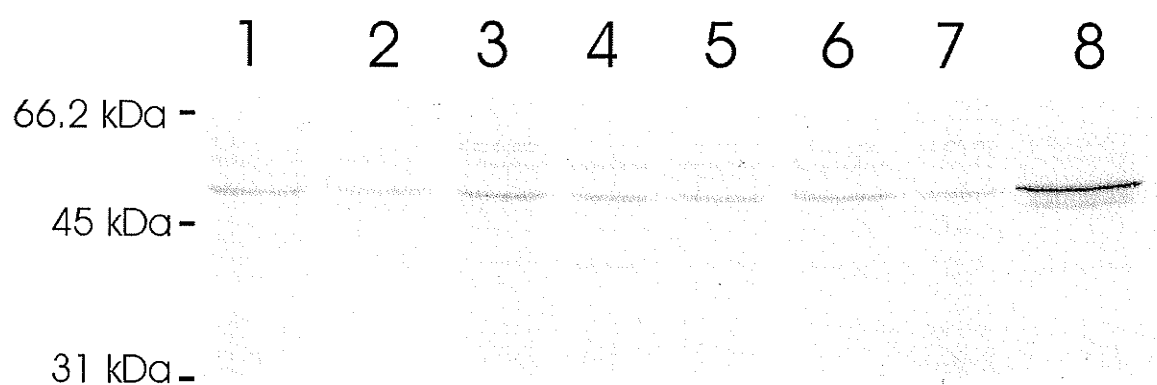


Figure 27. Sample of immunodetection HK screening. All lanes were loaded with 20 μ g protein from crude extracts, and screening with affinity purified α -HK IgGs. Lane 1 contained control line P2007. While lanes 2-8 were loaded with AD21008 (AS-2), AD23019 (AS-2), AD24007 (AS-2), AD24011 (AS-2), L12006 (AS-1), AG51008 (AS-3) and B22003 (S-1) respectively.

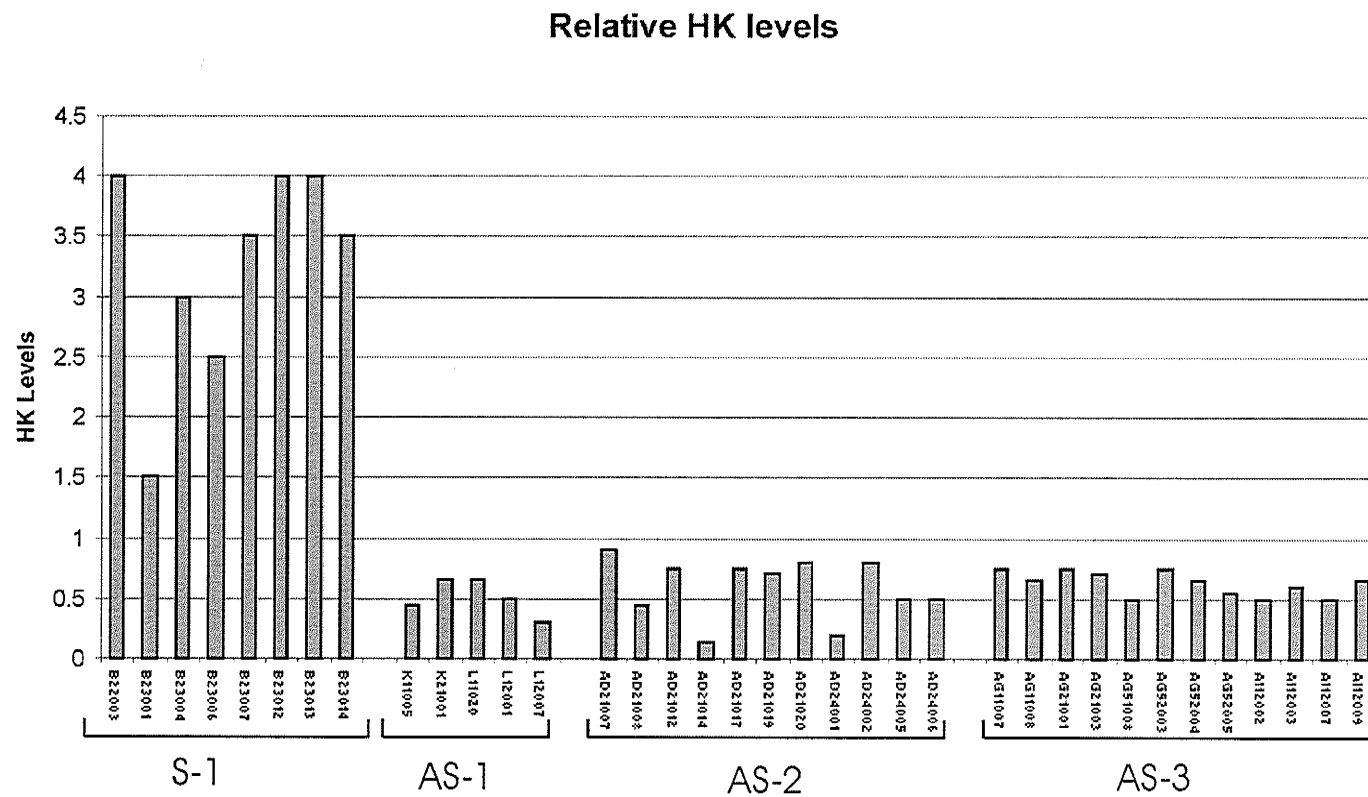


Figure 28. HK levels of individual root lines. HK levels were determined by comparing staining intensities of immunoblots against control lines, HK level = measured value/control value. 2 or 3 separate measurements were performed for each line. The lines B22003 - B23014 are contain the S-1 constructs, K11005- L12007 contain the AS-1 construct , AD21007 - AD24006 contain the AS-2 construct and AG11007-AI12009 contain the AS-3 construct.

None of the 13 S-1 lines tested displayed any significant reduction in protein level. Gene silencing of endogenous genes by co-suppression is dependent on the degree of sequence similarity. Co-suppression can occur more than 25% of the time when endogenous genes are used to transform plants (van der Krol *et al.* 1990a). The fact that no co-suppression was observed in the sense lines was surprising, given to the very high similarity between SCHK and STHK2. However, a sample size of only 13 was statistically insufficient to conclude that there was no co-suppression in any of the transgenic lines; screening of additional S-1 lines may reveal reduction in HK2 protein.

Table 3. The efficiency of altering HK levels of the individual constructs.

| Construct | Number of Lines Screened | Number with Altered HK Protein Levels |
|-----------|--------------------------|---------------------------------------|
| S-1 | 13 | 8 (increased) |
| AS-1 | 19 | 5 (decreased) |
| AS-2 | 31 | 11 (decreased) |
| AS-3 | 38 | 12 (decreased) |

Identification of root lines displaying reduced HK levels was far more difficult than identifying overexpressing lines. Difficulty of identification of the antisense lines was due to the relatively low intensity of the HK band, since the signal to noise ratio is relatively low. The efficiency for decreasing HK protein levels is highest in AS-2

constructs (Table 3). Thirty five % of the AS-2 lines screened revealed a reduction in HK levels as compared to 26% for AS-1 and 31% for AS-3. The degree of decrease in HK protein levels was also highest in the AS-2 lines screened, 2 AS-2 lines (AD24001 and AD21014) displayed levels under 0.2-fold that of the controls. The lowest HK level observed in AS-1 was 0.3-fold control levels (L12007) and the lowest AS-3 lines observed were 0.5-fold control levels (AG51008, AI2002 and AI2007) (Figure 28).

The level of reduction in HK protein was significantly greater in our antisense HK potato roots than observed in transgenic antisense HK1 *Arabidopsis*. In *Arabidopsis* 0.5-fold control levels of HK1 were present in 6 day old seedlings and there was almost no reduction of HK1 in 18 day old seedlings (Jang *et al.* 1997). Similar to what was seen by Jang *et al.* (1997) only the HK isoform that the antibody was raised against displayed any reduction in protein level.

4.6 Hexokinase activity measurements

The lines displaying altered HK protein levels were analyzed *in vitro* for altered enzyme activity. The change in protein level was expected to alter the enzyme activity proportionately. The activity was measured using both glucose and fructose as substrates. Phosphorylation activity using glucose (1 mM) as a substrate is called glucokinase (GK) activity, while activity when fructose (1 mM) is used as a substrate is called fructokinase (FK) activity. All activity measurements were calculated as mU/ mg protein as described in the Materials and Methods. The activity measurements were repeated several times in order to establish whether or not the observed differences were significant.

4.6.1 Control lines

Two control lines were used for measuring the GK and FK activities. The HK activities were determined to be 7.30 ± 0.78 mU GK and 13.98 ± 1.52 mU FK for P2012. For P2004 the values were 9.84 ± 0.93 mU and 17.5 ± 1.25 mU for GK and FK respectively (Table 4). These values represent the average of the range of activities displayed by the control lines (Figure 28). The GK activity in P2012 was 60 ± 6.25 mU/gram fresh weight (g-fw), which is similar to the GK activities reported in wild type potato leaves of 61-72 mU/g-fw (Veramendi *et al.* 1999). The GK levels in control roots are significantly lower than the values reported for tubers of 101-106 mU/g-fw (Veramendi *et al.* 1999). This is not unexpected since the requirement of sugar phosphorylation varies from tissue to tissue (Renz *et al.* 1993).

The FK/GK ratios for the control lines were 1.92 and 1.78 respectively (Table 4). The FK/GK ratio from control roots differed significantly from that observed in growing potato tubers and leaflets (Renz *et al.* 1993). There, the FK/GK ratio varies from 18.9 in young growing tubers to 0.45 in germinating tubers, while leaf tissue has a ratio of 2.5 (Renz *et al.* 1993). The root FK/GK ratio most closely resembles that of stored tubers of 1.5 (Renz *et al.* 1993), where both SuSy and invertase are used in sucrose metabolism. The root lines used in our activity measurement experiments were grown in liquid MS media, which contained 3% w/v sucrose. This high concentration of sucrose in the root lines may alter the activity of invertase and SuSy as compared to non-transformed roots. Growing the roots on sucrose free media may result in different FK/GK ratios.

Table 4. Hexokinase activity of the various transgenic root lines. Activities are in mU/mg protein in all cases. Glucokinase (GK) activity was determined by assaying in the presence of 1 mM glucose. Fructokinase (FK) activity was determined by assaying in the presence of 1 mM fructose. ND is not determined.

| Root Line (Construct) | Number of Replicates | GK Activity +/- SE | FK Activity +/- SE | FK/GK ratio |
|--------------------------|----------------------------|-----------------------|-----------------------|----------------|
| AD24001 (AS-2) | 9 | 5.44 +/- 0.43 | 10.91 +/- 0.69 | 2.00 |
| AD21014 (AS-2) | 6 | 5.78 +/- 0.29 | 13.39 +/- 0.72 | 2.32 |
| AG52005 (AS-3) | 4 | 6.31 +/- 0.99 | 17.53 +/- 1.94 | 2.78 |
| L12007 (AS-1) | 6 | 7.48 +/- 0.96 | ND | ND |
| AG11008 (AS-3) | 4 | 7.81 +/- 1.52 | 22.38 +/- 3.01 | 2.87 |
| AD24006 (AS-2) | 4 | 8.10 +/- 0.81 | 17.46 +/- 2.08 | 2.15 |
| AD24005 (AS-2) | 7 | 8.21 +/- 1.08 | ND | ND |
| AD21008 (AS-2) | 4 | 8.83 +/- 0.40 | ND | ND |
| AD21019 (AS-2) | 4 | 9.79 +/- 2.51 | ND | ND |
| AG11007 (AS-3) | 4 | 9.66 +/- 1.05 | 20.66 +/- 1.17 | 2.14 |
| P2012 (Control) | 4 | 7.30 +/- 0.78 | 13.98 +/- 1.52 | 1.92 |
| P2004 (Control) | 7 | 9.84 +/- 0.93 | 17.55 +/- 1.25 | 1.78 |
| B23006 (S-1) | 7 | 12.34 +/- 0.22 | 21.69 +/- 1.70 | 1.76 |
| B23014 (S-1) | 5 | 26.17 +/- 2.62 | 35.25 +/- 3.13 | 1.35 |
| B23012 (S-1) | 4 | 43.03 +/- 10.42 | ND | ND |
| B22003 (S-1) | 4 | 55.03 +/- 8.18 | 70.57 +/- 0.37 | 1.28 |

4.6.2 Sense lines

The level of HK activity measured in the sense lines represented a significant increase over the controls in all cases. The HK values ranged from 12.34 \pm 0.22 mU GK, 21.69 \pm 1.70 mU FK for B23006 to 55.03 \pm 8.18 mU GK, 70.6 \pm 0.37 mU FK for line B22003 (Table 4). This represents a GK activity range comprised between 1.4 to 6.4-fold of controls (Figure 29) and a FK activity range of 1.4 to 4.5-fold. The FK/GK activity ratio is 1.75 for both lines B23006 and B23014, however B22003 line has a lower ratio of 1.3.

The level of increase in HK activity is greater than that observed in transgenic potato leaves and tubers overexpressing HK1 (Veramendi *et al.* 1999). Leaves overexpressing HK1 had an increase in activity as great as 4.8-fold compared to wild type levels. Tubers had a maximal HK activity increase of 2-fold wild type (Veramendi *et al.* 1999). Similar values were found in transgenic *Arabidopsis* seedlings overexpressing HK1, where HK increased up to 5-fold control levels (Jang *et al.* 1997). Transgenic tomatoes homozygous for *Arabidopsis* HK1 overproduction have increases in GK activity of 7-fold the wild type levels (Dai *et al.* 1999). The increase in GK activity of the transgenic roots is within the ranges of those observed in other plants overexpressing HK genes.

The transgenic sense potato roots had a decreased FK/GK ratio as compared to the control lines (Table 4). The decrease in the FK/GK ratio is due to potato HK2 having a V_{max} for fructose of 58% as compared to glucose (HK2 V_{max} 900 mU/mg-protein for glucose, and 528 mU/mg-protein fructose) (Renz and Stitt 1993). Therefore, the greater the increase in SCHK level in potato the lower the FK/GK ratio will become. This was

observed in the line B22003, which had the highest level of HK activity and the lowest FK/GK ratio (Table 4).

4.6.3 Antisense lines

The level of HK activity in the antisense lines varies from 5.44 \pm 0.43 mU GK for AD24001 to 9.79 \pm 2.51 mU GK for AD21019. The GK values represented a range from 0.63 to 1-fold that of the controls. The FK values varied from 10.9 \pm 0.69 mU line AD24001 to 22.3 \pm 3.01 mU line AG11008. The FK values represent a range from 0.7 to 1.4-fold the control levels. A significant increase in FK activity over that of the control lines was observed in lines AG11008 and AG11007, which, may be indicative of a FK activity compensation for reduced GK activity. The FK/GK ratios in the antisense lines ranged from 2.0 in line AD24001 to 2.85 in line AG11008.

The level of GK activity decrease was lower than that observed in previous experiments. In antisense HK1 potato leaves the activity was reduced as much as 80% while in tubers the reduction in activity was nearly 70% (Veramendi *et al.* 1999).

The reduction in HK activity observed in the antisense root lines was less than that observed in tubers and leaves (Veramendi *et al.* 1999). Since there is no published information describing the isoform distribution in potato root the explanation for this is unclear. If there was a greater proportion of HK1 in the roots, using antisenses with HK2 would be less efficient than if the main root HK isoform was HK2. As seen in Veramendi *et al.* (1999) the reduction of HK2 activity was approximately 50% in antisense HK1 tubers. This is supported by the increases in the FK/GK ratios of the antisense lines.

Reduction in HK2 levels as expected would lead to an increase in the FK/GK ratios since all other HK isozymes have equal or higher activities with fructose (Renz and Stitt 1993).

The increase of FK activity in several of the antisense lines as compared to the controls is interesting. This induction of FK activity may occur in order to compensate for the decrease in glucose phosphorylation, and switching to the use of fructose as the primary glycolytic substrate. The reaction catalyzed by SuSy converts sucrose to fructose and UDP-glucose (Figure 2). This may serve as an alternative to HK phosphorylation of glucose, while glycolysis is continued using FK and UDP-glucose pyrophosphorylase.

From the antisense constructs used in the production of transgenic roots the greatest reduction in GK activity was found in the AS-2 construct. This was observed both in protein level through western blots and through enzyme assays (Figure 29). Two of the AS-3 lines, AG52005 and AG11008 had reduced GK activity as compared to the controls. Very few of AS-1 lines were analyzed by activity measurements, due to the lack of tissue produced required for the required sampling. Several factors apart from degree of sequence similarity affect the efficiency of gene silencing by antisense DNA. These factors include, blocking of translation sites and blocking the formation of secondary structures. However, the prediction of the degree of gene silencing by antisense DNA is inaccurate and using several constructs using various lengths increases the chances of significant gene silencing (Mol *et al.* 1990).

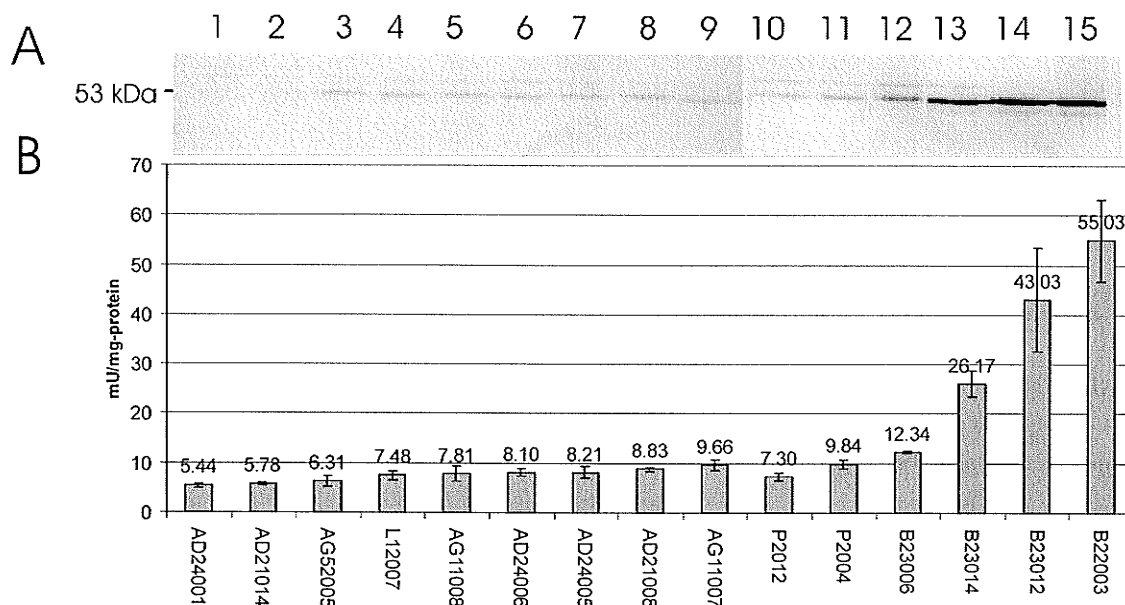


Figure 29. GK activity corresponding to HK protein levels. B. The GK levels for individual lines as measured spectrophotometrically. Bars indicate standard error. A. The western blot overlays the HK protein levels within the individual extract, with 10 μ g of protein from the crude extract loaded. Lanes 1-9 are antisense lines, 10 and 11 are control lines and 12-15 sense lines.

The alteration in GK activity corresponded to a decrease in protein level from Western blots (Figure 29). The level of reduction in protein levels in the antisense lines was not proportionate to the level of decrease in enzyme activity. Presumably this is due to only measuring the level of HK2 accurately by immunodetection. The other HK isoforms (HK1 and HK3) could not be determined by immunodetection, however their activity would still contribute towards the total. In the sense constructs increase in activity corresponded approximately equally with an increase in banding intensity through immunodetection. The banding intensity between B23012 and B22003 cannot be differentiated from these blots, indicating that the banding intensity has reached a point of saturation (Lanes 14 and 15, Figure 29).

4.7 Future studies

The further characterization of the transgenic roots will also be investigated looking at the HK isoform profiles will be generated from the control, antisense and sense root lines. These profiles will determine which HK isoforms are decreased in the antisense and increased in the sense lines, similar to the work published by Veramendi *et al.* (1999) with potato tubers. The isoform profile from the control lines can serve to complement the previously published profiles of potato tubers and leaves (Renz and others 1993). Western blot analysis of the collected HK isoforms will also verify the speculations made in respect to multiple bands visualized during immunodetection of crude protein extracts.

The ultimate application of this research is to determine the effect of HK on the rate of glycolysis during O₂ limitations. The degree of regulation that HK exerts will be measured using Metabolic Control Analysis. The rate of glycolytic flux will be measured for the individual root lines during anoxia, by tracking the path of radioactive carbon (¹⁴C). A comparison will then be made between the rate of glycolytic flux to the relative HK activity within the root line. This comparison is the flux control coefficient (FCC), which is a measure of the degree of control that HK exerts on glycolysis. If the FCC for HK in potato roots is high, as it has been found in animal systems (Rapoport *et al.* 1974; Agius *et al.* 1996), it may be used as a potential target for genetic engineering of resistance to anoxic and hypoxic stress. These findings will help to indicate the significance of HK induction during O₂ limitation.

5.0 CONCLUSIONS

In plant systems, hexokinase (HK) has been speculated to play a key role in controlling the rate of glycolytic flux. This hypothesis is supported by three main lines of evidence. i) HK is preferentially induced during anoxia in some plant systems. ii) during anoxia, HK activity is decreased by a reduction in cellular pH and ATP/ADP ratios. iii) experimental evidence in animal systems where the control that HK displays was determined to be very high. In this thesis, the initial requirements for the determination of the degree of control HK exerts on plant glycolysis were developed. This included the sequencing of a HK cDNA clone, the production of an antibody raised against recombinant HK, development and characterization of transgenic potato root lines with altered HK levels.

A HK cDNA clone from *Solanum chacoense* was sequenced and then compared to various plant and non-plant HKs. The nucleotide and amino acid sequence was nearly identical to *S. tuberosum* HK2. There was also significant similarity between the SCHK clone and various plant HKs examined, including STHK1 making an ideal gene for use in genetic engineering. The similarity was less when compared to mammalian and yeast HKs, however the domains responsible for phosphate binding were conserved similar to those observed in previous studies.

Recombinant SCHK was produced using a prokaryotic expression system. This protein was purified and used to produce rabbit α -HK antiserum. The specificity of the crude antiserum was low and affinity purification was required. The production of antibodies against plant HKs are rare in the literature, the only example was in *Arabidopsis* where α -HK1 antibodies were produced. The α -HK IgGs identified four

clear bands from immunodetection of crude potato root extracts, which may correspond to the different HK isoforms in potato. HK isoform purification would be required in order to confirm this antibody recognize the three isoforms.

Through the use of sense and antisense constructs, it was possible to engineering potato roots to produce altered levels of HK, by using *Agrobacterium rhizogenes* mediated transformations. The transgenic roots were screened by immunodetection with the α -HK IgG and by activity assays using both glucose and fructose as substrates. Modification of HK protein level corresponded to a proportional alteration in HK enzyme activity indicating the transgenic protein is active.

The transgenic lines produced provided a wide range of HK levels, ranging from 0.6 to 6.4-fold the control HK activity when using glucose (GK) as a substrate and 0.7 to 4.8-fold with fructose (FK). This range is comprised of 16 different transgenic root lines and is similar to the range of HK activities engineered in transgenic potato leaves. The ratio of activities of FK/GK increased compared to controls with decreasing total HK activity, and the ratio decreased with increasing total activity. This was expected due to the altered HK2 activity from potato when using different substrates. This range of lines is broad enough to perform detailed studies using Metabolic Control Analysis (MCA).

With the use of MCA, the extent of control exerted by HK on anoxia metabolism can be determined using these transgenic lines. The findings from these studies should provide scientist with an improved, general understanding of the regulation of primary plant metabolism. This knowledge could have implications to improve the process of metabolic engineering whereby carbon flux could be redirected from glycolysis in order to produce desired chemical compounds.

REFERENCES

- Agius L, Peak M, Newgard CB, Gomez-Foix AM, Guinovart JJ. 1996. Evidence for a role of glucose-induced translocation of glucokinase in the control of hepatic glycogen synthesis. *J Biol Chem* 271:30479-86.
- An G, Ebert PR, Mitra A, Ha SB. 1988. Binary Vectors. *Plant Mol Biol* A3:1-19.
- Anderson CM, Stenkamp RE, McDonald RC, Steitz TA. 1978b. A refined model of the sugar binding site of yeast hexokinase B. *J Mol Biol* 123:207-19.
- Anderson CM, Stenkamp RE, Steitz TA. 1978a. Sequencing a protein by x-ray crystallography. II. Refinement of yeast hexokinase B co-ordinates and sequence at 2.1 Å resolution. *J Mol Biol* 123:15-33.
- Andrews DL, Cobb BG, Johnson JR, Drew MC. 1993. Hypoxic and anoxic induction of alcohol dehydrogenase in roots and shoots of seedlings of *Zea mays*. Adh transcripts and enzyme activity. *Plant physiol* 101:407-14.
- Andrews DL, Drew MC, Johnson JR, Cobb BG. 1994. The response of maize seedlings of different ages to hypoxic and anoxic stress. Changes in induction of Adh1 mRNA, ADH activity, and survival of anoxia. *Plant physiol* 105:53-60.
- ap Rees T, Hill SA. 1994. Metabolic control analysis of plant metabolism. *Plant cell environ* 17:587-99.
- Appleby CA, Bogusz D, Dennis ES, Peacock WJ. A role for haemoglobin in all plant roots? *Plant cell environ.* 11, 359-367. 1988.
- Armstrong W. 1979. Aeration in higher plants. *Adv Botany Research* 7:225-32.
- Atkinson DE, Walton GM. 1967. Adenosine triphosphate conservation in metabolic regulation. Rat liver citrate cleavage enzyme. *J Biol Chem* 242:3239-41.
- Bahramian MB, Zarbl H. 1999. Transcriptional and posttranscriptional silencing of rodent alpha1(I) collagen by a homologous transcriptionally self-silenced transgene. *Mol Cell Biol* 19:274-83.
- Barclay AM, Crawford RMM. 1982. Plant growth and survival under strict anaerobiosis. *J Exp Bot* 33:541-9.
- Benfey PN, Ren L, Chua NH. 1990. Tissue-specific expression from CaMV 35S enhancer subdomains in early stages of plant development. *EMBO J* 9:1677-84.

Bennett WS, Jr., Steitz TA. 1980. Structure of a complex between yeast hexokinase A and glucose. II. Detailed comparisons of conformation and active site configuration with the native hexokinase B monomer and dimer. *J Mol Biol* 140:211-30.

Bork P, Sander C, Valencia A. 1992. An ATPase domain common to prokaryotic cell cycle proteins, sugar kinases, actin, and hsp70 heat shock proteins. *Proc Natl Acad Sci U S A* 89:7290-4.

Bork P, Sander C, Valencia A. 1993. Convergent evolution of similar enzymatic function on different protein folds: the hexokinase, ribokinase, and galactokinase families of sugar kinases. *Protein Sci* 2:31-40.

Bosher JM, Labouesse M. 2000. RNA interference: genetic wand and genetic watchdog. *Nat Cell Biol* 2:E31-E36.

Bouny JM, Saglio PH. 1996. Glycolytic flux and hexokinase activities in anoxic maize root tips acclimated by hypoxic pretreatment. *Plant physiol* 111:187-94.

Boyer JS. 1982. Plant Productivity and environment. *Science* 218:443-8.

Bradford MM. 1976. A rapid and sensitive method for the quantitation of microgram quantities of protein utilizing the principle of protein-dye binding. *Anal Biochem* 72:248-54.

Bucher M, Kuhlemeier C. 1993. Long-term anoxia tolerance. Multi-level regulation of gene expression in the amphibious plant *Acorus calamus* L. *Plant physiol* 103:441-8.

Bucher M, Brändle R, Kuhlemeier C. 1994. Ethanolic fermentation in transgenic tobacco expressing *Zymomonas mobilis* pyruvate decarboxylase. *EMBO J* 13:2755-63.

Cardenas ML, Cornish-Bowden A, Ureta T. 1998. Evolution and regulatory role of the hexokinases. *Biochim Biophys Acta* 1401:242-64.

Carystinos GD, MacDonald HR, Monroy AF, Dhindsa RS, Poole RJ. 1995. Vacuolar H(+)-translocating pyrophosphatase is induced by anoxia or chilling in seedlings of rice. *Plant physiol* 108:641-9.

Chilton MD, Tepfer DA, Petit A, David C, Casse-Delbart F, Tempe J. 1982. *Agrobacterium rhizogenes* inserts T-DNA into the genome of the host plant root cells. *Nature* 295:432-4.

Chuang CF, Meyerowitz EM. 2000. Specific and heritable genetic interference by double-stranded RNA in *Arabidopsis thaliana*. *Proc Natl Acad Sci U S A* 97:4985-90.

Cogoni C, Macino G. 1999. Gene silencing in *Neurospora crassa* requires a protein homologous to RNA-dependent RNA polymerase. *Nature* 399:166-9.

- Couée I, Defontaine S, Carde JP, Pradet A. 1992. Effects of anoxia on mitochondrial biogenesis in rice shoots--modification of in organelle translation characteristics. *Plant physiol* 98:411-21.
- da Silva WS, Rezende GL, Galina A. 2001. Subcellular distribution and kinetic properties of cytosolic and non- cytosolic hexokinases in maize seedling roots: implications for hexose phosphorylation. *J Exp Bot* 52:1191-201.
- Dai N, Schaffer A, Petreikov M, Shahak Y, Giller Y, Ratner K, Levine A, Granot D. 1999. Overexpression of *Arabidopsis* hexokinase in tomato plants inhibits growth, reduces photosynthesis, and induces rapid senescence. *Plant Cell* 11:1253-66.
- Davies D-D, Grego S, Kenworthy P. 1974. The control of the production of lactate and ethanol by higher plants. [Peas, parsnips]. *Planta* 118:296-310.
- De Atauri P, Acerenza L, Kholodenko BN, De L, I, Guinovart JJ, Agius L, Cascante M. 2001. Occurrence of paradoxical or sustained control by an enzyme when overexpressed: necessary conditions and experimental evidence with regard to hepatic glucokinase. *Biochem J* 355:787-93.
- de la Riva GA, Gonzalez-Cabrera J, Vazquez-Padron R, Ayra-Pardo C. 1998. *Agrobacterium tumefaciens*: a natural tool for plant transformation. *Elect J Biotech* 1:1-16.
- Dennis ES, Gerlach WL, Pryor AJ, Bennetzen JL, Inglis A, Llewellyn D, Sachs MM, Ferl RJ, Peacock WJ. 1984. Molecular analysis of the alcohol dehydrogenase (Adh1) gene of maize. *Nucleic Acids Res* 12:3983-4000.
- Dennis ES, Sachs MM, Gerlach WL, Finnegan EJ, Peacock WJ. 1985. Molecular analysis of the alcohol dehydrogenase 2 (Adh2) gene of maize. *Nucleic Acids Res* 13:727-43.
- Doehlert DC. 1989. Separation and characterization of four hexose kinases from developing maize kernels. *Plant physiol* 89:1042-8.
- Doehlert DC. 1990. Fructokinases from developing maize kernels differ in their specificity for nucleoside triphosphates. *Plant physiol* 93:353-5.
- Drew MC. 1997. Oxygen deficiency and root metabolism: injury and acclimation under hypoxia and anoxia. *Annu rev plant physiol plant mol biol* 48:223-50.
- Drew MC, Saglio PH, Pradet A. 1985. Larger adenylate energy charge and ATP/ADP ratios in aerenchymatous roots of *Zea mays* in anaerobic media as a consequence of improved internal oxygen transport. *Planta* 165:51-8.
- Duff SMG, Moorhead GBG, Lefebvre DD, Plaxton WC. 1989. Phosphate starvation inducible "bypasses" of adenylate and phosphate dependent glycolytic enzymes in *Brassica nigra* suspension cells. *Plant physiol* 90:1275-8.

- Fan TW, Higashi RM, Lane AN. 1988. An in vivo ^1H and ^{31}P NMR investigation of the effect of nitrate on hypoxic metabolism in maize roots. *Arch Biochem Biophys* 266:592-606.
- Fell DA. 1992. Metabolic control analysis: a survey of its theoretical and experimental development. *Biochem-J* 286:313-30.
- Fire A. 1999. RNA-triggered gene silencing. *Trends Genet* 15:358-63.
- Fire A, Xu S, Montgomery MK, Kostas SA, Driver SE, Mello CC. 1998. Potent and specific genetic interference by double-stranded RNA in *Caenorhabditis elegans*. *Nature* 391:806-11.
- Fox TC, Green BJ, Kennedy RA, Rumpho ME. 1998. Changes in hexokinase activity in *Echinochloa phyllopogon* and *Echinochloa crus-galli* in response to abiotic stress. *Plant physiol* 118:1403-9.
- Fox TC, Kennedy RA, Rumpho ME. 1994. Energetics of Plant Growth Under Anoxia: Metabolic Adaptations of *Oryza sativa* and *Echinochloa phyllopogon*. *Annals of botany* 74:445-55.
- Fox TC, Mujer CV, Andrews DL, Williams AS, Cobb BG, Kennedy RA, Rumpho ME. 1995. Identification and gene expression of anaerobically induced enolase in *Echinochloa phyllopogon* and *Echinochloa crus-galli*. *Plant physiol* 109:433-43.
- Freeling M. 1973. Simultaneous induction by anaerobiosis or 2,4-D of multiple enzymes specified by two unlinked genes: differential Adh1-Adh2 expression in maize. *Mol Gen Genet* 127:215-27.
- Gancedo JM, Clifton D, Fraenkel DG. 1977. Yeast hexokinase mutants. *J Biol Chem* 252:4443-4.
- Gerlach WL, Pryor AJ, Dennis ES, Ferl RJ, Sachs MM, Peacock WJ. 1982. cDNA cloning and induction of alcohol dehydrogenase gene (adh1) in maize. *Proc Natl Acad Sci U S A* 79:2981-5.
- Giri A, Narasu ML. 2000. Transgenic hairy roots: recent trends and applications. *Biotech-Adv* 18:1-22.
- Gonzalez C, Ureta T, Sanchez R, Niemeyer H. 1964. Multiple molecular forms of ATP:hexose 6-phosphotransferase from rat liver. *Biochem Biophys Res Commun* 16:347-52.
- Gonzali S, Pistella L, Bellis LD, Alpi A. 2001. Characterization of two *Arabidopsis thaliana* fructokinases. *Plant Science* 160:1107-14.
- Good AG, Crosby WL. 1989. Anaerobic induction of alanine aminotransferase in barley root tissue. *Plant physiol* 90:1305-9.

- Griffin LD, Gelb BD, Adams V, McCabe ER. 1992. Developmental expression of hexokinase 1 in the rat. *Biochim Biophys Acta* 1129:309-17.
- Hajurezaei M, Stitt M. 1991. Contrasting roles of pyrophosphate: Fructose-6-phosphate phosphotransferase during aging of tissue slices from potato tubers and carrot storage tissues. *Plant Science* 77:177-83.
- Hake S, Kelley PM, Taylor WC, Freeling M. 1985. Coordinate induction of alcohol dehydrogenase 1, aldolase, and other anaerobic RNAs in maize. *J Biol Chem* 260:5050-4.
- Hansen G. 2000. Evidence for *Agrobacterium*-induced apoptosis in maize cells. *Mol Plant Microbe Interact* 13:649-57.
- Hanson AD, Jacobsen JV. 1984. Control of lactate glycolysis, lactate fermentation and -amalyse by O₂ deficit in barley aleurone layers. *Plant physiol* 75:566-72.
- Hanson AD, Jacobsen JV, Zwar JA. 1984. Regulated expression of three alcohol dehydrogenase genes in barely aleurone layers. *Plant physiol* 75:573-81.
- He CJ, Morgan PW, Drew MC. 1996. Transduction of an Ethylene Signal Is Required for Cell Death and Lysis in the Root Cortex of Maize during Aerenchyma Formation Induced by Hypoxia. *Plant physiol* 112:463-72.
- Hengartner H, Zuber H. 1973. Isolation and characterization of a thermophilic glucokinase from *Bacillus stearothermophilus*. *FEBS Lett* 37:212-6.
- Hernalsteens JP, Thiatoong L, Schell J, VanMontagu, M. 1984. An *Agrobacterium* transformed cell-culture from the monocot *Asparagus officinalis*. *EMBO J* 3 :3039-41.
- Hiei Y, Ohta S, Komari T, Kumashiro T. 1994. Efficient transformation of rice (*Oryza sativa* L.) mediated by *Agrobacterium* and sequence analysis of the boundaries of the T-DNA. *Plant J* 6:271-82.
- Higgins TJ, Easterby JS. 1974. Wheatgerm hexokinase: physical and active-site properties. *Eur J Biochem* 45:147-60.
- Hoffman NE, Bent AF, Hanson AD. 1986. Induction of lactate dehydrogenase isozymes by oxygen deficit in barley root tissue. *Plant physiol* 82:658-63.
- Hooykaas PJJ. 1989. Transformation of plant cells via *Agrobacterium*. *Plant Mol Biol* 13:327-36.
- Inouye M. 1988. Antisense RNA: its functions and applications in gene regulation--a review. *Gene* 72:25-34.
- Izant JG, Weintraub H. 1984. Inhibition of thymidine kinase gene expression by anti-sense RNA: a molecular approach to genetic analysis. *Cell* 36:1007-15.

- Jang JC, Leon P, Zhou L, Sheen J. 1997. Hexokinase as a sugar sensor in higher plants. *Plant Cell* 9:5-19.
- Johnson JR, Cobb BG, Drew MC. 1989. Hypoxic induction of anoxic tolerance in *Zea mays*. *Plant physiol* 91:837-41.
- Kacser H, Burns JA. 1973. The control of flux. *Symp Soc Exp Biol* 27:65-104.
- Kacser H, Burns JA. 1979. Molecular democracy: Who shares the controls? *Biochem Soc Trans* 7:1149-61.
- Kacser H, Burns JA. 1995. The control of flux: 21 years on. *Biochem Soc Trans* 23(2):341-66.
- Kanayama Y, Granot D, Dai N, Petreikov M, Schaffer A, Powell A, Bennett AB. 1998. Tomato fructokinases exhibit differential expression and substrate regulation. *Plant physiol* 117:85-90.
- Katzen HM, Soderman DD, Cirillo VJ. 1968. Tissue distribution and physiological significance of multiple forms of hexokinase. *Ann N Y Acad Sci* 151:351-8.
- Kelley PM. 1989. Maize pyruvate decarboxylase mRNA is induced anaerobically. *Plant Mol Biol* 13:213-22.
- Kelley PM, Freeling M. 1984a. Anaerobic expression of maize fructose-1,6-diphosphate aldolase. *J Biol Chem* 259:14180-3.
- Kelley PM, Freeling M. 1984b. Anaerobic expression of maize glucose phosphate isomerase I. *J Biol Chem* 259:673-7.
- Kengen SW, Tuininga JE, de Bok FA, Stams AJ, de Vos WM. 1995. Purification and characterization of a novel ADP-dependent glucokinase from the hyperthermophilic archaeon *Pyrococcus furiosus*. *J Biol Chem* 270:30453-7.
- Koch KE, Ying Z, Wu Y, Avigne WT. 2000. Multiple paths of sugar-sensing and a sugar/oxygen overlap for genes of sucrose and ethanol metabolism. *J Exp Bot* 51:417-27.
- Kooter JM, Matzke MA, Meyer P. 1999. Listening to the silent genes: transgene silencing, gene regulation and pathogen control. *Trends Plant Sci* 4(9):340-7.
- Laemmli UK. 1970. Cleavage of structural proteins during the assembly of the head of bacteriophage T4. *Nature* 227:680-5.
- Lal SK, Johnson S, Conway T, Kelley PM. 1991. Characterization of a maize cDNA that complements an enolase-deficient mutant of *Escherichia coli*. *Plant Mol Biol* 16:787-95.
- Lal SK, Lee C, Sachs MM. 1998. Differential regulation of enolase during anaerobiosis in maize. *Plant physiol* 118:1285-93.

- Lessard PA, Kulaveerasingam H, York GM, Strong A, Sinskey AJ. 2002. Manipulating gene expression for the metabolic engineering of plants. *Metab Eng* 4:67-79.
- Martinez-Barajas E, Krohn BM, Stark DM, Randall DD. 1997. Purification and characterization of recombinant tomato fruit (*Lycopersicon esculentum* Mill.) fructokinase expressed in *Escherichia coli*. *Protein Expr Purif* 11:41-6.
- Martinez-Barajas E, Randall DD. 1998. Purification and characterization of a glucokinase from young tomato (*Lycopersicon esculentum* L. Mill.) fruit. *Planta* 205:567-73.
- Matzke MA, Matzke AJM. 1995. How and why do plants inactivate homologous (trans)genes? *Plant physiol* 107:679-85.
- Menegus F, Cattaruzza L, Chersi A, Fronza G. 1989. Differences in the anaerobic lactate-succinate production and in the changes of cell sap pH for plants with high and low resistance to anoxia. *Plant physiol* 90:29-32.
- Menu T, Rothan C, Dai N, Petreikov M, Etienne C, Destrac-Irvine A, Schaffer A, Granot D, Ricard B. 2001. Cloning and characterization of a cDNA encoding hexokinase from tomato. *Plant Science* 160:209-18.
- Mertens E. 1991. Pyrophosphate-dependent phosphofructokinase, an anaerobic glycolytic enzyme?. *FEBS Lett* 285:1-5.
- Mertens E, Larondelle Y, Hers HG. 1990. Induction of pyrophosphate:fructose 6-phosphate 1-phosphotransferase by anoxia in rice seedlings. *Plant physiol* 93:584-7.
- Miernyk JA, Dennis DT. 1983. Mitochondrial, plastid, and cytosolic isozymes of hexokinase from developing endosperm of *Ricinus communis*. *Arch Biochem Biophys* 226:458-68.
- Miernyk JA, Dennis DT. 1984. Enolase isozymes from *Ricinus communis*: partial purification and characterization of the isozymes. *Arch Biochem Biophys* 233:643-51.
- Misset O, Bos OJ, Opperdoes FR. 1986. Glycolytic enzymes of *Trypanosoma brucei*. Simultaneous purification, intraglycosomal concentrations and physical properties. *Eur J Biochem* 157:441-53.
- Mol JN, van der Krol AR, van Tunen AJ, van Blokland R, de Lange P, Stuitje AR. 1990. Regulation of plant gene expression by antisense RNA. *FEBS Lett* 268:427-30.
- Monson EK, Ditta GS, Helinski DR. 1995. The oxygen sensor protein, FixL, of *Rhizobium meliloti*. Role of histidine residues in heme binding, phosphorylation, and signal transduction. *J Biol Chem* 270:5243-50.
- Monson EK, Weinstein M, Ditta GS, Helinski DR. 1992. The FixL protein of *Rhizobium meliloti* can be separated into a heme-binding oxygen-sensing domain and a functional C-terminal kinase domain. *Proc Natl Acad Sci U S A* 89:4280-4.

- Muench DG, Good AG. 1994. Hypoxically inducible barley alanine aminotransferase: cDNA cloning and expression analysis. *Plant Mol Biol* 24:417-27.
- Murashige T, Skoog F. 1962. A revised medium for rapid growth and bioassays with tissue cultures. *Plant physiol* 15:473-97.
- Nakanishi Y, Maeshima M. 1998. Molecular cloning of vacuolar H(+)-pyrophosphatase and its developmental expression in growing hypocotyl of mung bean. *Plant physiol* 116:589-97.
- Napoli C, Lemieux C, Jorgensen RA. 1990. Introduction of a Chimeric Chalcone Synthase Gene into Petunia Results in Reversible Co-Suppression of Homologous Genes in trans. *Plant Cell* 2:279-89.
- Newsholme EA, Crabtree B. 1979. Theoretical principles in the approaches to control of metabolic pathways and their application to glycolysis in muscle. *J Mol Cell Cardiol* 11:839-56.
- Pal-Bhadra M, Bhadra U, Birchler JA. 1999. Cosuppression of nonhomologous transgenes in *Drosophila* involves mutually related endogenous sequences. *Cell* 99:35-46.
- Peschke VM, Sachs MM. 1993. Multiple pyruvate decarboxylase genes in maize are induced by hypoxia. *Mol Gen Genet* 240:206-12.
- Phillips NF, Horn PJ, Wood HG. 1993. The polyphosphate glucokinase. *Arch Biochem Biophys* 300:309-19.
- Plaxton WC. 1989. Molecular and immunological characterization of plastid and cytosolic pyruvate kinase isozymes from castor-oil-plant endosperm and leaf. *Eur J Biochem* 181(2):443-51.
- Plaxton WC. 1990. Glycolysis. *Methods in Plant Biochemistry* 3:145-72.
- Pollard-Knight D, Cornish-Bowden A. 1987. Kinetics of hexokinase D ('glucokinase') with inosine triphosphate as phosphate donor. Loss of kinetic co-operativity with respect to glucose. *Biochem J* 245:625-9.
- Potrykus I. 1991. Gene transfer to plants: Assessment of published approaches and results. *Annu rev plant physiol plant mol biol* 42:205-25.
- Pradet A, Raymond P. Adenine nucleotide ratios and adenylate charge in energy metabolism of plants and enzyme activities. *Annu rev plant physiol plant mol biol*. 34, 199-224. 1983.
- Rapoport TA, Heinrich R, Jacobasch G, Rapoport S. 1974. A linear steady-state treatment of enzymatic chains. A mathematical model of glycolysis of human erythrocytes. *Eur J Biochem* 42:107-20.

Renz A, Merlo L, Stitt M. 1993. Partial purification from potato tubers of three fructokinases and three hexokinases which show differing organ and developmental specificity. *Planta* 190:156-65.

Renz A, Stitt M. 1993. Substrate specificity and product inhibition of different forms of fructokinases and hexokinases in developing potato tubers. *Planta* 190:166-75.

Ricard B, Rivoal J, Pradet A. 1989. Rice cytosolic glyceraldehyde 3-phosphate dehydrogenase contains two subunits differentially regulated by anaerobiosis. *Plant Mol Biol Int J Mol Biol Biochem Genet Eng* 12:131-9.

Ricard B, van Toai TV, Chourey P, Saglio P. 1998. Evidence for the critical role of sucrose synthase for anoxic tolerance of maize roots using a double mutant. *Plantphysiol* 116:1323-31.

Ricard B, Rivoal J, Spiteri APA. 1991. Anaerobic stress induces the transcription and translation of sucrose synthase in rice. *Plant physiol* 95:669-74.

Rivoal J, Hanson AD. 1993. Evidence for a large and sustained glycolytic flux to lactate in anoxic roots of some members of the halophytic genus *Limonium*. *Plant physiol* 101:553-60.

Rivoal J, Hanson AD. 1994. Metabolic control of anaerobic glycolysis. Overexpression of lactate dehydrogenase in transgenic tomato roots supports the Davies-Roberts hypothesis and points to a critical role for lactate secretion. *Plant physiol* 106:1179-85.

Rivoal J, Ricard B, Pradet A. 1989. Glycolytic and fermentative enzyme induction during anaerobiosis in rice seedlings. *Plant physiol biochem* 27:43-52.

Rivoal J, Ricard B, Pradet A. Lactate dehydrogenase in *Oryza sativa* L. seedlings and roots. Identification and partial purification. *Plant physiol* 95, 682-686. 1991.
Ref Type: Generic

Rivoal J, Thind S, Pradet A, Ricard B. 1997. Differential induction of pyruvate decarboxylase subunits and transcripts in anoxic rice seedlings. *Plant-physiol* 114:1021-9.

Roberts JKM, Andrade FH, Anderson IC. 1985. Further evidence that cytoplasmic acidosis is a determinant of flooding intolerance in plants. *Plant physiol* 77:492-4.

Roberts JKM, Callis J, Jardetzky O, Walbot V, Freeling M. 1984a. Cytoplasmic acidosis as a determinant of flooding intolerance in plants. *Proc Natl Acad Sci U S A* 81:6029-33.

Roberts JKM, Callis J, Wemmer D, Walbot V, Jardetzky O. 1984b. Mechanism of cytoplasmic pH regulation in hypoxic maize root tips and its role in survival under hypoxia. *Proc Natl Acad Sci U S A* 81:3379-84.

- Rocha FA, de Meis L. 1998. Reversibility of H⁺-ATPase and H⁺-pyrophosphatase in tonoplast vesicles from maize coleoptiles and seeds. *Plant physiol* 116:1487-95.
- Rolland F, Moore B, Sheen J. 2002. Sugar sensing and signaling in plants. *Plant Cell* 14 Suppl:S185-S205.
- Rolland F, Winderickx J, Thevelein JM. 2001. Glucose-sensing mechanisms in eukaryotic cells. *Trends Biochem Sci* 26:310-7.
- Rothstein SJ, DiMaio j, Strand M, Rice D. 1987. Stable and heritable inhibition of the expression of nopaline synthase in tobacco expressing anti-sense RNA. *Proc Natl Acad Sci U S A* 84:8439-43.
- Ruiz F, Vayssie L, Klotz C, Sperling L, Madeddu L. 1998. Homology-dependent gene silencing in *Paramecium*. *Mol Biol Cell* 9:931-43.
- Russell DA, Sachs MM. 1989. Differential expression and sequence analysis of the maize glyceraldehyde-3-phosphate dehydrogenase gene family. *Plant Cell* 1:793-803.
- Sachs MM, Subbaiah CC, Saab IN. Anaerobic gene expression and flooding tolerance in maize. *J Exp Bot* 47:1-15. 1996.
- Sachs MM, Freeling M, Okimoto R. 1980. The anaerobic proteins of maize. *Cell* 20:761-7.
- Saglio PH, Raymond P, Pradet A. 1980. Metabolic activity and energy charge of excised root tips under anoxia. *Plant physiol* 66 :1053-7.
- Salas J, Salas M, Vinuela E, Sols, A. 1965. Glucokinase of rabbit liver. *J Biol Chem* 240:1014-8.
- Sanger F, Nicklen S, Coulson AR. 1977. DNA sequencing with chain-terminating inhibitors. *Proc Natl Acad Sci U S A* 74:5463-7.
- Schafer W, Gorz A, Kahl G. 1987. T-DNA integration and expression in a monocot crop plant after induction of *Agrobacterium*. *Nature* 327:529-32.
- Schleucher J, Vanderveer PJ, Sharkey TD. 1998. Export of carbon from chloroplasts at night. *Plant physiol* 118:1439-45.
- Schnarrenberger C. 1990. Characterization and compartmentation, in green leaves, of hexokinases with different specificities for glucose, fructose, and mannose and for nucleoside triphosphates. *Planta* 181:249-55.
- Schumacher K, Vafeados D, McCarthy M, Sze H, Wilkins T, Chory J. 1999. The *Arabidopsis* det3 mutant reveals a central role for the vacuolar H⁽⁺⁾-ATPase in plant growth and development. *Genes Dev* 13:3259-70.

- Sebastian S, Wilson JE, Mulichak A, Garavito RM. 1999. Allosteric regulation of type I hexokinase: A site-directed mutational study indicating location of the functional glucose 6-phosphate binding site in the N-terminal half of the enzyme. *Arch Biochem Biophys* 362:203-10.
- Shanks JV, Morgan J. 1999. Plant 'hairy root' culture. *Curr Opin Biotechnol* 10:151-5.
- Shelp BJ, Bown AW, McLean MD. 1999. Metabolism and functions of gamma-aminobutyric acid. *Trends Plant Sci* 4:446-52.
- Sowa AW, Duff SMG, Guy PA, Hill RD. 1998. Altering hemoglobin levels changes energy status in maize cells under hypoxia. *Proc Natl Acad Sci U S A* 95:10317-21.
- Springer B, Werr W, Starlinger P, Bennett DC, Zokolica M, Freeling M. 1986. The Shrunk gene on chromosome 9 of *Zea mays* L is expressed in various plant tissues and encodes an anaerobic protein. *Mol Gen Genet* 205:461-8.
- Stachelek C, Stachelek J, Swan J, Botstein D, Konigsberg W. 1986. Identification, cloning and sequence determination of the genes specifying hexokinase A and B from yeast. *Nucleic Acids Res* 14:945-63.
- Subbaiah CC, Bush DS, Sachs MM. 1994b. Elevation of cytosolic calcium precedes anoxic gene expression in maize suspension-cultured cells. *Plant Cell* 6:1747-62.
- Subbaiah CC, Zhang J, Sachs MM. 1994a. Involvement of intracellular calcium in anaerobic gene expression and survival of maize seedlings. *Plant physiol* 105:369-76.
- Tanizawa Y, Koranyi LI, Welling CM, Permutt MA. 1991. Human liver glucokinase gene: cloning and sequence determination of two alternatively spliced cDNAs. *Proc Natl Acad Sci U S A* 88:7294-7.
- Theodorou ME, Cornel FA, Duff SM, Plaxton WC. 1992. Phosphate starvation-inducible synthesis of the alpha-subunit of the pyrophosphate-dependent phosphofructokinase in black mustard suspension cells. *J Biol Chem* 267:21901-5.
- Thomas S, Mooney PJ, Burrell MM, Fell DA. 1997a. Finite change analysis of glycolytic intermediates in tuber tissue of lines of transgenic potato (*Solanum tuberosum*) overexpressing phosphofructokinase. *Biochem J* 322:111-7.
- Thomas S, Mooney PJ, Burrell MM, Fell DA. 1997b. Metabolic Control Analysis of glycolysis in tuber tissue of potato (*Solanum tuberosum*): explanation for the low control coefficient of phosphofructokinase over respiratory flux. *Biochem J* 322:119-27.
- Trethewey RN, ap Rees T. 1994. A mutant of *Arabidopsis thaliana* lacking the ability to transport glucose across the chloroplast envelope. *Biochem J* 301:449-54.
- Turner JF, Chensee QJ, Harrison DD. 1977. Glucokinase of pea seeds. *Biochim Biophys Acta* 480:367-75.

Umeda M, Hara C, Matsubayashi Y, Li HH, Liu Q, Tadokoro F, Aotsuka S, Uchimiya H. 1994. Expressed sequence tags from cultured cells of rice (*Oryza sativa* L.) under stressed conditions: analysis of transcripts of genes engaged in ATP-generating pathways. *Plant Mol Biol* 25(3):469-78.

Ureta T, Fernandez WY, Centelles JJ, Cascante M. 2000. In vivo measurements of control coefficients for hexokinase and glucose- 6-phosphate dehydrogenase in *Xenopus laevis* oocytes. *FEBS Lett* 475:145-9.

van der Krol AR, Lenting PE, Veenstra J, van der Meer IM, Koes RE, Gerats AGM, Mol JN, Stuitje AR. 1988a. An anti-sense chalcone synthase gene in transgenic plants inhibits flower pigmentation. *Nature* 333:866-9.

van der Krol AR, Mol JN, Stuitje AR. 1988b. Antisense genes in plants: an overview. *Gene* 72:45-50.

van der Krol AR, Mur LA, Beld M, Mol JN, Stuitje AR. 1990a. Flavonoid genes in petunia: addition of a limited number of gene copies may lead to a suppression of gene expression. *Plant Cell* 2:291-9.

van der Krol AR, Mur LA, de Lange P, Mol JN, Stuitje AR. 1990b. Inhibition of flower pigmentation by antisense CHS genes: promoter and minimal sequence requirements for the antisense effect. *Plant Mol Biol* 14:457-66.

van West P, Kamoun S, 't Klooster JW, Govers F. 1999. Internuclear gene silencing in *Phytophthora infestans*. *Mol Cell* 3:339-48.

Veramendi J, Roessner U, Renz A, Willmitzer L, Trethewey RN. 1999. Antisense repression of hexokinase 1 leads to an overaccumulation of starch in leaves of transgenic potato plants but not to significant changes in tuber carbohydrate metabolism. *Plant physiol* 121:123-34.

Wassenegger M, Pelissier T. 1998. A model for RNA-mediated gene silencing in higher plants. *Plant Mol Biol* 37:349-62.

Webb J, Jackson MB. 1986. A transmission and cryo-scanning electron microscopy study of aerenchyma (cortical gas filled space) in adventitious roots of rice (*Oryza sativa*). *J Exp Bot* 37:832-41.

Wiese A, Groner F, Sonnewald U, Deppner H, Lerchl J, Hebbeker U, Flugge U, Weber A. 1999. Spinach hexokinase I is located in the outer envelope membrane of plastids. *FEBS Lett* 461:13-8.

Wilson JE. 1995. Hexokinases. *Rev Physiol Biochem Pharmacol* 126:65-198.

Womack FC, Welch MK, Nielsen J, Colowick SP. 1973. Purification and serological comparison of the yeast hexokinases P-I and P-II. *Arch Biochem Biophys* 158:451-7.

Xia JH, Saglio PH. 1992. Lactic acid efflux as a mechanism of hypoxic acclimation of maize root tips to anoxia. *Plant physiol* 100:40-6.

Xia JH, Robers JKM. 1994. Improved Cytoplasmic pH Regulation, Increased Lactate Efflux, and Reduced Cytoplasmic Lactate Levels Are Biochemical Traits Expressed in Root Tips of Whole Maize Seedlings Acclimated to a Low-Oxygen Environment. *Plant physiol* 105:651-7.

Zeng Y, Wu Y, Avigne WT, Koch KE. 1998. Differential regulation of sugar-sensitive sucrose synthases by hypoxia and anoxia indicate complementary transcriptional and posttranscriptional responses. *Plant physiol* 116:1573-83.

Zeng Y, Wu Y, Avigne WT, Koch KE. 1999. Rapid repression of maize invertases by low oxygen. Invertase/sucrose synthase balance, sugar signaling potential, and seedling survival. *Plant physiol* 121:599-608.